

Cretaceous Crocodyliforms from the Sahara

Paul C. Sereno^{1,†}, Hans C.E. Larsson^{2,‡}

1 Department of Organismal Biology and Anatomy, University of Chicago, Chicago, Illinois 60637, USA

2 Redpath Museum, McGill University, Montreal, Quebec H3A 2K6, Canada

† [urn:lsid:zoobank.org:pub:A979ECDE-871F-4AFC-9ABA-63A0FD6DC323](https://zoobank.org/pub:A979ECDE-871F-4AFC-9ABA-63A0FD6DC323)

‡ [urn:lsid:zoobank.org:author:F1B7E0C5-C76A-44ED-852C-58BF7AB961DB](https://zoobank.org/author:F1B7E0C5-C76A-44ED-852C-58BF7AB961DB)

Corresponding author: Paul C. Sereno (dinosaur@uchicago.edu)

Academic editor: Hans Sues | Received 13 November 2009 | Accepted 16 November 2009 | Published 19 November 2009

[urn:lsid:zoobank.org:pub:A979ECDE-871F-4AFC-9ABA-63A0FD6DC323](https://zoobank.org/pub:A979ECDE-871F-4AFC-9ABA-63A0FD6DC323)

Citation: Sereno PC, Larsson HCE (2009) Cretaceous Crocodyliforms from the Sahara. ZooKeys 28: 1–143. doi: 10.3897/zookeys.28.325

Abstract

Diverse crocodyliforms have been discovered in recent years in Cretaceous rocks on southern landmasses formerly composing Gondwana. We report here on six species from the Sahara with an array of trophic adaptations that significantly deepen our current understanding of African crocodyliform diversity during the Cretaceous period. We describe two of these species (*Anatosuchus minor*, *Araripesuchus wegneri*) from nearly complete skulls and partial articulated skeletons from the Lower Cretaceous Elrhaz Formation (Aptian-Albian) of Niger. The remaining four species (*Araripesuchus rattoides* **sp. n.**, *Kaprosuchus saharicus* **gen. n. sp. n.**, *Laganosuchus thaumastos* **gen. n. sp. n.**, *Laganosuchus maghrebensis* **gen. n. sp. n.**) come from contemporaneous Upper Cretaceous formations (Cenomanian) in Niger and Morocco.

Keywords

crocodyliforms, Metasuchia, Notosuchia, Crocodylia

Introduction

Crocodyliforms were particularly diverse during the Cretaceous period and long have been a focal point for paleobiogeographic hypotheses regarding the timing of the break-up of Gondwana (Buffetaut and Taquet 1979; Buffetaut and Rage 1993; Sereno

at al. 2003; Turner 2004). South America has the most complete fossil record of Cretaceous crocodyliforms. More than a dozen genera are known from Late Cretaceous rocks in Argentina and Brazil, which are characterized by a broad range of skull shapes pertaining to terrestrial carnivores, piscivores and herbivores (Ortega et al. 2000; Martinelli 2003; Candeiro et al. 2006; Candeiro and Martinelli 2006; Fiorelli and Calvo 2008; Marinho and Carvalho 2009). A similar range of Cretaceous crocodyliforms, although less taxonomically diverse, has been described recently from other southern landmasses, namely Madagascar (Buckley and Brochu 1999; Buckley et al. 2000; Turner 2006; Turner and Buckley 2008), Indo-Pakistan (Wilson and Gingerich 2001; Prasad and Broin 2002) and Australia (Salisbury et al. 2006).

In this paper, we provide an initial description of a range of Cretaceous crocodyliforms from continental Africa that rivals the record from South America in taxonomic and morphological diversity (Table 1). These African crocodyliforms, discovered in fossiliferous horizons in Morocco and Niger (Fig. 1), offer new insights into the evolution of crocodyliform trophic and locomotor adaptations and have significant impact on the understanding of Cretaceous paleobiogeography on southern landmasses.

Table 1. Fossil material described in this report.

Taxon	Number	Material	Country, Formation, Age
<i>Anatosuchus minor</i>	(holotype) MNN GAD603	Juvenile skull	Niger, Elrhaz Formation, Lower Cretaceous (Aptian-Albian)
	MNN GAD17	Skull and partial skeleton	
	MNN GAD18	Partial dentary	
	MNN GAD19	Cranium	
<i>Araripesuchus wegeneri</i>	MNN GAD20–24	Partial skulls and skeletons on block	Niger, Elrhaz Formation, Lower Cretaceous (Aptian-Albian)
	MNN GAD25	Partial skeleton	
	MNN GAD26	Juvenile dentary	
<i>Araripesuchus rattoides</i>	(holotype) CMN 41893	Right dentary	Morocco, Kem Kem Beds, Upper Cretaceous (Cenomanian)
	UCRC PV3	Dentary section	
<i>Araripesuchus</i> sp.	MNN GAD27	Large dentary	Niger, Elrhaz Formation, Lower Cretaceous (Aptian-Albian)
<i>Kaprosuchus saharicus</i>	(holotype) MNN IGU12	Skull	Niger, Echkar Formation, Upper Cretaceous (Cenomanian)
<i>Laganosuchus thaumastos</i>	(holotype) MNN IGU13	Lower jaws	Niger, Echkar Formation, Upper Cretaceous (Cenomanian)
<i>Laganosuchus maghrebensis</i>	(holotype) UCRC PV2	Dentary section	Morocco, Kem Kem Beds, Upper Cretaceous (Cenomanian)

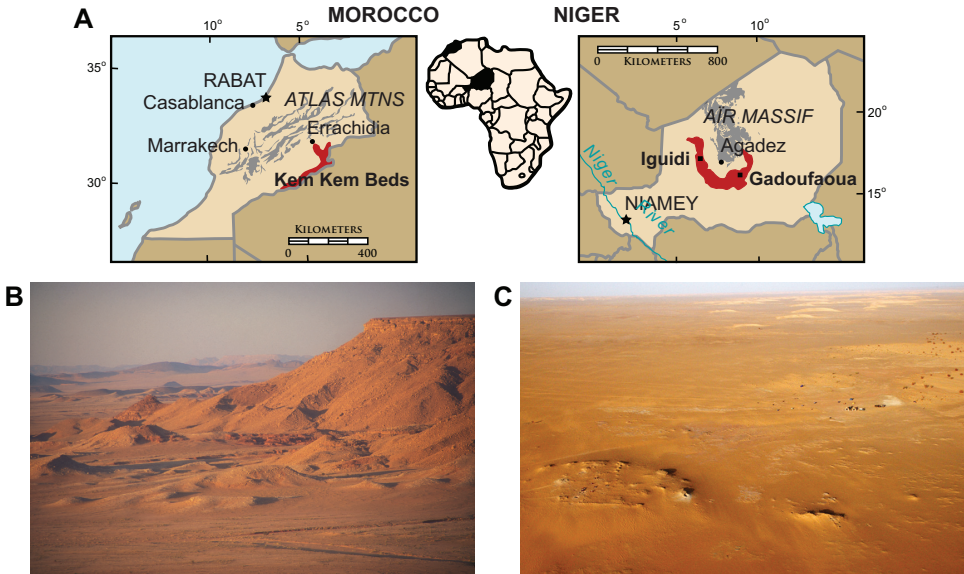


Figure 1. Map showing location of field areas in Morocco and Niger. Principal Cretaceous outcrops yielding Cretaceous crocodyliforms shown in red. **A** Exposures of the early late Cretaceous (Cenomanian) Kem Kem Beds in eastern Morocco (left) and late Early Cretaceous (Aptian-Albian) exposures at Gadoufaoua and early late Cretaceous exposures (Cenomanian) at Iguidi in Niger (right). **B** Exposures of the Upper Cretaceous Kem Kem Beds in eastern Morocco on the slope below the cliff edge, which is held by the overlying Cenomanian-Turonian limestone. **C** Aerial view of Gadoufaoua and the peneplain exposure of the Lower Cretaceous Elrhaz Formation in central Niger. The Elrhaz Formation consists of low-lying patches of purplish outcrop exposed among the dune fields of the Ténéré Desert.

Fossil evidence from Africa

Circum-Sahara. The earliest discoveries of Cretaceous crocodyliforms in Africa were made in Cenomanian-age rocks in the eastern Sahara in Egypt. Stromer described a “blunt-snouted” skull as *Libycosuchus brevirostris* (Stromer 1914) and a much longer, “duck-faced” skull as *Stomatosuchus inermis* (Stromer 1925, 1936) (Fig. 2). The holotype skull of *Libycosuchus*, one of the few fossil vertebrates from Stromer’s Egyptian collection to survive World War II, has since been widely interpreted as a basal notosuchian (Price 1959; Goman 1997; Ortega et al. 2000; Carvalho et al. 2004; Pol and Apesteguía 2005; Fiorelli and Calvo 2008), following initial comments by Price (1955). *Stomatosuchus*, given its unusual morphology and the loss of the holotype and only known remains, has not been placed with confidence within crocodyliform phylogeny, although often compared and sometimes allied with the South American Cenozoic eusuchian clade “Nettosuchidae” (Steel 1973). Its flattened, U-shaped skull is nearly two meters in length, its lower jaws are slender, and its teeth are small and closely set, as described by the only authors to examine the original material (Stromer 1925, 1936; Nopsca 1926). Discovery of a closely related genus from Niger and Mo-

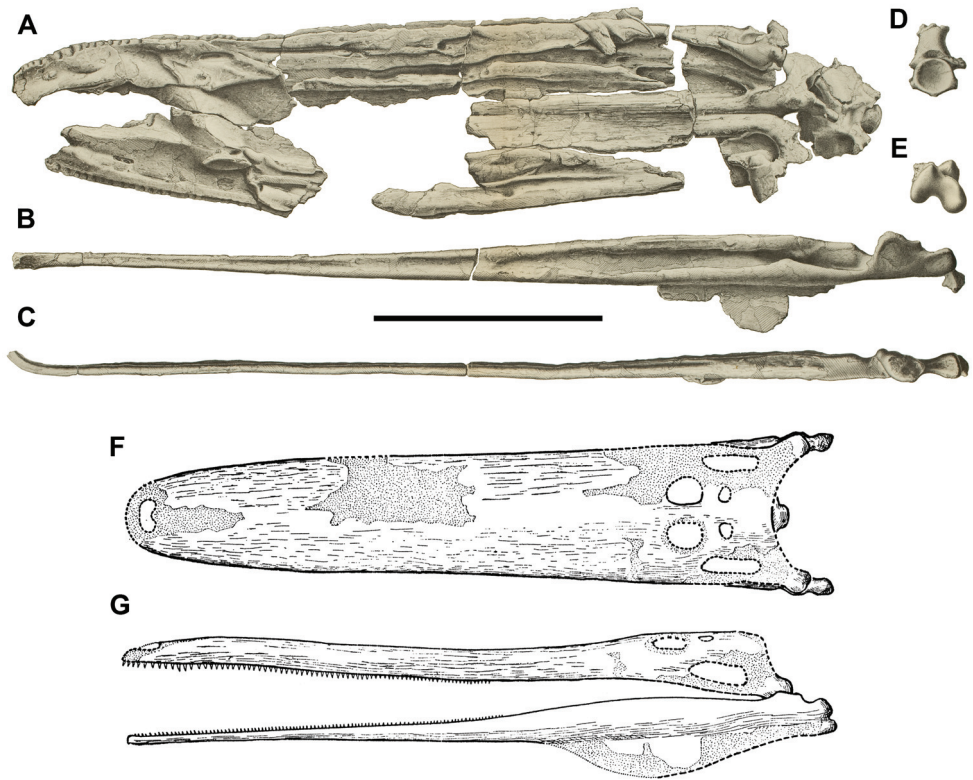


Figure 2. Skull and cervical vertebra of the crocodyliform *Stomatosuchus inermis*. **A** Cranium in ventral view. **B** Right lower jaw in medial view. **C** Right lower jaw (reversed) in dorsal view. **D** cervical vertebra in anterior view. **E** Right quadrate in ventral view. **F** Skull reconstruction in dorsal view. **G** Skull reconstruction in lateral view. Scale bar for A-E equals 50 cm. A-E from Stromer (1925); F and G from Stromer (1936).

rocco, described below, represents the first new information available for this highly specialized crocodyliform clade.

The remaining Cretaceous crocodyliform taxa known from the circum-Saharan region come from Lower Cretaceous (Aptian-Albian) and Late Cretaceous (Cenomanian) horizons, which are best exposed and explored in Morocco and Niger (Fig. 1). Well preserved crocodyliforms were first discovered from Aptian-Albian horizons at Gadoufaoua, a richly fossiliferous area along the western edge of the Ténéré Desert in Niger. Two species were initially described, the giant *Sarcosuchus imperator* (Broin and Taquet 1966; Buffetaut and Taquet 1977) and a new species, *Araripesuchus wegneri* Buffetaut and Taquet 1979; Buffetaut 1981), which was assigned to a genus originally described from northeastern Brazil (Price 1959). Recovery and study of more complete skulls and partial skeletons of *Sarcosuchus* has clarified its phylogenetic position among pholidosaurid crocodyliforms (Sereno et al. 2001). The generic assignment of *A. wegneri*

and its associated biogeographic significance have remained controversial (Ortega et al. 2000), given the fragmentary nature of the holotype (a partial snout with only a few teeth bearing complete crowns). The much more complete remains described below, however, leave no doubt about its assignment to *Araripesuchus*, a genus that may reside at the base of Notosuchia (Price 1955, 1959; Sereno et al. 2003; Pol and Apesteguía 2005; Fiorelli and Clavo 2008).

More recently two additional crocodyliforms were described from Aptian-Albian horizons at Gadoufaoua in Niger. *Stolokrosuchus*, a narrow-snouted crocodyliform based on a nearly complete skull (Larsson and Gado 2000), has been interpreted as close to *Peirosaurus* (Price 1955) among basal neosuchians (Larsson and Gado 2000; Fiorelli and Calvo 2008). *Anatosuchus*, a blunt-snouted notosuchian based on a juvenile skull (Sereno et al. 2003), is reconsidered below in the light of a well preserved adult skull and partial skeleton.

Well preserved crocodyliforms have also been described from Cenomanian horizons in Morocco and Algeria. *Hamadasuchus*, originally based on a partial dentary (Buffetaut 1994), is now known from complete cranial remains with generalized skull proportions (Larsson and Sues 2007). *Elosuchus* (Broin 2002), a narrow-snouted crocodyliform originally based on fragmentary remains from Algeria referred to *Thoracosaurus* (Lavocat 1955), is now also known from well preserved cranial remains from Niger and has been considered a close relative of *Stolokrosuchus* (Broin 2002). Cenomanian horizons in Morocco and Niger have yielded molariform teeth (Larsson and Sidor 1999) and other specimens that suggest a diverse array of specialized crocodyliforms was present during the Late Cretaceous on Africa similar to that known from South America (Montefeltro et al. 2009). Below we describe three new species from these horizons.

Post-Cenomanian crocodyliforms from circum-Saharan Africa are limited to isolated elements collected from a small exposure of “Senonian” beds in Niger (Buffetaut 1976). The genus *Trematochampsia* was erected on the basis of an isolated right lacrimal, and several additional species have been assigned to *Trematochampsia* from distant locales in Madagascar (Buffetaut and Taquet 1979) and Argentina (Chiappe 1988). The validity of the original genus and species has long been questioned (Gasparini et al. 1991), and a new genus (*Miadanasuchus*) was recently erected for material from Madagascar (Rasmusson Simons and Buckley 2009). Restudy of the collection from Niger will be needed to resolve its taxonomic affinities.

Eastern Africa. Two blunt-snouted notosuchians with multicusped teeth have been described from continental eastern Africa based on partial skeletons with well preserved skulls. The first, *Malawisuchus*, comes from Lower Cretaceous beds in eastern Malawi (Gomani 1997). Its molariform, multicusped posterior maxillary crowns closely resemble those of the Brazilian notosuchid *Candidodon* (Carvalho 1994; Zaher et al. 2006) and engaged opposing crowns in anteroposterior (proal) jaw movement (Gomani 1997), as in the notosuchians *Mariliasuchus* (Zaher et al. 2006) and *Notosuchus* (Price 1959; Lecuona and Pol 2008).

The second is a new blunt-snouted species (O'Connor et al. 2008) discovered recently in Lower Cretaceous horizons in southwestern Tanzania (Roberts et al. 2004). The dentition is markedly heterodont with incisiform, caniniform and molariform teeth that may have accommodated fore-aft jaw movement similar to that described above.

Methods

Preparation. Fossil material was prepared using pin vice, pneumatic air scribe, and air-powered abrasives. To reduce color distractions in photographic images, some fossils were molded in silicone and cast in matt-grey epoxy.

Imaging. Computed tomography was undertaken for several of the skulls and one postcranial skeleton. The skull of *Kaprosuchus saharicus* (MNN IGU12) was scanned by a Philips Brilliance 64-slice scanner at 80 Kv in the University of Chicago Hospitals. The cranium of *Araripesuchus wegneri* (MNN GAD19), a dentary section of *Araripesuchus rattoides* (UCRC PV3), and the skull and partial skeleton of *Anatosuchus minor* (MNN GAD17) were scanned at the High-Resolution X-ray Computed Tomography Facility at The University of Texas at Austin.

Anatomical terms. We employ traditional, or “Romerian”, anatomical and directional terms over veterinarian alternatives (Wilson 2006). We use “anterior” and “posterior” as directional terms, for example, rather than the veterinarian alternatives “rostral” or “cranial” and “caudal”. For the dentition, we use “mesial” and “distal” rather than “anterior” and “posterior” to accommodate reorientation of the crown along an arched dental arcade.

For crocodyliform skull shape, we employ five terms from the literature (Langston, 1973; Busbey 1994; Brochu 2001) that have been used to describe the rostrum, the most variable aspect of the crocodyliform skull: (1) generalized, (2) blunt-snouted, (3) narrow-snouted, (4), duck-faced (= platyrostral); and (5) deep-snouted (= ziphodont or oreinirostral). Despite their utility, these skull shape categories do not neatly divide crocodyliform skull shape in multivariate space (Brochu 2001).

For tooth identification, we use tooth number and a letter abbreviation for dentary (d), premaxillary (pm), and maxillary (m) teeth (e.g., “pm4” = fourth premaxillary tooth). For tooth form, we avoid the term “ziphodont” in order to separate tooth shape and the ornamentation of the carina. For tooth shape, we employ the terms “incisiform,” “caniniform” and “postcaniniform” in species with differentiated dentitions, as defined below. For tooth ornamentation, we use the term “denticle” to identify subconical projections along the carina that are directed apically and “serration” for subrectangular projections that are directed at a right angle to the carina.

Taxonomic terms. We use a small number of suprageneric taxa to tag specific clades within Crocodylomorpha (Fig. 3). Phylogenetic definitions were proposed for these

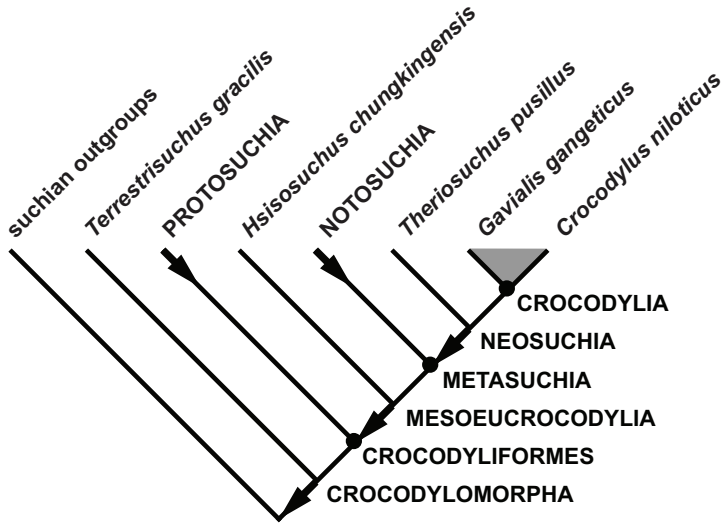


Figure 3. Higher level taxonomic framework. Phylogenetic taxonomic framework employed in the present work (following Sereno et al. 2001). Taxa surrounding two important junctions within Crocodylomorpha are stabilized with node-stem triplets, in which a node-based taxon (Crocodyliformes, Metasuchia) is composed of two subordinate stem-based taxa (Protosuchia + Mesoeucrocodylia; Notosuchia + Neosuchia). Dots and arrows indicate node-based and stem-based definitions, respectively. Tone indicates extant crocodylians.

taxa with the aim of stabilizing their meaning (Sereno et al. 2001). These definitions specify Crocodylomorpha and Crocodylia as stem and node-based taxa, respectively. The latter comprises the crown clade, as specified by the species *Gavialis gangeticus* and *Crocodylus niloticus*. Two node-stem triplets (Sereno 2005) are positioned at two important nodes between Crocodylomorpha and Crocodylia. These include Crocodyliformes, composed of stem-based Protosuchia and Mesoeucrocodylia, and Metasuchia, composed of Notosuchia and Neosuchia. Data concerning the historical usage for these six taxa and their phylogenetic definitions are available online (Sereno 2005; Sereno et al. 2005).

The crocodyliforms in this paper would be widely regarded as metasuchians, their position within that clade comprising the central phylogenetic question. The taxonomic framework outlined here specifies a split within Metasuchia, the fundamental phylogenetic question being whether the new crocodyliforms are closer to *Notosuchus terrestris* or *Crocodylus niloticus*. This is a heuristic taxonomic framework, given the current state of flux in basal metasuchian phylogeny.

Institutional and collection abbreviations:

AMNH American Museum of Natural History, New York, New York, USA

CMN Canadian Museum of Nature, Ottawa, Ontario, Canada

FMNH Field Museum of Natural History, Chicago, Illinois, USA

- LH** Las Hoyas collection, Museo de Cuenca, Cuenca, Spain
MCNA Museo de Ciencias Naturales y Antropológicas (J. C. Moyano) de Mendoza, Mendoza, Argentina
MNN Muséum National du Niger, Niamey, République de Niger
TMM TMM, Texas Memorial Museum, Austin, Texas, USA
UCRC University of Chicago Research Collection, Chicago, Illinois, USA

Results

Systematic Paleontology

Systematic hierarchy:

Crocodylomorpha Hay, 1930 *sensu* Walker, 1970

Crocodyliformes Hay, 1930

Mesoeucrocodylia Whetstone & Whybrow, 1983

Metasuchia Benton & Clark, 1988

Notosuchia Gasparini, 1971

Anatosuchus minor Sereno et al., 2003

Figs. 4–10, 12, 13

Tables 2–6

Sereno et al. (2001, figs. 1, 2)

Holotype. MNN GAD603; nearly complete skull with lower jaws of a subadult individual; margins of the skull are eroded away. The holotype was previously catalogued as “GDF603” (Sereno et al. 2003).

Type locality. Gadoufaoua, Agadez District, Niger Republic (N 16° 46', E 9° 22') (Fig. 1A, C).

Horizon. Elrhaz Formation, Tegama Series; Lower Cretaceous (Aptian-Albian), ca. 110 Mya (Taquet 1976). In association with a diverse dinosaurian fauna (Taquet 1976; Sereno et al. 1998, 1999, 2007; Taquet and Russell 1999; Sereno and Brusatte 2008) and the crocodyliforms *Sarcosuchus imperator* (Broin and Taquet 1966; Sereno et al. 2001), *Araripesuchus wegneri* (Buffetaut and Taquet 1979), and *Stolokrosuchus lapparenti* (Larsson and Gado 2000). At a single field locality (G109), specimens were recovered that are referable to *Anatosuchus minor* (MNN GAD18) and *Araripesuchus wegneri* (MNN GAD19).

Referred material. MNN GAD17 (Figs. 4–8, 12, 13), nearly complete skull with lower jaws lacking only the anterolateral corner of the snout in articulation with a postcranial skeleton lacking the right pectoral girdle and forelimb, most of both hind limbs, sacrum, and tail; MNN GAD18 (Fig. 9), mid-section of the left dentary preserving alveoli 7–14 and the anterior tip of the left splenial.

Revised diagnosis. Small-bodied metasuchian (< 1.0 m) with low transversely expanded snout that forms the broadest portion of the cranium, broad-based anteriorly projecting pointed internarial bar, lenticular-shaped external nares, elevated narial bridge which expands transversely behind the external nares, prominent median edentulous dentary margin, laterally projecting vascularized dentary shelf on parasagittal portion of dentary ramus, enlarged neurovascular foramina located along the anterior snout margin, anterior snout margin smooth, vertical and sharply defined on the premaxilla and maxilla, oval splenic fenestra on the anterior transverse portion of the lower jaw, six premaxillary teeth, premaxillary and anterior maxillary tooth row that angles ventrolaterally toward the corner of the snout at approximately 25°, largest upper and lower teeth positioned along the bend in the L-shaped tooth row (m4, d12), three pairs of cervical osteoderms that decrease in size posteriorly, large manus (30% skull length), elongate poorly recurved manual unguals on digits I–III, and manual digit IV with six phalanges.

The initial description was based on an immature skull embedded in a hematitic concretion (MNN GAD603). The concretion was discovered on the surface with prominent edges of the skull, such as the anterior end of the snout, trimmed by erosion (Serenio et al. 2003). The likeness drawn between *Anatosuchus* and the South American genus *Comahuesuchus* was based on a few seemingly unique features, such as a diastema between the premaxillary tooth rows, which we can now say arose in the immature skull of *Anatosuchus* as an artifact of erosion. The revised diagnosis is based mainly on a referred adult skull and partial articulated postcranium (MNN GAD17) that preserves an intact portion of the paravertebral shield (Fig. 4). This well preserved skull was found embedded in sandstone, the right corner of the snout, right limbs, sacrum and tail lost to erosion. The additional information available for both *Anatosuchus* and *Comahuesuchus* confirms Martinelli's (2003) view that these genera are not closest relatives among known notosuchians.

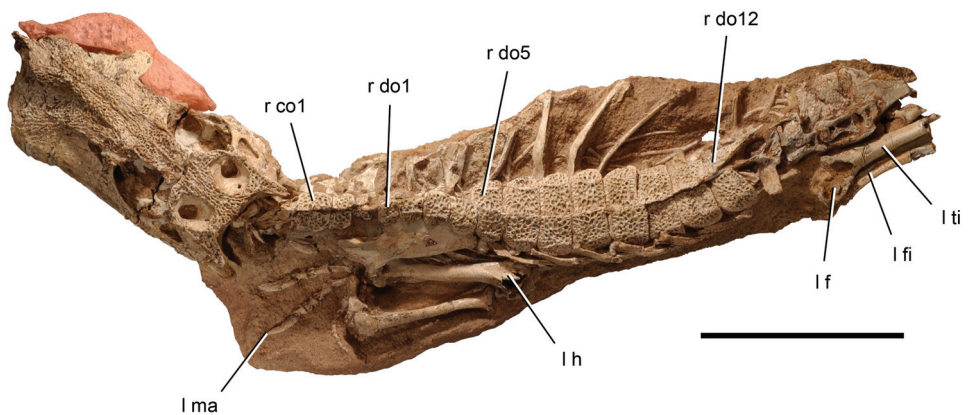


Figure 4. Skeleton of the crocodyliform *Anatosuchus minor*. Skull and partial postcranial skeleton (MNN GAD17) in dorsal view. Scale bar equals 10 cm. Pink tone indicates restored snout margin. Abbreviations: *co1*, cervical osteoderm 1; *do1*, 5, 12, dorsal osteoderm 1, 5, 12; *f*, femur; *fi*, fibula; *h*, humerus; *l*, left; *ma*, manus; *r*, right; *ti*, tibia.

Dorsal skull roof. In *A. minor* the snout becomes relatively broader and longer during growth. In the juvenile holotype specimen MNN GAD603, the width of the skull across the rounded anterior corner of the snout is subequal to that across the suborbital ramus of the jugal (Sereno et al. 2003). Preorbital length, in addition, is subequal to that of the remainder of the skull. In mature individuals, in contrast, the anterior snout corner is the broadest region of the skull, and preorbital length is approximately 20% greater than the posterior portion of the skull (MNN GAD17; Figs. 5, 6; Tables 2, 3). The following description is based primarily on this specimen.

The *premaxilla* is a broad bone housing six recurved teeth. The base of the internarial process is broad, unlike that in *Araripesuchus*, but similar in this regard to *Simosuchus* (Buckley et al. 2000). It extends anteriorly at approximately 30° above the horizontal, and tapers to a point, where it joins at a sharp angle the nearly horizontal internarial process of the nasal (Figs. 5, 6). The external nares, as a result, are dorsoventrally compressed and appear as a narrow slit in lateral view. In dorsal view, the external nares are elliptical, the floor of the narial passage broadly exposed to each side of the tapering internarial process of the nasal. The floor of the narial passage, which is formed by the premaxilla, is raised and slightly extended anterolaterally by a short tongue-shaped flange (Figs. 5B, 6B, 7A). The anterior half of the external nares projects beyond the first premaxillary tooth, a narial structure that projects anteriorly more prominently than in any other crocodyliform.

The narial fossa is clearly demarcated as a smooth subtriangular surface located lateral to the external nares and restricted to the premaxilla. In glancing light, a subtle division of the surface is visible. A teardrop-shaped fossa within the narial fossa is the largest surface, its tip emerging from under the lip of the rim of the external naris. In ventral view, the anterior projection is smooth and incorporates into the narial fossa the alveolar margin dorsal to premaxillary teeth 1–3. The lateral margin of the narial fossa is delimited by a shallow trough from the smooth, highly vascularized, vertical alveolar margin, which extends laterally toward the premaxilla-maxilla suture. No

Table 2. Dimensions (mm) of the holotype skull of *Anatosuchus minor* (MNN GAD603).

Measurement	Length
Cranium, preserved length	97.0
Snout, maximum transverse width	50.3
Snout, minimum transverse width	45.0
Cranium, width across quadrate condyles	44.4
Pterygoid mandibular processes, maximum transverse width	38.6
Choana, maximum anteroposterior length	17.0
Foramen magnum, maximum transverse width	9.6
Foramen magnum, maximum dorsoventral depth	6.0
Lower jaw, maximum length (anterior tip to end of retroarticular process)	97.0
Dentary ramus, maximum anteroposterior width at symphysis	10.6

other crocodyliform known thus far closely approaches the form and orientation of the external nares in *A. minor*.

The remainder of the external surface of the premaxilla can be divided into the alveolar margin and the ramus that tapers between the nasal and maxilla. The alveolar

Table 3. Dimensions (mm) of the referred skull of *Anatosuchus minor* (MNN GAD17). Paired structures are measured on left side except as indicated.

Structure	Measurement	Length
Dorsal skull roof	Cranium, maximum length	142.4
	Cranium, width across posterior tip of squamosals	48.6
	Cranium, width across quadrate condyles	57.1
	Snout, maximum transverse width	94.2
	Snout, minimum transverse width	75.4
	External naris, anteroposterior length	15.1
	External naris, maximum transverse width	6.7
	Narial fossa, maximum transverse width	37.0
	Antorbital fossa length	23.6
	Antorbital fenestra length	12.4
	Antorbital fenestra, maximum height	6.5
	Interorbital skull roof, minimum width	15.3
	Orbital anteroposterior diameter	36.6
	Orbital dorsoventral diameter	30.1
	Jugal orbital ramus, depth at mid-length	7.2
	Jugal lower temporal bar, minimum depth	3.6
	Postorbital bar, minimum anteroposterior diameter	3.2
	Laterotemporal fenestra length	12.8
	Laterotemporal fenestra depth	7.3
	Supratemporal fossa, anteroposterior length	18.7
	Supratemporal fossa, transverse width	14.7
Palate	Quadrate shaft length	13.4
	Quadrate condyles, transverse width	14.5 ¹
	Pterygoid mandibular processes, maximum transverse width	53.6
	Choana, maximum anteroposterior length	13.5
Lower jaw	Lower jaw, maximum length (to end of retroarticular process)	136.3
	Lower jaw, anterior end, transverse width	82.6
	Lower jaw, mid-section end, transverse width	81.4
	Lower jaw, retroarticular processes, transverse width	57.7
	Symphysis (dentary and splenial)	16.9
	External mandibular fenestra, length	15.3 ¹
	External mandibular fenestra, depth	7.8 ¹
	Retroarticular process, length	15.3
	Retroarticular process, transverse width at mid-length	7.4

¹Measurement from right side.

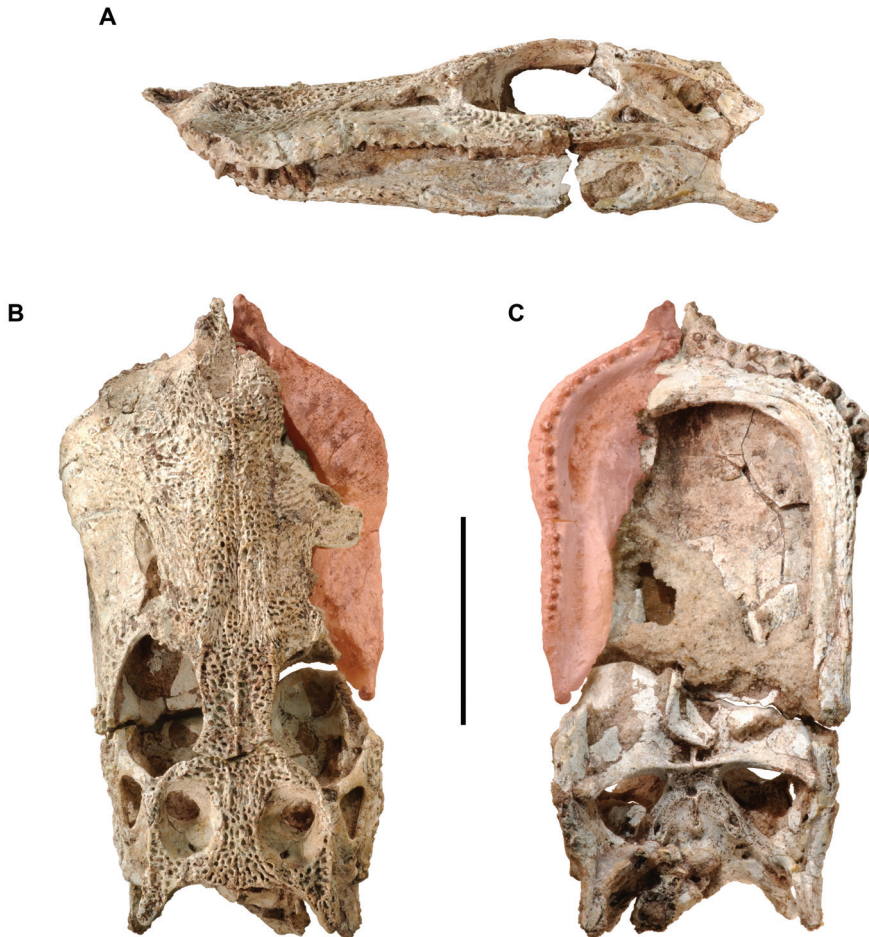
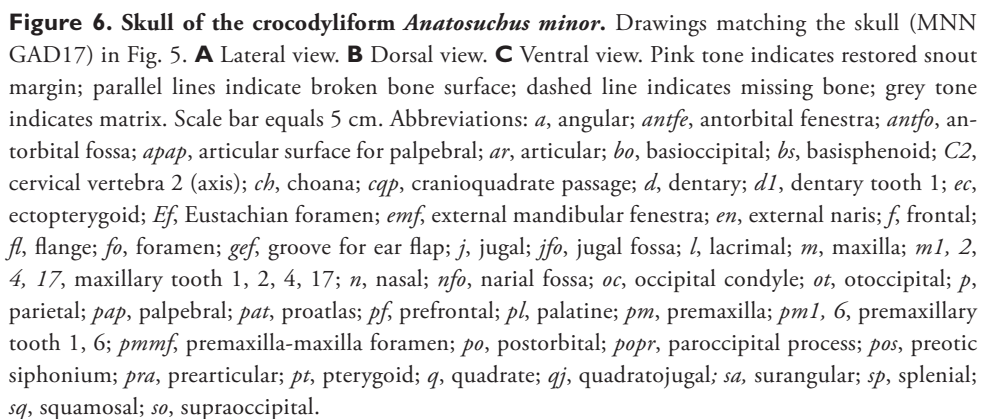


Figure 5. Skull of the crocodyliiform *Anatosuchus minor*. Partial skull in articulation with the atlas and the anterior portion of the axis (MNN GAD17). **A** Lateral view. **B** Dorsal view. **C** Ventral view. Pink tone indicates restored snout margin. Scale bar equals 5 cm.

margin faces primarily anteriorly, has a vertical orientation, and is gently transversely convex (Fig. 7A, B). As in *Araripesuchus wegneri*, two large neurovascular foramina are situated between the narial fossa and the premaxilla-maxilla foramen. The ventral margin is scalloped to match the position of the lateral three premaxillary teeth (Fig. 7B) as occurs in *Simosuchus*, but unlike the straight margin in *Araripesuchus*. The dorsal margin meets the dorsal surface of the snout at nearly a right angle along a rugose edge. Small foramina and grooves for impressed vessels are visible on the dorsal surface of the snout near the narial fossa and alveolar margin. That texture becomes deeply pitted as the premaxilla tapers to a point on the lateral aspect of the nasal bridge.



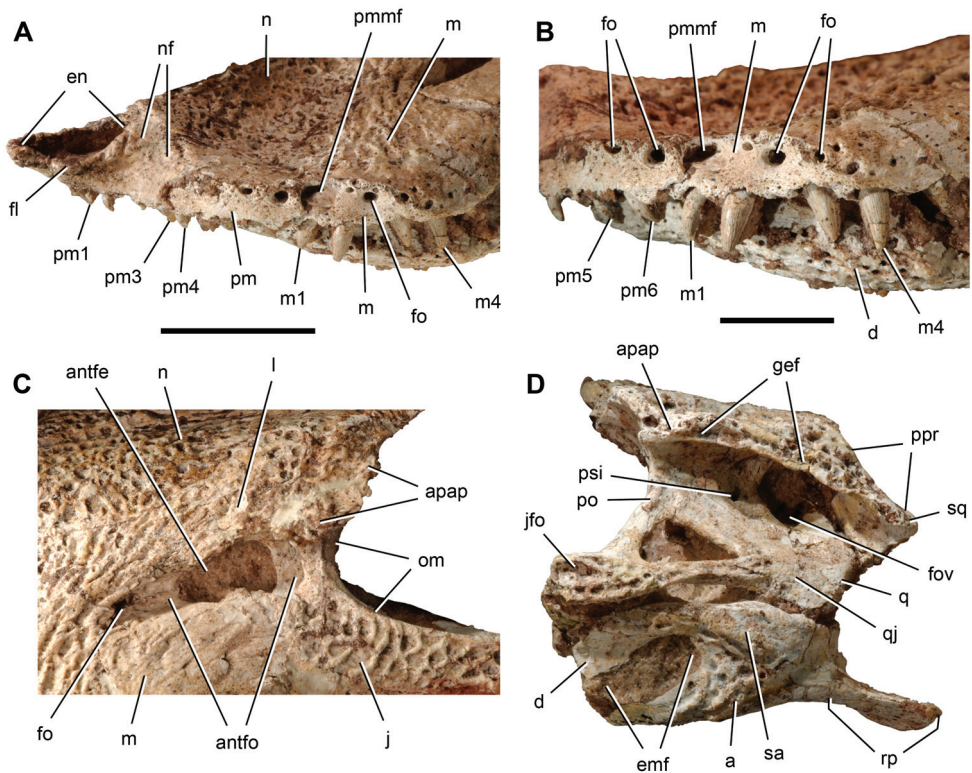


Figure 7. Skull of the crocodyliform *Anatosuchus minor*. Detailed views of the skull (MNN GAD17).

A Left snout margin in anterolateral view. **B** Left maxillary teeth in anterolateroventral view. **C** left antorbital region in lateral view. **D** Posterior portion of the skull in left lateral view. Scale bar for A, C and D equals 2 cm; scale bar for B equals 1 cm. Abbreviations: *a*, angular; *antfe*, antorbital fenestra; *antfo*, antorbital fossa; *apap*, articular surface for a palpebral; *d*, dentary; *emf*, external mandibular fenestra; *en*, external naris; *fl*, flange; *fo*, foramen; *fov*, fenestra ovalis; *gef*, groove for the ear flap; *j*, jugal; *jfo*, jugal fossa; *l*, lacrimal; *m*, maxilla; *m1*, 4, maxillary tooth 1, 4; *n*, nasal; *nf*, narial fossa; *om*, orbital margin; *pm*, premaxilla; *pm1*, 3, 4, 5, 6, premaxillary tooth 1, 3, 4, 5, 6; *pmmf*, premaxilla-maxilla foramen; *po*, postorbital; *ppr*, posterior process; *psi*, preotic siphonium; *q*, quadrate; *qj*, quadratojugal; *rp*, retroarticular process; *sa*, surangular; *sq*, squamosal.

In ventral view, the premaxilla is divided between the transversely convex surface of the internarial bar, the raised edges of the alveoli that scallop the alveolar margin, and the flat palatal surface, which is only partially exposed (Figs. 5C, 6C).

The *maxilla* is the most expansive bone in the skull and forms most of the snout. Its external surface is composed of a narrow alveolar margin and broader posterodorsal and posteroventral rami that extend above and below the antorbital opening, respectively. Like the premaxilla, the alveolar surface is vertical (Fig. 7B). It faces anterolaterally, borders the premaxilla-maxilla foramen, and gives passage to one additional large neurovascular foramen. The dorsal edge protrudes over this foramen before curving posteroventrally to join the scalloped ventral margin near the overhanging corner of

the snout adjacent to the fourth maxillary tooth. Several large foramina are present just above this edge on the corner of the snout (Fig. 7B).

The dorsal surface of the maxilla remains lightly textured along a band near the sharp anterior margin of the snout from the narial fossa to the anterolateral corner. This same low texture is present across the posteroventral ramus lateral to the antorbital depression, a muted textural pattern that resembles that seen in *Simosuchus*. In both taxa most of the maxilla below the antorbital opening is only lightly textured. In *Araripesuchus*, by contrast, the comparable region of the maxilla above m3 and m4 is more deeply sculpted with pits (Figs. 14A, 15A). As in most crocodyliforms, in *A. minor* a row of neurovascular foramina runs above the alveolar margin along the posteroventral ramus, although these are smaller than those at the anterior end of the snout. The maxilla forms the smooth and elongate anterior wall of the antorbital fossa, which is pierced by a foramen (Fig. 7C). The posterodorsal ramus of the maxilla is deeply pitted and slightly elevated as it passes over the antorbital depression to join the lacrimal and prefrontal.

The *nasal* extends from the tip of the internarial bar anteriorly to a subquadrate process posteriorly. The texture is reduced on the nasals immediately posterior to the external nares. Nonetheless, shallow sculpting is present, and the nasals do not contribute to the smooth narial fossa, which is isolated on the premaxilla as in *Araripesuchus* (Fig. 16A), *Simosuchus* (Buckley et al. 2000) and other crocodyliforms. The elevated nasal bridge is narrowest in width at mid-length along the snout, after which it broadens slightly to equal interorbital width (Figs. 5B, 6B). A narrow median trough is present from mid-snout to the subrectangular interdigitating ends of the nasals.

The L-shaped *lacrimal* has anterior and ventral rami, which join near a laterally prominent process for articulation with a missing anterior palpebral (Fig. 7C). The lacrimal foramen is tucked under this process within the orbit. The anterior ramus is deeply pitted and joins the maxilla along a subrectangular suture. The ventral ramus is smooth and divided into an orbital margin and medially inset posterior margin of the antorbital fossa.

The *palpebrals* are disarticulated in both known skulls. In the adult skull, however, they have fallen into orbital and temporal spaces, where they are partially exposed. A pair of articular fossae, the anterior on the lacrimal and *prefrontal* and the posterior on the postorbital, supported anterior and posterior palpebrals, respectively, as in many crocodyliforms (Fig. 7C, D). The prefrontal-frontal suture courses anteriorly, extending parallel to the inset of the fossa for the anterior palpebral. The prefrontal narrows in mid-section, where it contacts the lacrimal, and then extends anteriorly to contact the maxilla, effectively separating the nasal and lacrimal. The prefrontal pillar angles ventromedially and slightly posteriorly, tapering strongly from the skull roof to the palate.

The *frontal* and *parietal* are fused to their opposites and joined to each other by an interdigitating frontoparietal suture in both the adult and subadult skulls. The deeply pitted frontals have a median crest. The flat skull table formed by the parietals is also deeply pitted and separates the supratemporal fossae to a greater degree than in *Simosuchus* (Buckley et al. 2000). During growth in *A. minor*, interorbital width expands relative to the width of the skull table, such that the two measurements are subequal

in a subadult (Sereno et al. 2003) whereas the former is nearly twice the latter in an adult (Figs. 5B, 6B).

In the adult skull the frontal forms the anteromedial rim and distinctive corner of the supratemporal fossa, which is not the case in the subadult skull. That corner, in addition, is invaded by diverticulae from the supratemporal fossa. Although there is a similar corner in the rim of the fossa in *Araripesuchus wegeneri*, the rim is not undercut by pneumatic invagination. *Simosuchus*, on the other hand, has diverticulae resembling the condition in *A. minor* that undercut the anterior rim of the supratemporal fossa, a condition that has arisen a few times among crocodyliforms.

The frontal contributes to the rim of the supratemporal fossa and reaches the fossa in dorsal view. Frontal participation in these supratemporal structures seems to occur with maturity, given the exclusion of the frontal in a subadult skull (Sereno et al. 2003). The posterior margin of the skull table is scalloped to each side of a short posteromedian projection formed by the supraoccipital, which joins the parietals along a shallow V-shaped suture. *Simosuchus*, in contrast, is shown with a nearly straight posteromedian margin. In this case, notching of the posterior margin of the parietals by the supraoccipital may have been obliterated by coossification.

The right side of the skull has rotated slightly posterolaterally, an asymmetry best seen in dorsal view (Figs. 5B, 6B). Because there is no pattern of postmortem distortion of the skull, this asymmetry appears to be pathological rather than preservational in origin. The articular notch for the posterior palpebral on the right side is shifted posterolaterally, altering the shape of the supratemporal fossa. The right fossa has a convex lateral margin and its maximum parasagittal length is about 10% longer than the left side.

The *postorbital* is notched by an articular facet for a small posterior palpebral. The surface of the postorbital between the facet and the supratemporal fossa varies, remaining textured with pits in some species, such as *A. gomesii* (Price 1959) and *A. tsangatsangana* (Turner 2006), and smooth in others such as *A. patagonicus* (Ortega et al. 2000). In *A. wegeneri* that surface between the palpebral facet and supratemporal fossa is smooth and convex (Figs. 14B, 15B).

The *squamosal* is distinctly triradiate in dorsal view, the anterior process that contacts the postorbital the most slender. The dorsal surface of the anterior process is deeply pitted and depressed to form a shallow arcuate fossa (Figs. 5B, 6B). The posterior process is offset below the skull table and has a more subdued texture.

The *jugal* approaches, but does not contact, the posteroventral corner of the antorbital fossa (Fig. 7C). The anterior ramus is moderately expanded dorsoventrally toward its anterior end and is deeply pitted, with an oval fossa located beneath the orbit (Fig. 7D). The relatively slender postorbital process is inset at its base, the location for a very small siphonal opening. The posterior ramus is also relatively slender under the laterotemporal fenestra, where it terminates in a shallow inset articulation on the quadratojugal.

The L-shaped *quadratojugal* is partially fused to the quadrate near the quadrate condyle, where it approaches, but does not contribute to, the jaw articulation. The suture with the quadrate shaft is relatively straight, and surface texture is low and limited to the anterior portion of the bone.

Palate. The configuration of palatal sutures, shape and position of the suborbital fenestra, form of the mandibular rami of the pterygoid and ectopterygoid, position of the choanae, and form of the choanal septum (Figs. 5C, 6C) correspond well with those of *Araripesuchus* (Price 1959) (Figs. 14C, 15C) and differ markedly from the palatal configuration described in *Simosuchus* (Buckley et al. 2000). In these regards, *A. minor* is less derived than *Simosuchus*.

The premaxillary portion of the palate is restricted to a broad-based triangle near the anterior margin. The premaxilla-maxilla suture, however, is exposed only near the alveolar margin. The premaxilla-maxilla foramen may communicate with the palate as in *A. wegneri*; a foramen is present at the anterior margin of the maxilla just posterior to the premaxilla-maxilla suture, as is the case on one side of a cranium of *A. wegneri* (Figs. 14C, 15C). Furthermore, as in another skull of that species (Fig. 20B), this palatal foramen appears to be associated with the tip of the fourth dentary crown (MNN GAD17, GAD603)

The maxilla and *palatine* form the majority of the palate in *A. minor* (Figs. 5C, 6C). The median one-third appears to preserve its natural arching toward the midline, whereas the lateral one-third on each side lies closer to the horizontal. Neither the vomer nor pterygoid are exposed in the midline as in *Simosuchus* (Buckley et al. 2000). A slit-shaped foramen opens on the maxilla. Canted along an anterolateral-posteromedial axis, opening anterolaterally, and associated with a small palatal fossa, the foramen is far from the alveolar margin and may not correspond to maxillary foramina associated with the alveolar margin in other notosuchians.

The *pterygoid* and *ectopterygoid* form the posterior portion of the palate, including the posteroventrally projecting mandibular rami. The distal end of this process is modestly expanded as in *Araripesuchus* and lies in its natural position adjacent to the adductor fossa of the lower jaw. The ectopterygoid overlaps the ventral aspect of the pterygoid on the lateral edge of the palate.

The suborbital fenestra, which is best exposed in the subadult skull (Sereno et al. 2003), is subequal in size to the paired choanae and located farther anteriorly. The palatine-pterygoid suture, preserved on the right side, courses across a broad palatal border lateral to the choanae. In the midline of the adult skull, the posterior one-half of the very thin choanal septum is exposed, the remainder covered from view by extraneous bone pieces. The choanae are located as far posterior on the pterygoids as possible, butting against a posterior palatal ridge formed by the pterygoids. During growth the sigmoid curve of the posterior palatal ridge in the subadult becomes a broad arch in the adult (Figs. 5C, 6C). Unlike in some other species of *Araripesuchus* (*A. gomesii*, *A. wegneri*), there is no development of a pair of parasagittal flanges extending from the posterior palatal ridge.

The *quadrate* angles posteroventrally from the recessed otic region toward the quadrate condyles. In the otic region, a large opening constitutes the fenestra ovalis and confluent cranioquadrate passage. Anterior to this opening is the preotic siphonium, ventral to which is a circular fossa (Fig. 7D) as in *Araripesuchus wegneri*.

A sharp vertical crest on the quadrate contributes to the posterior skull margin, joining the paroccipital process with the rim of the medial condyle. In posterior view,

a foramen aërum opens on the posterior aspect of the quadrate shaft just above the medial condyle (Fig. 8). In lateral view, the posterior margin of the quadrate angles anteroventrally as in *Simosuchus* (Buckley et al. 2000) rather than posteroventrally as in nearly all other crocodyliforms. The quadrate condyles are relatively flat and separated by a marked V-shaped cleft (Fig. 7D).

Braincase. The braincase is well preserved and exposed in the holotype and referred skulls (Figs. 5C, 6C). The *supraoccipital* forms a small median pitted triangle on the dorsal skull roof. On the occiput, the supraoccipital forms a short vertical nuchal keel with broad flanges extending to either side, more closely resembling that in *Simosuchus* than in *Araripesuchus*. The proatlantal elements are fused together forming an inverted chevron that is preserved in articulation with the protruding dorsal rim of the foramen magnum (Figs. 5B, 6B). The paroccipital processes project to each side, arching ventrolaterally to a sharp edge that connects the squamosal above and quadrate condyles below (Fig. 8). The ends of the paroccipital processes are marked by a series of striations or ridges as in *Araripesuchus* and extant crocodylians.

The ventrally deflected occipital condyle is formed almost exclusively by the *basioccipital*. The remainder of the bone angles anteroventrally at approximately 45° and forms most of the braincase floor posterior to the palate. A small posterior Eustachian

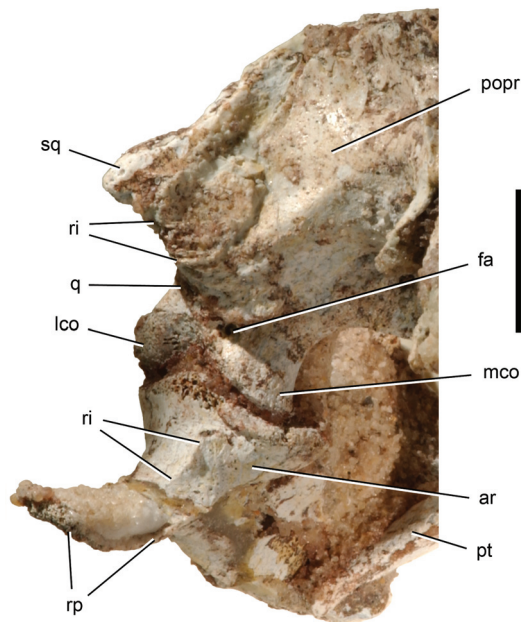


Figure 8. Skull of the crocodyliform *Anatosuchus minor*. Detailed view of the jaw articulation and retroarticular process in posteromedial view (MNN GAD17). Scale bar equals 1 cm. Abbreviations: *ar*, articular; *fa*, foramen aërum; *lco*, lateral condyle; *mco*, medial condyle; *popr*, paroccipital process; *pt*, pterygoid; *q*, quadrate; *ri*, ridge; *rp*, retroarticular process; *sq*, squamosal.

foramen is located in the midline just anterior to the occipital condyle. Farther anteriorly, a median crest rises (larger in the subadult skull), followed by a large anterior Eustachian foramen. This circular foramen opens posterodorsally between the basioccipital and basisphenoid. The lateral edges of the basioccipital curl against the medial edge of low basal tubera formed by the anterior extremity of the exoccipital.

A large lateral Eustachian foramen opens posterodorsally on the anterior side of each basal tuber between the *otoccipital* (exoccipital + opisthotic) and *basisphenoid*. As in *Araripesuchus*, four foramina are present adjacent to the occipital condyle, the largest an anteroventrally opening foramen for the internal carotid. Along the lateral edge of the braincase, a pair of low crests is present running anteromedially from the quadrate to the pterygoid. In lateral view, the otoccipital extends from the very large cranioquadrate passage anteriorly to the paroccipital process posteriorly, just separating the squamosal and quadrate (Figs. 5A, 6A). The basisphenoid has only a narrow, V-shaped ventral exposure. It floors a narrow depression between the pair of lateral crests and a small median patch between the basioccipital and the posterior margin of the palate.

Endocast. An endocast, generated from the computed-tomographic scan of cranium MNN GAD17 (Fig. 10), closely resembles that for *Araripesuchus* (Fig. 22). In both the cerebral hemispheres are spade-shaped as seen in dorsal view and measure ap-

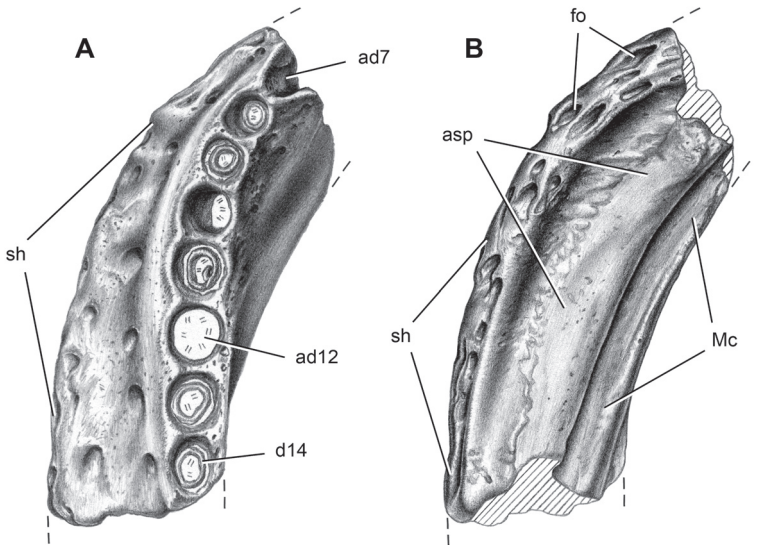


Figure 9. Dentary of the crocodyliform *Anatosuchus minor*. Pencil drawing of mid-section of the left dentary including alveoli 7–14 (MNN GAD18). **A** Dorsal view. **B** Ventral view (reversed). Parallel lines indicate broken bone; double-dash pattern indicates matrix. Scale bar equals 1 cm. Abbreviations: *ad7*, 12, alveolus of dentary tooth 7, 12; *asp*, articular surface for splenial; *d14*, dentary tooth 14; *fo*, foramen; *Mc*, Meckel's canal; *sh*, shelf.

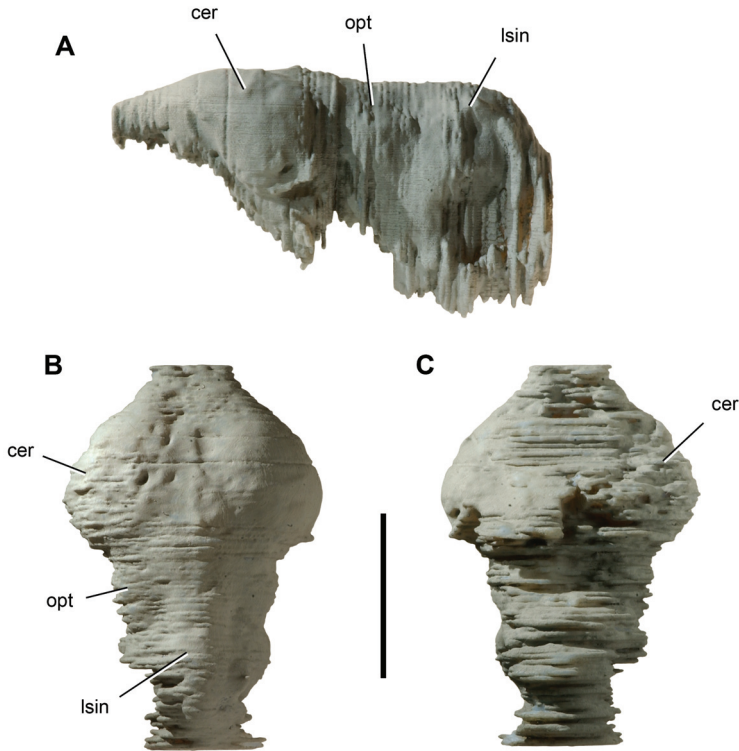


Figure 10. Endocast of the crocodyliform *Anatosuchus minor*. Endocast (UCRC PVC2) prototyped from a computed-tomography scan of skull MNN GAD18. The endocast lacks a portion of the pituitary fossa and right and left labyrinths. **A** Lateral view. **B** Dorsal view. **C** Ventral view. Scale bar equals 2 cm. Abbreviations: *cer*, cerebrum; *lsin*, longitudinal sinus; *opt*, optic lobe.

proximately one-half of total endocast length. In general the forebrain in the endocast compares more closely with that reported for *Sebecus* (Hopson 1979) than the more rounded, symmetrical cerebral hemispheres in *Alligator* (Fig. 11) or *Caiman* (Hopson 1979). A sagittal venous sinus flanked by shallow longitudinal depressions outlines the medial aspect of each hemisphere. In lateral view, the cerebral hemispheres are compressed dorsoventrally. In *A. minor* the posterior portion of the hemisphere is a little deeper than in *Araripesuchus wegneri*. In ventral view, the absence in *A. minor* of the ventromedian fossa between the hemispheres observed in *A. wegneri* may be an artifact of the quality of the scan. Swellings for optic lobes are visible posterior to the cerebral hemispheres. Although not well preserved in *A. minor*, the dorsal surface of the cerebellar region is near the height of the cerebral hemispheres.

Dentition. There are 6 premaxillary teeth, 19 maxillary teeth, and 21 dentary teeth, as established on the basis of the exposed teeth and a computed-tomographic scan of skull MNN GAD17. In a subadult skull (MNN GAD603), there are 6 premaxillary teeth,

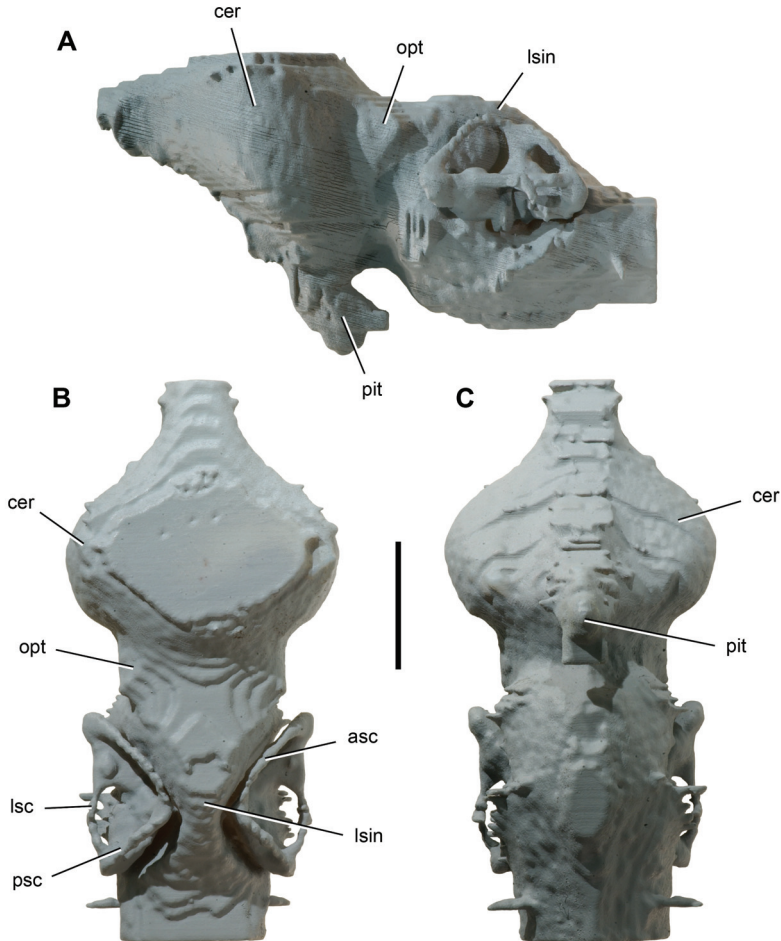


Figure 11. Endocast of *Alligator mississippiensis*. Endocast (UCRC PVC6) prototyped from a computed-tomography scan of a recent skull (TMM M-983). **A** Lateral view. **B** Dorsal view. **C** Ventral view. Scale bar equals 1 cm. Abbreviations: *asc*, anterior semicircular canal; *cer*, cerebrum; *lsc*, lateral semicircular canal; *lsin*, longitudinal sinus; *opt*, optic lobe; *pit*, pituitary fossa; *psc*, posterior semicircular canal.

15 maxillary teeth, and an unknown number of dentary teeth. Sereno et al. (2003) originally reported 5 premaxillary teeth in the subadult skull, although it is now clear that the first premaxillary tooth was broken away on both sides based on comparison with the adult skull. Premaxillary tooth number thus appears to be stable in the final 30% of growth in the skull, while maxillary and probably dentary tooth counts increase by a comparable percentage. The lower jaws and tooth rows become much more U-shaped during maturation. The diagnostic breadth of the snout and transverse orientation of the anterior ends of each dentary emerge late in post-hatching growth. On the other hand, the characteristic inclination of the anterior dentition from the midline to the

Table 4. Length (mm) of crowns in the right upper jaw of *Anatosuchus minor* (MNN GAD603). Parentheses indicate estimated measurement. Abbreviations: *m*, maxillary; *pm*, premaxillary.

Tooth	Length
pm1	2.3
pm2	2.7
pm5	3.7
pm6	3.8
m1	3.8
m2	5.5
m3	7.3
m4	(8.6)
m5	5.5
m12	(3.8)
m17	3.6

corner of the snout changes very little; the tooth row in anterior view of both subadult and adult skulls is angled at approximately 25° from the horizontal.

Upper and lower crowns are subconical with the base of the crown very slightly expanded from the root. The crowns curve lingually. There is no distinct neck or marked constriction between root and crown. All but the first premaxillary crown have unornamented mesial and distal carinae and very fine interweaving striae, which can be seen under strong magnification on the labial side of premaxillary and maxillary crowns. Tooth wear is not nearly as pronounced as in *Araripesuchus*. There are no wear facets and only a few crown tips with thinned enamel or exposed dentine from apical abrasion.

Six *premaxillary teeth* are one or two more than common among crocodyliforms. Pm1–3 project ventrally unopposed by dentary teeth, the first of which projects between pm3 and pm4. The tip of d4 projects dorsally into a fossa between pm6 and m1 (MNN GAD17, GAD603), a typical dental configuration among crocodyliforms. If the teeth at the junction of premaxilla, maxilla and dentary teeth are regarded as homologous with those in other crocodyliforms, additional premaxillary teeth must have been added to the original plesiomorphic tooth count of four or five teeth, beginning at the medial end of the tooth row.

The crown of pm1 is approximately 20% smaller than the crowns of pm2–6, lacks carinae, and is positioned lateral to the midline. The alveolar margins of opposing premaxillae are separated in the midline by a subtriangular gap, such that the opposing first premaxillary crowns are separated by a median diastema approximately twice that between ipsilateral premaxillary crowns.

Premaxillary teeth 2–6 are very similar in size and crown detail. The alveoli of all premaxillary teeth are raised as rugose cylinders. The inner set of alveoli (pm1–3) are separated by concave intercrown festoons, whereas the raised rim of the alveolus in the outer set (pm4–6) are linked together by a rugose alveolar ridge. The festooning of the inner set, thus, is the result of the concave margin between alveoli; festooning in the

outer set and in the maxillary series, by contrast, is the result of the dorsally concave labial rim of the alveoli (Fig. 7B).

The mesial premaxillary crowns (pm1–3) are functionally distinctive. They oppose a prominent edentulous edge of the dentary, which is 9 mm in transverse width in the adult skull. As confirmed by computed tomography, the first dentary tooth is positioned 11 mm from the dentary symphysis. That tooth (d1) projects toward the base of the fourth premaxillary alveolus. Successive dentary crowns (d2–4) project toward small circular fossae between pm5 and pm6 and into a large palatal opening, respectively. The palatal opening is visible on both available skulls and possibly connected with the nearby premaxilla-maxilla foramen. Given that a similarly positioned fossa in *Araripesuchus* receives the tip of the caniniform fourth dentary tooth, the dental and palatal relationships in *A. minor* appear to be modified from that observed in other notosuchians.

The *maxillary teeth* have crowns that are more closely spaced than the premaxillary teeth with alveoli that begin to coalesce toward the distal end of the tooth row. The first maxillary crown is approximately 20% larger than the sixth premaxillary crown. Crown size reaches its maximum in m4 at the depressed corner of the snout, distal to which it gradually decreases (m5–20). A caniniform crown is not differentiated. All maxillary crowns curve lingually with carinae that are shifted lingually. Were the crown to be split by a plane through the carinae, the labial portion would comprise most of crown volume.

The *dentary teeth* are more poorly exposed. Crown shape seems similar to that in the maxilla and they equal opposing maxillary crowns in size. Crown size reaches its maximum in d11–13 at the depressed corner of the snout (Fig. 8A), distal to which it gradually decreases (d14–21). A caniniform crown is not differentiated, and the dentary series ends mesial to the maxillary series; tooth d21 opposes m14 or m15, leaving at least m16–20 free of opposing dentary crowns. The differential between upper and lower tooth rows in *A. minor* is greater than that in *Araripesuchus*.

Lower jaw. The lower jaw broadens significantly during growth, gaining its distinctive U-shape with maturity. This shape is similar to that in the lower jaws of mature individuals of *Simosuchus* as seen in dorsal view (Buckley et al. 2000). The lower jaw in *A. minor*, however, is anteroposteriorly nearly twice as long as its maximum width; in *Simosuchus* jaw length and width are subequal. The profile of the lower jaw differs from that in either *Simosuchus* or *Araripesuchus*. With jaws abducted, the anterior portion of the lower jaws fits within the snout and is obscured in lateral view (Figs. 5A, 6A). The lateral ramus of the dentary gradually increases in depth to a point ventral to the postorbital bar and dorsal to the external mandibular fenestra, after which it tapers rapidly to an elongate, narrow retroarticular process.

The *dentary* has an immobile interdigitating symphysis with its opposite in the midline. The medial 9 mm of the dentary projects anterodorsally at about 45° with an articular edge for the premaxillary palate that protrudes to the height of adjacent dentary crowns. In ventral view, the process has a gently convex articular edge in contact with the premaxillary palate. In cross-sectional views derived from the computed-

tomographic scan, the edentulous margin appears to narrow to a sharp cutting edge. This masticatory structure has no parallel among other crocodyliforms (Figs. 5C, 6C).

Lateral to the median process, the dentary decreases in width and twists into a subhorizontal plane as it approaches the corner of the snout. As it turns the corner, it becomes broader transversely than deep, a very unusual proportion and quite different from *Simosuchus* (Buckley et al. 2000). Much of the additional width is due to the highly vascularized dentary shelf, which extends lateral to the scalloped alveolar margin (Fig. 9). In ventral view, Meckel's canal lies in a groove along the medial edge, lateral to which is a broad articular surface for the splenial (Fig. 9B).

The dentary extends posteriorly, its deep posterodorsal ramus forming the anterior portion of the coronoid process and anterodorsal margin of the external mandibular fenestra. There is a small triangular posteroventral ramus that terminates on the angular ventral to the external mandibular ramus, as evident in several species of *Araripesuchus* (Price 1959).

The *splenial* contributes to the median symphysis anteriorly (Figs. 5A, 6A). Its posterior margin at the symphysis is damaged in the adult skull. In the subadult skull there is some development of a posteromedian thickening; it seems likely there was a posteromedian splenial “peg” in the adult as in many other notosuchians. In *Simosuchus* the posteromedian eminence is formed by the dentary, as the splenial approaches but fails to reach the symphysis. The splenial extends laterally from the symphysis as a thin sheet of bone with a near horizontal orientation, similar to that of the dentary. That orientation is maintained around the corner of the lower jaw, after which a vertical ramus expands across the medial side of the dentary. A large oval foramen opens on the transverse ramus of the splenial and continues as a groove medially toward the posterior margin of the symphysis.

The *surangular* extends from the jaw articulation anterodorsally along the top of the coronoid process, a ramus that is swollen laterally with pitted ornamentation except where it bounds the external mandibular fenestra (Fig. 7D). It appears to form the lateralmost portion of the jaw articulation, after which it continues as a slender unornamented process between the articular and angular to the tip of the long retroarticular process (Fig. 7D). The *angular* also has raised pitted ornamentation except for the portion contributing to the margin of the external mandibular fenestra (Fig. 7D). It extends as a slender unornamented process to the tip of the retroarticular process.

The *articular* forms the saddle-shaped glenoid for the quadrate condyles (Fig. 8). The surface is transversely convex to accommodate the cleft between the condyles and gently concave anteroposteriorly, the medial socket situated farther ventrally than the lateral socket. There is no anterior or posterior lip to the glenoid. The shape of the quadrate condyles and accommodating surface on the articular is similar to that in *Araripesuchus*. In posterior view, there is a prominent attachment crest ventral to the jaw joint. The articular extends to the tip of the slender, dorsoventrally flattened retroarticular process, which is twisted to face dorsomedially.

Axial skeleton. The axial skeleton is preserved in articulation from the proatlas to the fifteenth dorsal vertebra. This is one of the most complete presacral series available for any

notosuchian. The axial column is well exposed immediately posterior to the skull and partially exposed, mainly in right lateral view, more posteriorly. Because this is one of the rare specimens that also shows the relationship between the osteoderms and vertebrae, we left all bones in place during preparation and obtained a computed-tomographic scan to observe details hidden from view. A subadult specimen of *Araripesuchus gomesii* is the other notable basal metasuchian preserving a complete cervicodorsal column (Hecht 1991).

Extant crocodylians have a proatlas, 8 cervical vertebrae and 16 dorsal vertebrae (Mook 1921). The ribs for C3–7 are short, overlapping, and parallel the vertebral column. The rib for C8 angles posteroventrally and is transitional to longer, broader-shafted dorsal ribs. There are typically 16 dorsal vertebrae in extant crocodylians (Chiasson 1962). Hecht (1991: 346) suggested there were “about seven cervicals” and 17 dorsal vertebrae (thoracic and lumbar) in the subadult specimen of *Araripesuchus gomesii*. The vertebra that would be the eighth cervical, however, is partially covered by the scapula. Its rib is transitional in form between the short cervical and long dorsal rib, which is typical of the eighth cervical rib in extant crocodylians (Mook 1921). A similar vertebral formula and transitional rib has recently been reported in *Araripesuchus tsangatsangana* (Turner 2006). The axial column in *A. minor* also appears to have 8 cervical vertebrae and probably 16 dorsal vertebrae. Only 15 dorsal vertebrae are preserved, but a sixteenth may be inferred from the position of the sacral vertebrae, which is based on the position of the associated hind limb (Fig. 4). Cervical centra are amphiplatan and lack hypapophyses. Dorsal centra become amphicoelous.

This vertebral formula differs from that described recently in the notosuchian *Notosuchus*. This genus may possess as many as 10 cervical vertebrae, 19 dorsal vertebrae, and 3 sacral vertebrae (Pol 2005; Fiorelli and Calvo 2008). The cervicodorsal column, thus, has 29 rather than 24 vertebrae and the sacrum 3 rather than 2 vertebrae.

A *proatlas* is preserved in articulation with the occiput in *A. minor*. It is an inverted V-shaped median element with a dorsal keel similar to that in extant crocodylians (Mook 1921). The *proatlas* in *A. minor* appears to be somewhat larger relative to the *atlas*, which is composed of separate, paired neural arches and an intercentrum. The transverse width of the *proatlas* is greater than that of the atlantal neural arches.

The *axis* has a low subrectangular neural spine that projects only slightly posterior to the centrum as in extant crocodylians (Mook 1921; Chiasson 1962). *Cervical vertebrae* three through eight have tall anteriorly tilted neural arches and vertical neural spines as described in the *Notosuchus* (Pol 2005). The neural spine in C3 is subrectangular, about twice as tall as long. The neural spine in C7 is considerably taller and narrower, about five times as tall as long. Tall neural arches may characterize notosuchians (Pol 2005).

The *dorsal vertebrae* are somewhat longer relative to their width in *A. minor* than in *Araripesuchus gomesii* (AMNH 24450; Hecht 1991). The broadest width in both taxa occurs in the posterior dorsal vertebrae, which have long transverse processes (Fig. 4). In *A. minor* maximum width across the transverse processes is approximately twice centrum length, whereas in *A. gomesii* maximum width is about three times centrum length. In both genera, the parapophysis migrates out onto the transverse process anterior to the diapophysis (D9–11), eventually coalescing to form a single rib articulation

(D12), as in extant crocodylians. Similar elevation and fusion of the parapophysis does not appear to occur in *Notosuchus* (Pol 2005; Fiorelli and Calvo 2008).

The straight *ribs* of the atlas and axis are preserved on the left side (Fig. 12). The shorter triradiate ribs of C3–8 are preserved on the right side in articulation with each other. After they clear the paravertebral shield, the shafts of the anterior dorsal ribs bend ventrally and expand slightly to form a flange along their anterior margin as in *A. gomesii* (Hecht 1991) and *A. tsangatsangana* (Turner 2006). In the posterior dorsal ribs, the capitulum and tuberculum lie in the same plane and eventually coalesce into a single head. *Gastralia* are preserved ventrally between the girdles (Fig. 4). There do not appear to be any ventral osteoderms in *A. minor*.

Parasagittal rows of *osteoderms* are preserved above the cervicodorsal column, with each pair joining its opposite in the midline along an interdigitating suture (Fig. 12; Table 5). Articulation between successive rows of osteoderms is limited to overlap by the posterior edge of a given osteoderm with the anterior edge of the successive ipsilateral osteoderm. As in *Araripesuchus* (Hecht 1991; Turner 2006), there is no development of anteromedial processes as is common among basal crocodylomorphs, and the

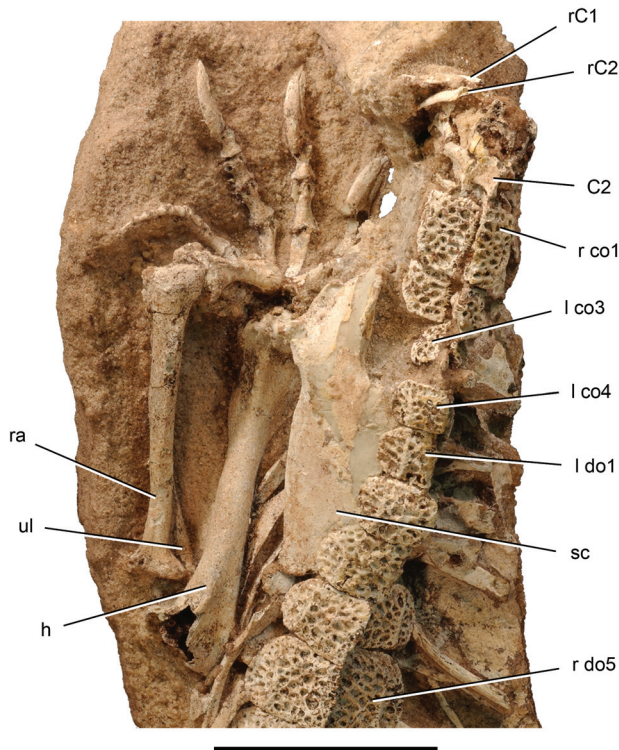


Figure 12. Pectoral girdle and forelimb of the crocodyliform *Anatosuchus minor*. Left pectoral girdle, forelimb and anterior portion of the paravertebral shield (MNN GAD17) in dorsal view. Scale bar equals 5 cm. Abbreviations: C2, axis; co1, 3, 4, cervical osteoderm 1, 3, 4; do1, 5, dorsal osteoderm 1, 5; h, humerus; l, left; r, right; ra, radius; rC1, atlantal rib; rC2, axial rib; sc, scapula; ul, ulna.

overlap within each parasagittal column of osteoderms is a narrow smooth articulation limited to the edges of the dorsal series.

No osteoderms are positioned over the proatlas, atlas or axis (Fig. 12). Four paired cervical osteoderms are associated with C3–8 and 12 osteoderms are positioned over D1–12. Osteoderms distal to the twelfth were weathered away. The first cervical osteoderm is the largest of the cervical series and articulates over the neural spines of C3–5. It has a trapezoidal shape with a broader anterior end and a low keel that is most promi-

Table 5. Dimensions (mm) of the skeleton of *Anatosuchus minor* (MNN GAD17). Measurements of individual bones are from the left side, except for dorsal osteoderm 12 (preserved only on the right side). Parentheses indicate estimated measurement. Ungual length is measured along longest chord from base to tip.

Bone	Measurement	Length
Axial skeleton	Cervical vertebral series, length	(75.0)
	Dorsal vertebral series, length	(268.0)
	Cervical osteoderm 1, maximum length	16.0
	" " 2, " "	11.5
	" " 3, " "	9.6
	" " 4, " "	9.9
	Dorsal osteoderm 1, maximum length	11.2
	" " 2, " "	12.6
	" " 3, " "	14.4
	" " 4, " "	15.3
	" " 5, " "	16.6
	" " 6, " "	17.3
	" " 7, " "	18.6
	" " 8, " "	18.9
	" " 9, " "	18.3
	" " 10, " "	19.2
	" " 11, " "	18.2
	" " 12, " "	18.7
Scapula	Maximum length	68.2
	Neck, minimum dorsoventral height	15.2
Coracoid	Distal width	(23.0)
Humerus	Maximum length	80.8
	Minimum shaft diameter	7.5
Radius	Maximum length	69.3
	Maximum proximal width	13.6
	Maximum distal width	13.4
	Minimum shaft diameter	4.1
Radiale	Maximum length	23.0
	Maximum proximal width	13.8
	Maximum distal width	10.8

Bone	Measurement	Length
Manus	Metacarpal 1 length	13.0
	Phalanx I-1 length	9.3
	Phalanx I-3 (ungual) length	18.6
	Phalanx II-1 length	11.1
	Phalanx II-2 length	8.0
	Phalanx II-3 (ungual) length	19.6
	Phalanx III-1 length	10.0
	Phalanx III-2 length	6.9
	Phalanx III-3 length	6.0
	Phalanx III-4 (ungual) length	17.0
	Phalanx IV-1 length	9.7
	Phalanx IV-2 length	6.7
	Phalanx IV-3 length	5.3
	Phalanx IV-4 length	5.1
	Phalanx IV-5 length	4.2
	Phalanx IV-6 length	3.4
Pes	Phalanx II-3 length	12.5
	Phalanx III-2 length	11.8
	Phalanx III-3 length	8.3
	Phalanx III-4 (ungual) length	8.0
	Phalanx IV-2 length	10.2
	Phalanx IV-3 length	6.9
	Phalanx IV-4 length	5.4

nent on the posterior one-half of the osteoderm. As in the other cervical osteoderm rows, there is some asymmetry in the paired plates. The keel in the first cervical osteoderm row is laterally displaced on the left but centered on the right side. The second cervical osteoderm is smaller and articulates with the neural spine of C6. Its shape is similar to the first cervical osteoderm, the keel now reduced to a swelling along the rounded posterolateral corner on the left side or centered on the right side. The third cervical osteoderm is the smallest among all preserved and articulates with the neural spine of C7. It is subtriangular on the left and subquadrate on the right and does not have a keel. The fourth and final cervical osteoderm is slightly larger than the third cervical osteoderm and has a shape reminiscent of many of the succeeding dorsal osteoderms. The laterally displaced keel is low and set back from the anterior margin of the plate. The lateral corners of the plate are rounded, the anterolateral corner more so than the posterolateral corner. There is no overlap between the last cervical and first dorsal osteoderm. The cervical osteoderms would allow considerable lateral and dorsoventral flexibility of the cervical series as may have been needed during foraging on land or subaquatic feeding.

The dorsal osteoderms have a one-to-one relationship with underlying dorsal vertebrae as described in extant crocodylians (Ross and Mayer 1984) (Figs. 4, 12). Each

dorsal osteoderm contacts the neural spine of its respective vertebrae, extends posteriorly across the interspinous gap, and rests on the anterior portion of the successive neural spine. This is well exposed in the middle of the dorsal series, where the right column of osteoderms is displaced ventrally against the transverse processes, exposing the natural articulation between the neural spines and the left column of osteoderms. The junction between the osteoderms appears to be positioned so as to coincide functionally with the joints between the centra to enhance mobility of the trunk (Salisbury et al. 2006).

The first dorsal osteoderm closely resembles the last cervical osteoderm but is slightly larger and extends over the leading edge of the successive osteoderm. Each dorsal osteoderm has a smooth beveled leading edge approximately 1.75 mm broad for articulation with the next anterior osteoderm. The sculpted pitting is reduced in a narrow parallel band of slightly greater width adjacent to the leading articular surface. Dorsal osteoderms 2–12 are more flexed than more anterior osteoderms, the portion of the plate lateral to the keel deflected ventrally. The keel remains parallel to the midline across the series. Osteoderm length gradually increases until about the middle of the series (Table 5). Osteoderm shape remains very similar throughout the series, the rounding of the anterolateral corner somewhat less in posterior dorsal osteoderms.

Appendicular skeleton. The left pectoral girdle and forelimb and portions of the left tibia, fibula and pedal phalanges are preserved in association with the adult skull (Figs. 3, 11; Table 5). The left *scapula* has broad proportions comparable to those in *Araripesuchus gomesii* (Hecht 1991). The blade does not appear to flare as strongly distally as in *A. tsangatsangana* (Turner 2006). The distal end of the blade is tucked under the edge of the anterior dorsal osteoderms as in extant crocodylians (Fig. 12). The elongate coracoid is exposed distally near its contact with the interclavicle.

The *humerus* has a straight shaft and gracile proportions, with shaft diameter less than 10% of its length (Turner 2006) (Table 5). The deltopectoral crest is directed anteriorly, and the fossa for the olecranon process is well developed distally as in *Araripesuchus* (Hecht 1991; Turner 2006). The proximal end of the *radius* is strongly flared, measuring more than twice mid-shaft diameter. Flaring of the proximal end of the radius to this degree is also present in *Araripesuchus* (Fig. 25B) and *Notosuchus* (Pol 2005). The radius is shorter than the *ulna*, because the ulna extends along the lateral side of the radiale. The ulna in *A. minor* is only partially exposed, its shaft noticeably curved. The differential in length between the radius and ulna is about 10%, as preserved in articulation in *Araripesuchus* (Fig. 25B). The *radiale* is a very robust bone in *A. minor*, its shaft just slightly less robust than the mid-shaft of the radius (Fig. 13A). The broad lateral facet for the ulna on the proximal end confirms the offset in the joint between the forearm bones (radius, ulna) and the proximal carpals (radiale, ulnare). From the radiale, it is clear that this offset is also present in *A. tsangatsangana* (Turner 2006) and *Notosuchus terrestris* (Pol 2005). Very little of the ulnare is not exposed in *A. minor*, but the bone would have been considerably smaller than the radiale. The offset at the forelimb-carpus joint, the general robustness of the radiale, and the differential

in robustness between the radiale and ulnare are primitive for Crocodylomorpha, given their presence in *Terrestrisuchus* (Crush 1984), *Hesperosuchus* (Clark et al. 2000), *Dibothrosuchus* (Wu and Chatterjee 1993), *Junggarsuchus* (Clark et al. 2004), and *Protosuchus* (Colbert and Mook 1951), although often muted in extant crocodylians (Mook 1921).

The *manus* is well preserved and exposed (Fig. 13A). As in *A. wegeneri* (Fig. 26A), the metacarpals and phalanges have well developed distal condyles marked by dorsal extensor pits. The *manus* is very large relative to the forearm. Digit three is approximately 80% the length of the radius, whereas in other terrestrial crocodylomorphs that percentage is between 50 to 60% (Mook 1921; Colbert and Mook 1951; Crush 1984; Wu and Chatterjee 1993; Clark et al. 2000; Clark et al. 2004). Besides its size, two other features of the *manus* are unusual. Digit IV has six phalanges, two more than is usual among crocodylomorphs (Fig. 13B). Total length of the phalanges of digit IV is approximately 80% the length of the phalanges of digit III, a typical crocodylian proportion. Much of the length of the phalanges of digits I–III is due to elongate unguals. The phalanges of digit IV are longer than the nonungual phalanges of digit III. The unguals of the inner digits are unusually long. The unguals have a narrow attachment groove that extends toward from the base to the tip (Fig. 13B). This groove converges with the dorsal margin of the ungual. The ventral margin is arched proximally and straight distally toward the tip. These unusual features, which are absent in the more typical *manus* in *Araripesuchus wegeneri* (Fig. 26A), are indicative of specialized function.

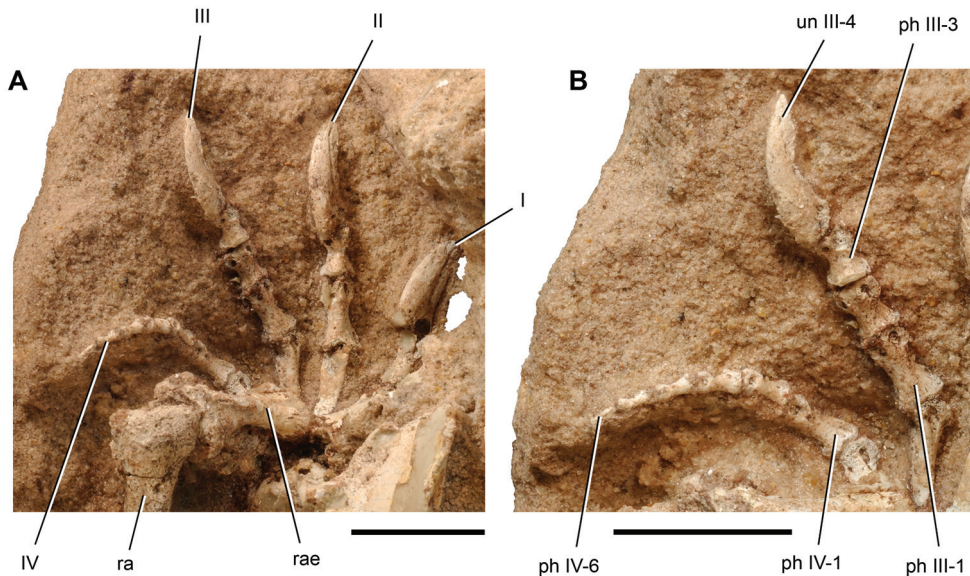


Figure 13. Manus of the crocodyliform *Anatosuchus minor*. Left carpus and manus (MNN GAD17). **A** Left carpus and manus in dorsal view. **B** Left manual digits III and IV in dorsomedial view. Scale bars equal 2 cm. Abbreviations: *I–IV*, digits I–IV; *ph*, phalanx; *ra*, radius; *rae*, radiale; *un*, ungual.

Araripesuchus Price, 1959

Referred species. *A. gomesii* (Price 1959), *A. wegneri* (Buffetaut and Taquet 1979), *A. patagonicus* (Ortega et al. 2000), *A. buitrerensis* (Pol and Apesteguía 2005), *A. tsangatsangana* (Turner 2006).

Revised diagnosis. Small-bodied metasuchians with autapomorphies including (1) trapezoidal snout cross-section just anterior to the orbit in which the lacrimal is split between dorsal and lateral rami; (2) premaxilla external surface smooth with ornamentation limited to the distal end of the ascending ramus; (3) presence of one or two neurovascular foramina opening anterolaterally or anteroventrally just posterior to the narial fossa; (4) premaxillary teeth 1–4 aligned in a straight row; (5) maxillary postcaniniform alveolar margin dorsally arched; (6) smooth buccal emargination on lateral maxillary and dentary alveolar margins adjacent to postcaniniform teeth; (7) confluent alveoli for postcaniniform maxillary and mid- and posterior postcaniniform dentary teeth; (8) medial alveolar wall absent along mid- and posterior postcaniniform dentary teeth with root crypts enclosed medially by the splenial.

Discussion. The monophyly of the genus *Araripesuchus* has been controversial. Some features that were initially thought to be diagnostic for the genus were discovered to have broader distributions among notosuchians such as *Uruguaysuchus*. The generic assignment of one species in particular, *A. wegneri*, has been questioned (Ortega et al. 2000). Comparison among species has been difficult due to incomplete specimens and descriptions. The dentition, for example, is critical for evaluation of species and generic distinction, but the morphology of a relatively fresh (unworn) dentition is not available for most species within *Araripesuchus* or immediate outgroups (e.g., *Uruguaysuchus*). Here we describe derived features that may unite some or all of the species in the genus *Araripesuchus*.

The geometric shape of the cross-section at the base of the snout (Ortega et al. 2000) involves a distinct flexure in the body of the lacrimal that gives the snout a trapezoidal cross section just anterior to the orbit. The vertical portion of the lacrimal is not broadly exposed in dorsal view of the skull (Figs. 14B, 15B). The lacrimal is gently arched and broadly visible in dorsal view in most short-snouted notosuchians, such as *Mariliassuchus* (Zaher et al. 2006), or long-snouted neosuchians, such as *Hamadasuchus* (Larsson and Sues 2007). The lacrimal in *Uberabasuchus* (Carvalho et al. 2004) and *Stolokrosuchus* (Larsson and Gado 2000) are closest in form to that in *Araripesuchus*.

Most of the premaxilla is smooth and lacks the rugose texture and small foramina typical of other regions of the snout in the vast majority of crocodyliforms. Only the tip of the ascending ramus is textured, as it curves onto the dorsal aspect of the snout tapering between similarly textured surfaces of the nasal and maxilla (Fig. 16A). The body of the premaxilla is also smooth in *A. gomesii* (Price 1959: pl. 1) and *A. tsangatsangana* (Turner 2006: fig. 20), whereas the condition in *A. patagonicus* (Ortega et al. 2000) and *A. buitrerensis* (Pol and Apesteguía 2005) remains poorly known.

Two large neurovascular foramina open on the lateral surface of the premaxilla on a smooth surface just posterior to a depression (narial fossa) and just anterior to the premaxilla-maxilla foramen (Fig. 15A). The same pair are present in the same position

in *A. gomesii* (AMNH 24450; Hecht 1991), although there appears to be only a single large foramen in the smaller species *A. tsangatsangana* (Turner 2006: figs. 19, 20). In other genera, such as *Hamadasuchus* (Larsson and Sues 2007: fig. 3) or *Stolokrosuchus* (Larsson and Gado 2000), small foramina are often present but are not relatively as large, isolated, or located on a smooth surface related to the margins of the narial fossa.

The straight, rather than labially convex, arrangement of alveoli 1–4 in the premaxillary tooth row is unusual. The external profile of the alveolar margin of the premaxilla, likewise, is also straight or even slightly concave in ventral view (Figs. 13C, 14C). This feature is currently known in *A. wegneri*, *A. gomesii* (Price 1959; Turner 2006; AMNH 24450), and *A. tsangatsangana* (Turner 2006). A similar premaxillary margin was very likely present in a new species of *Araripesuchus* described below, given the opposing straight, anteromedially oriented margin at the anterior end of the dentary (Figs. 27C, 28). In *A. tsangatsangana* the alveolar margin of the premaxilla is gently concave (Turner 2006: fig. 49A), and the corresponding anteriormost dentary teeth also have a straight, rather than curved, alignment [Turner 2006: fig. 41A]. This unusual feature may eventually be shown to characterize other closely related notosuchians, such as *Libycosuchus*, which shows a similar condition (Stromer 1914). In *Uruguaysuchus* the premaxillary margin is not well described but has been shown as gently convex (Rusconi 1933; Price 1959). *Anatosuchus* (Figs. 5, 6), *Uberabasuchus* (Carvalho et al. 2004), *Hamadasuchus* (Larsson and Sues 2007) and most other crocodyliforms show the plesiomorphic condition; a line drawn through the centroids of the premaxillary crowns arches from the midline to the lateral aspect of the snout.

The postcaniniform alveolar margin on the maxilla is dorsally arched, above which is a smooth buccal emargination (Figs. 14–16). Both features characterize *Araripesuchus*. Although in some other crocodylomorphs the alveolar margin of the maxilla is sinuous, the portion distal to the caniniform that is dorsally convex is limited to several crowns and followed by a margin that is ventrally convex, as in *Hamadasuchus* (Larsson and Sues 2007). *Araripesuchus* is distinctive because the entire postcaniniform series has a dorsally convex margin (Figs. 14A, 15A). This appears to be related to the enlargement of the opposing dentary teeth (Fig. 20A); when the enlargement of opposing crowns is more limited, the arching of the maxillary series is more subtle, as in *A. patagonicus* (Ortega et al. 2000) and *A. tsangatsangana* (Turner 2006). In *Uruguaysuchus* the postcaniniform series also appears to be very gently arched and may ultimately share this feature with *Araripesuchus*. The buccal emargination is also present on the dentary dorsal to a row of neurovascular foramina (Figs. 18A, 31A). As discussed below, there may have been a fleshy cheek margin functioning for temporary storage during mastication parallel to that in basal ornithischian and sauropodomorph dinosaurs (Taquet 1976).

As discussed most notably by Pol and Apesteguía (2005), the alveoli are confluent for postcaniniform maxillary and for mid- and posterior postcaniniform dentary teeth in *Araripesuchus*. In other words, the posterior two-thirds of both upper and lower dentitions, have incompletely divided alveoli. This is well preserved in the upper and lower jaws of *A. wegneri* (Figs. 14C, 15C, 16C, 19B, 20A, 21B, 27C). In the maxilla,

medial and lateral walls of the alveoli extend ventrally to an equal degree, so the incomplete septa separating the alveoli are best seen in ventral view (Figs. 14C, 15C, 16C). A similar condition may be present in the reduced postcaniniform series in *Libycosuchus* (Stromer 1914) as well as some other basal metasuchians, although more comparative detail is needed. In *Notosuchus* the alveolar septa are incomplete along the entire upper tooth row (Lecuona and Pol 2008).

In the dentary, the lateral alveolar margin is much taller than the medial margin, so the incomplete septa separating the alveoli are broadly visible in medial view of a disarticulated dentary (Figs. 18B, 21B, 27B). The lack of a medial wall enclosing these alveoli is a remarkable feature. The crypts for the roots of the mid- and posterior postcaniniform teeth in the dentary are actually enclosed medially by the splenial in *Araripesuchus* (Pol and Apesteguía 2005). This condition does not appear to be present in the stout mandibular rami of *Libycosuchus* (Stromer 1914).

Several features used previously to distinguish *Araripesuchus* (Ortega et al. 2000; Pol and Apesteguía 2005; Turner 2006) clearly have a broader distribution among genera that may be closely related within Notosuchia. These include teeth showing marked differentiation of tooth type into anterior incisiforms with bulbous subconical crowns, caniniforms, and squat postcaniniforms; a sharp transition in tooth form between the upper caniniform tooth (m3) and smaller and similar sized, squat-crowned, denticulate postcaniniforms; the presence of a basal constriction between crown and root in most teeth; and inclined denticles along the carinae of many upper and lower teeth. All of these features are present, for example, in *Uruguaysuchus* (Rusconi 1933) and *Uberabasuchus* (Carvalho et al. 2004), both of which may fall within Notosuchia.

The lateral bulge at the anterior end of the maxilla (Pol and Apesteguía 2005) is filled by the root of the maxillary caniniform (m3), as seen in a computed-tomographic scan of the cranium (Fig. 17C). Thus the degree of bulging in the maxilla of *Araripesuchus* is related to the relative size of the caniniform, as it is in many crocodyliforms. Interpreted in this manner, this feature is not restricted to *Araripesuchus* but has a much broader distribution. The corresponding bulge in *Hamadasuchus*, for example, occurs somewhat farther posteriorly, corresponding to the more posterior position of the caniniform (Larsson and Sues 2007).

The jugal ascending ramus diverges at a point posterior to the midpoint of the ventral rami in *Araripesuchus* (Pol and Apesteguía 2005), a feature also present in *Anatosuchus* (Figs. 5A, 6A) and *Uberabasuchus* (Carvalho et al. 2004). The ascending ramus, in contrast, is positioned at the midpoint of the ventral rami in *Uruguaysuchus* (Rusconi 1933) and many other basal crocodyliforms. The interpretation of this feature as a synapomorphy uniting species of *Araripesuchus* (Pol and Apesteguía 2005) thus is not clear.

Several features have an uncertain distribution or polarity to function as unambiguous synapomorphies uniting species of *Araripesuchus*. *A. wegneri*, *A. gomesii* (Price 1959) and *A. tsangatsangana* (Turner 2006) have five premaxillary teeth whereas *A. patagonicus* (Ortega et al. 2000) has four, a more common condition among crocodyliforms. A prominent wedge-shaped posteroventral (quadrate) process on the pterygoid

characterizes *A. wegeneri* (Figs. 14C, 15C, 16C, 17C) and *A. gomesii* (Price 1959) but is absent in *A. patagonicus* (Ortega et al. 2000) and *A. tsangatsangana* (Turner 2006). The polarity of this character is uncertain. The choanal septum has a flat ventral surface and T-shaped cross-section in *A. patagonicus*, but the condition in other species of *Araripesuchus* seems variable; the septum is flattened to a lesser degree in *A. buitrerensis* and a subadult specimen of *A. gomesii* (Pol and Apesteguía 2005) and is present as a narrow strut with a rounded ventral edge in *A. wegeneri* (Figs. 14C, 15C) and a mature specimen of *A. gomesii* (Price 1959).

Araripesuchus wegeneri Buffetaut & Taquet, 1979

Figs. 14–26

Tables 6–8

Buffetaut and Taquet (1979, fig. 1)

Ortega et al. (2000, fig. 9)

Turner (2006, figs. 5–7)

Holotype. MNHN GDF700; snout composed of articulated upper and lower jaws and preserved to mid-orbit on the right side with several teeth preserving their crowns.

Type locality. Gadoufaoua, Agadez District, Niger Republic (more precise locality unknown) (Fig. 1A, C).

Horizon. Elrhaz Formation, Tegama Series; Lower Cretaceous (Aptian-Albian), ca. 110 Mya (Taquet 1976).

Referred material. MNN GAD19, nearly complete cranium lacking only portions of the left lacrimal and prefrontal, the palpebrals, and some of the teeth (Figs. 14–17, 19); MNN GAD20, partial skeleton on block preserving the left side of the skull exposing the dentition in medial view and an articulated tail with dermal armor (Figs. 20, 21, 25A); MNN GAD21, partial skeleton on block preserving the ventral portion of the skull, an articulated partial forelimb, and an articulated tail with dermal armor (Fig. 24, 25B); MNN GAD22, partial skeleton on block preserving the ventral portion of the skull, an articulated right manus and pes, a right calcaneum, and an articulated tail with dermal armor (Fig. 26); MNN GAD23, isolated snout on block composed of articulated upper and lower jaws and preserved to mid-orbit on the right side; MNN GAD24, isolated left maxilla on block preserving the dentition; MNN GAD25, partial skeleton preserving the posterior ends of the lower jaws and most of the postcranial skeleton except the tail; MNN GAD26, edentulous right dentary from a juvenile (Fig. 18).

An exceptional series of specimens are preserved in close proximity on a single block of sandstone (MNN GAD20–24) (Fig. 23). Three individuals are fairly complete, partially articulated skeletons with their axial columns aligned side-by-side pointing in the same direction (MNN GAD20–22). One of the three (MNN GAD20) is slightly smaller than the other two. Also present are portions of at least two additional individuals, one represented by an articulated snout (MNN GAD23) and the other by an isolated maxilla (MNN GAD24). A minimum of five individuals thus are represented on the block.

Table 6. Measurements and proportions of forelimb elements of *Anatosuchus minor* (MNN GAD17), *Araripesuchus wegneri* (MNN GAD21, GAD25), *Alligator mississippiensis* (FMNH 22027), and *Crocodylus johnstoni* (FMNH 223669). Measurements are from the left side in *A. minor* and *A. wegneri* and from an average of left and right sides in *A. mississippiensis* and *C. johnstoni*. Measurements in *A. wegneri* are based on two partial forelimbs with radii of identical length (MNN GAD21, GAD25); only one preserved the humerus (MNN GAD25). Estimated measurements for metacarpal 3 in *A. minor* and *A. wegneri* are based on measurements of metacarpal 1 and 2, the former approximately 15% shorter and the latter slightly longer than metacarpal 3 (Mook 1921). Parentheses indicate estimated measurement.

	<i>Anatosuchus minor</i>	<i>Araripesuchus wegneri</i>	<i>Alligator mississippiensis</i>	<i>Crocodylus johnstoni</i>
Measurements (mm)				
Humerus	80.8	66.0	187.8	58.6
Radius	69.3	50.7	124.8	37.2
Radiale	23.0	20.4	35.2	9.6
Metacarpal 3	(15.0)	(13.0)	45.7	12.7
Ratios (%)				
Radius/humerus	86%	77%	67%	64%
Radiale/radius	33%	40%	28%	26%
Radiale/metacarpal 3	153%	157%	77%	76%

The close proximity and alignment of the three best preserved skeletons and the presence of additional individuals on a small block is unusual. Portions of the three best preserved skeletons (MNN GAD20–22) and the isolated snout (MNN GAD23) have been lost to postmortem surface erosion and would have been more complete. Some postmortem disarticulation is evident in all three of the most complete specimens (MNN GAD20–22), although there is no obvious preferred direction or orientation to displaced elements. The strong curvature of the distal tail in three skeletons, in addition, is difficult to attribute to postmortem water transport, as the curvature in one of the skeletons opposes the curvature in the other two.

Revised diagnosis. Small-bodied metasuchian (< 1.0 m) characterized by an anterior premaxillary foramen anterior to the first premaxillary tooth; infratemporal bar of jugal with marginal fossa; supratemporal fossa with marked anteromedial corner; scalloped posterior margin of skull table with median process; reduction of the premaxillary palate to parasagittal shelves; median elliptical incisive foramen; dentary with prominent labial alveolar margin that obscures all alveoli in lateral view; caniniform (d4) to the largest crowns in the postcaniniform series (d13) with relatively low, mesio-distally broad (crown width 60–80% of crown height), denticulate crowns; and largest postcaniniform crowns with lingually deflected mesial carina and associated trough.

Discussion. The referred cranium (MNN GAD19; Figs. 14–17, 19) removes any doubt about the assignment of the African species to *Araripesuchus*; the shape of the cranium and many of its structural details are close or identical with the type species *Araripesuchus gomesii* (Price 1959).

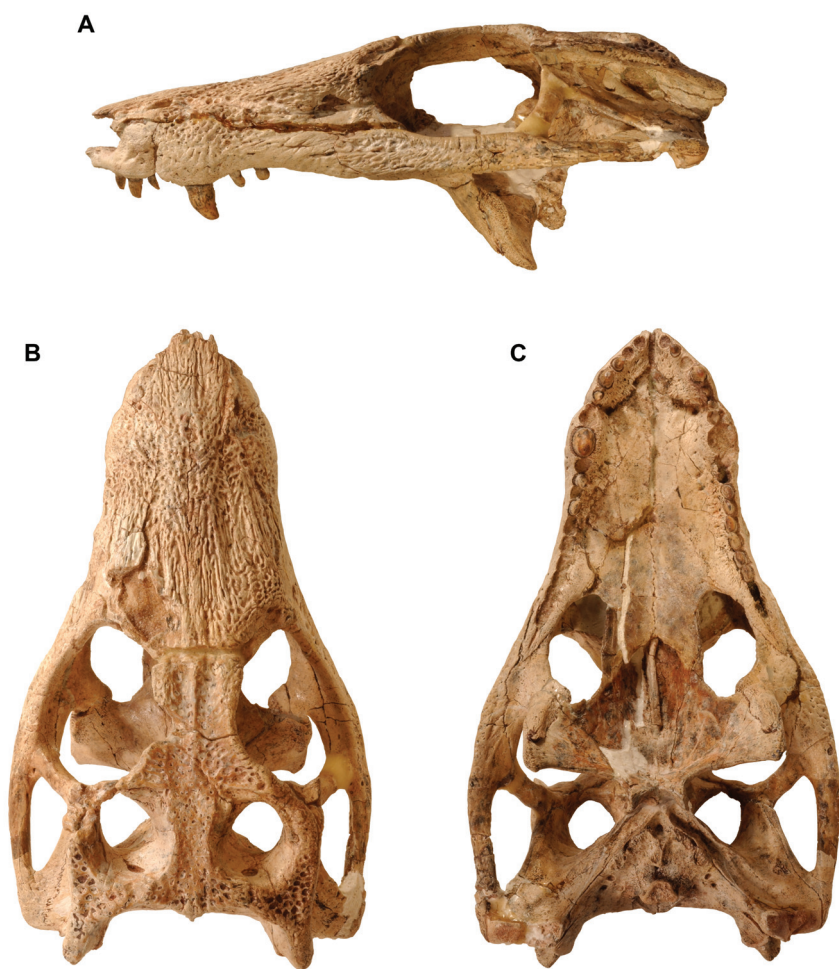


Figure 14. Skull of the crocodyliform *Araripesuchus wegeneri*. Cranium (MNN GAD19). **A** Lateral view (reversed). **B** Dorsal view. **C** Ventral view. Scale bar equals 5 cm.

Secondly, there is no doubt that cranium MNN GAD19 is correctly referred to *A. wegeneri*, because there are many features it shares only with the holotype, a partial snout (MNHN GDF700; Buffetaut and Taquet 1979). It is approximately 90% of the size of the holotype, based on measurements of the snout. Both have five premaxillary teeth. The jugal in both specimens expands in depth toward its anterior end and has a shallow sculpted fossa under the orbit. Other shared features found thus far only in the holotype and MNN GAD19 include a premaxillary sinus, small posterior spine on the maxilla that projects into the antorbital fenestra, flat strap-shaped border between the

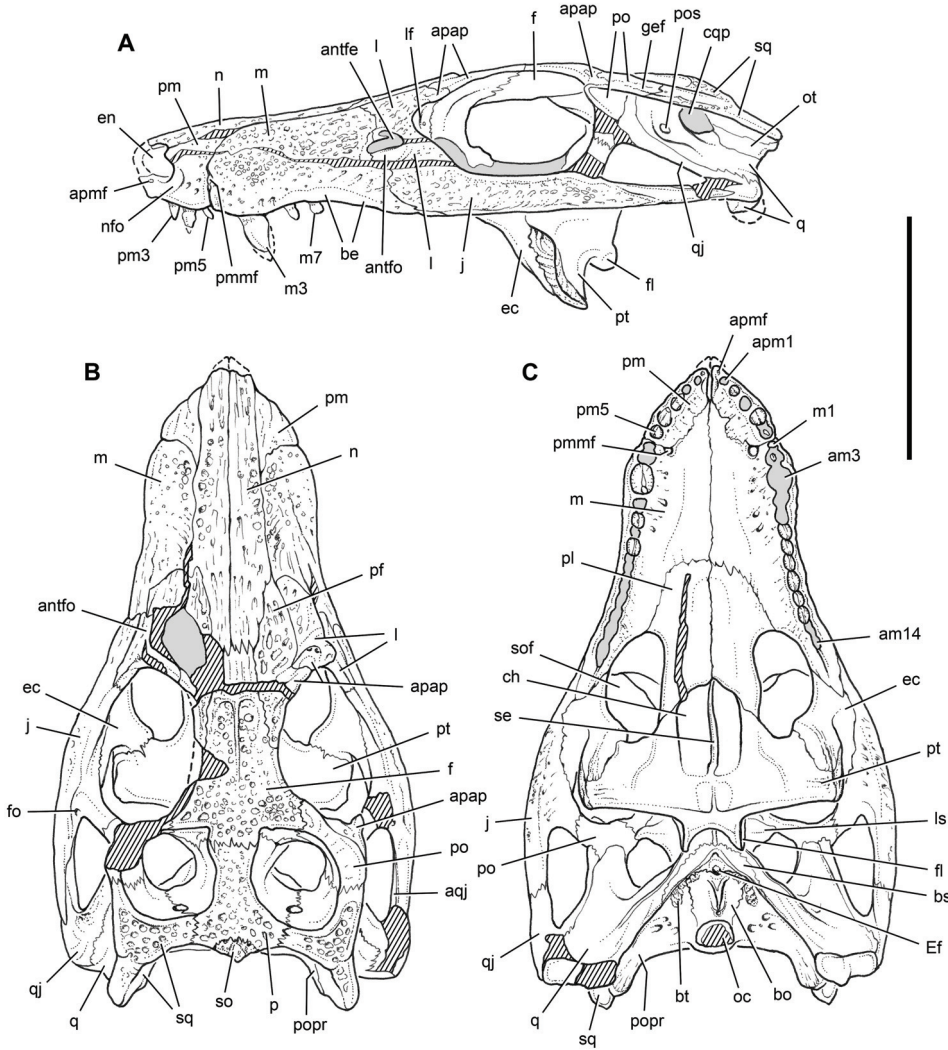


Figure 15. Skull of the crocodyliform *Araripesuchus wegneri*. Drawings matching the cranium (MNN GAD19) in Fig. 14. **A** Lateral view (reversed). **B** Dorsal view. **C** Ventral view. Parallel lines indicate broken bone surface; dashed line indicates missing bone or tooth crown; grey tone indicates matrix. Scale bar equals 5 cm. Abbreviations: *am3*, 14, alveolus for maxillary tooth 3, 14; *antfe*, antorbital fenestra; *antfo*, antorbital fossa; *apap*, articular surface for palpebral; *apm1*, alveolus for premaxillary tooth 1; *apmf*, anterior premaxillary foramen; *aqj*, articular surface for the quadratojugal; *be*, buccal emargination; *bo*, basioccipital; *bs*, basisphenoid; *bt*, basal tubera; *ch*, choana; *cqp*, cranioquadrate passage; *ec*, ectopterygoid; *Ef*, Eustachian foramen; *en*, external naris; *f*, frontal; *fl*, flange; *fo*, foramen; *gef*, groove for ear flap; *j*, jugal; *l*, lacrimal; *lf*, lacrimal foramen; *ls*, laterosphenoid; *m*, maxilla; *m1*, 3, 7, maxillary tooth 1, 3, 7; *n*, nasal; *nfo*, narial fossa; *oc*, occipital condyle; *ot*, otoccipital; *p*, parietal; *pf*, prefrontal; *pl*, palatine; *pm*, premaxilla; *pm3*, 5, premaxillary tooth 3, 5; *pmmf*, premaxilla-maxilla foramen; *po*, postorbital; *popr*, paroccipital process; *pos*, preotic siphonium; *pt*, pterygoid; *q*, quadrate; *qj*, quadratojugal; *se*, septum; *sq*, squamosal; *so*, supraoccipital; *sof*, suborbital fenestra.

choana and suborbital fenestra, and a V-shaped anterior margin of the choanae (Figs. 14, 15, 17). Finally, the fifth maxillary crown is preserved in both skulls and corresponds in detail regarding orientation, shape, and surface detail; the subcircular crown is angled posteroventrally, has a low short primary ridge near the crown apex laterally, has finely denticulate carinae, and has fine striations on the crown surface, some of which extend from the denticles.

Dorsal skull roof. The following abbreviated description is based primarily on the well preserved cranium MNN GAD19 (Figs. 14–17, 19, 22; Table 7) and a nearly complete dentition in skull MNN GAD20, which was hemisected by erosion (Figs. 20, 21).

The *premaxilla* exhibits many features important for determining phylogenetic position, the monophyly of *Araripesuchus*, and the distinction of *A. wegneri*. Most of the external surface of the bone is smooth, except for the tip of the posterodorsal ramus (Figs. 14A, B, 15A, B, 16A). At the anterior tip of the premaxilla, an anterior premaxillary foramen is present and passes posterodorsally into the nasal passage (Fig. 16A). On the lateral aspect of the premaxilla, the posterior boundary of the narial fossa is indicated by an arcuate depression, posterior to which are located two large neurovascular foramina (posterior premaxillary foramina) and one smaller accessory foramen. One large foramen with a similar anteroventral groove has been described or shown in *A. gomesii* (Price 1959) (also AMNH 24450), *A. patagonicus* (Ortega et al. 2000) and *A. tsangatsangana* (Turner 2006). Posterior to these foramina is located the larger premaxilla-maxilla foramen, which opens between these bones and extends ventrally to the alveolar margin as a narrow slit (Fig. 16A). In cross-section the body of the premaxilla posterior to the external nares is hollow (Fig. 17A), a highly unusual feature that is at least partially responsible for the inflated appearance of the premaxilla (Fig. 16A). This space, a premaxillary sinus, is also visible on the holotype, the cavity filled with matrix and exposed by erosion (MNHN GDF700). In the scan of *A. wegneri* and in an acid-prepared skull of *A. gomesii* (AMNH 24450; Hecht 1991), the canal of the premaxilla-maxilla foramen appears to have an anterior diverticulum that may pneumatize the premaxilla. The scan also shows that the pair of large lateral foramina on the body of the premaxilla anterior to the premaxilla-maxilla foramen also communicate with the premaxillary sinus.

The external surface of the *maxilla* is textured, except for a smooth surface along the arched, ventral alveolar margin dorsal to the postcaniniform teeth (Figs. 14A, 15A, 16A). The root of the caniniform tooth fills the swelling at the anterior end of the maxilla. The maxilla extends posteriorly to form the anterior margin of the antorbital fenestra and fossa. Above the fossa, a narrow prong of the maxilla contacts the prefrontal, separating the nasal and lacrimal. This is a sutural configuration present in *A. tsangatsangana* but absent in *A. gomesii* and *A. patagonicus* (Turner 2006), where the nasal contacts the lacrimal separating the maxilla and prefrontal.

The *nasal* is textured most deeply with circular pits in its mid-section and has a more elevated median nasal bridge than in other species (Figs. 14B, 15B). The nasal-frontal suture is interdigitated as in *A. gomesii* (Price 1959) and *A. patagonicus* (Ortega et al. 2000), a sutural configuration present in juveniles of *A. gomesii* (AMNH 24450).

Table 7. Dimensions (mm) of the referred cranium of *Araripesuchus wegneri* (MNN GAD19). Paired structures measured on left side except as indicated.

Structure	Measurement	Length
Dorsal skull roof	Cranium, maximum length (premaxilla to quadrate condyle)	127.3
	Cranium, maximum length (premaxilla to supraoccipital)	121.9
	Cranium, width across posterior tip of squamosals	50.4
	Cranium, width across quadrate condyles	69.5
	Snout, maximum transverse width (at caniniform tooth)	35.5
	External naris, dorsoventral height	7.7
	External nares, transverse width	13.3
	Narial fossa, maximum transverse width	23.5
	Antorbital fossa length	8.4
	Antorbital fenestra length	4.9
	Antorbital fenestra, maximum height	3.1
	Interorbital skull roof, minimum width	15.5
	Orbital anteroposterior diameter	32.4
	Orbital dorsomedial-ventrolateral diameter	30.0 ¹
	Jugal orbital ramus, depth at mid-length	7.8
	Jugal lower temporal bar, minimum depth	4.0
	Postorbital bar, minimum anteroposterior diameter	4.5
	Laterotemporal fenestra length	19.3
	Laterotemporal fenestra depth	10.6
	Supratemporal fossa, anteroposterior length	19.4
	Supratemporal fossa, transverse width	16.4 ¹
Palate	Quadrate condyles, transverse width	14.0
	Pterygoid mandibular processes, maximum transverse width	51.0
	Choana, maximum anteroposterior length	20.5
Braincase	Foramen magnum, maximum transverse width	9.4
	Foramen magnum, maximum dorsoventral depth	6.0

¹Measurement from right side.

The nasal-frontal suture shows less interdigitation in *A. tsangatsangana* (Turner 2006), and the frontal has a narrow anteromedian process in *A. buitreaensis* (Pol and Apes-teguia 2005).

The L-shaped *lacrima* forms nearly all of the smooth surface of the antorbital fossa, which has subequal margins posterior and ventral to the antorbital fenestra as in *A. gomesii* (Figs. 14A, 15A). The narrow continuation of the smooth margin of the fossa extends around the anterior corner of the antorbital fenestra and along the ventral margin of a posterior prong of the maxilla that partially divides the fenestra. None of the other species of *Araripesuchus* have a similar maxillary prong. In both *A. gomesii* and *A. patagonicus* (Ortega et al. 2000), the antorbital fossa is approximately twice the size of the opening in *A. wegneri* relative to the orbit and does not appear to change much in rela-

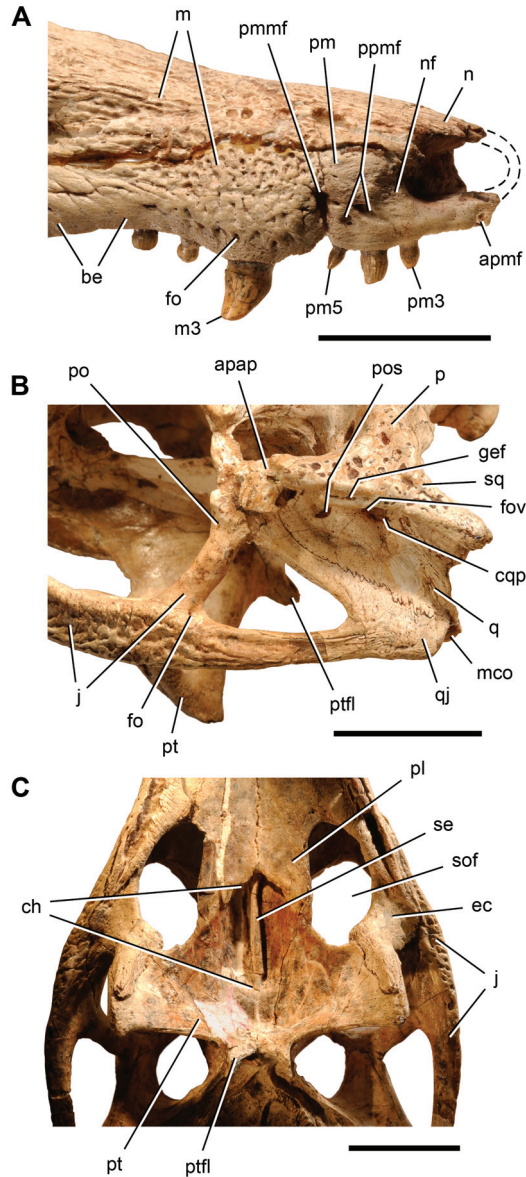


Figure 16. Skull of the crocodyliform *Araripesuchus wegneri*. Detailed views of the cranium (MNN GAD19). **A** Snout margin in anterolateral view. **B** Posterior portion of the skull in left lateral view. **C** Posterior palate in ventral view. Scale bars equal 2 cm. Abbreviations: *apap*, articular surface for the palpebral; *apmf*, anterior premaxillary foramen; *be*, buccal emargination; *cqp*, cranioquadrate passage; *ch*, choana; *ec*, ectopterygoid; *fo*, foramen; *fov*, fenestra ovalis; *gef*, groove for the ear flange; *j*, jugal; *pm*, premaxilla; *qj*, quadratojugal; *m*, maxilla; *m3*, maxillary tooth 3; *mco*, medial condyle; *n*, nasal; *nf*, narial fossa; *p*, parietal; *pl*, palatine; *pm*, premaxilla; *pm3*, 5, premaxillary tooth 3, 5; *pmmf*, premaxilla-maxilla foramen; *po*, postorbital; *pos*, preotic siphonium; *ppmf*, posterior premaxillary foramen; *pt*, pterygoid; *ptfl*, pterygoid flange; *q*, quadrate; *se*, septum; *sof*, suborbital fenestra; *sq*, squamosal.

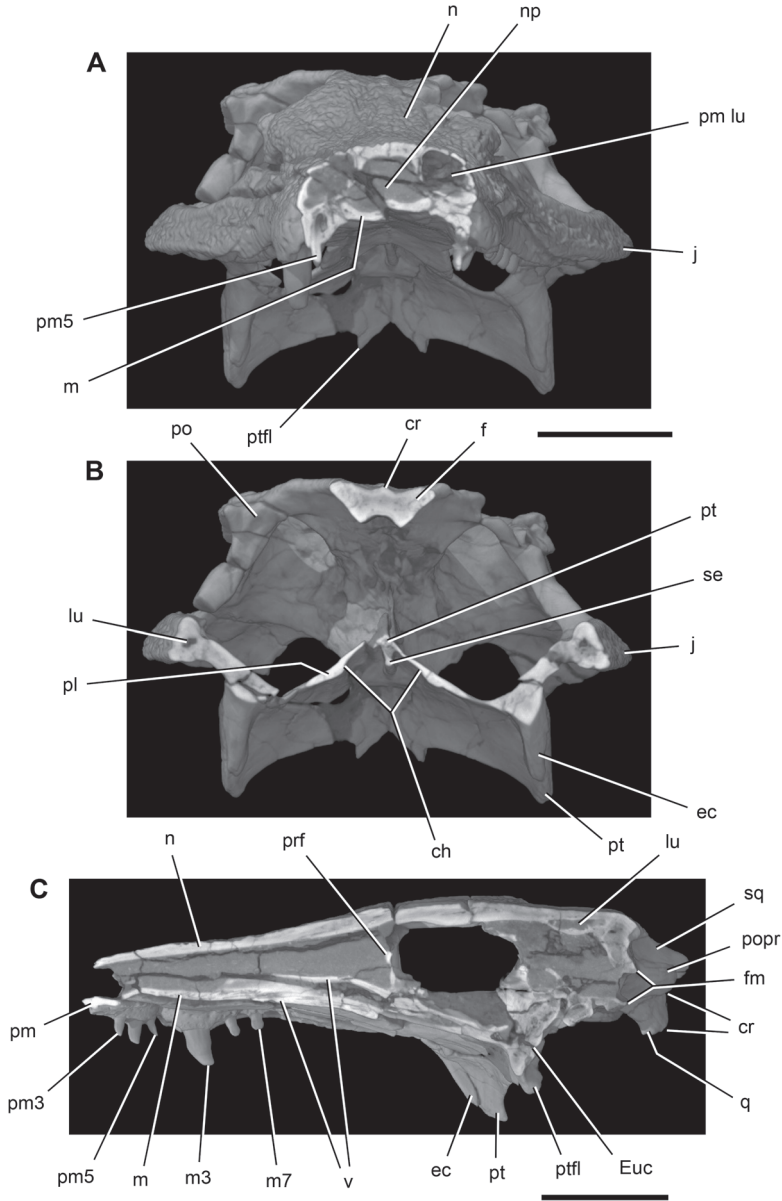


Figure 17. Skull of the crocodyliform *Araripesuchus wegneri*. Computed-tomographic cutaway views of the cranium (MNN GAD19). **A** Snout posterior to the external nares in anterior view. **B** Posterior portion of the skull in anterior view. **C** Cranium in sagittal section near midline. Scale bar for A and B equals 2 cm; scale bar for C equals 3 cm. Abbreviations: *ch*, choana; *cr*, crest; *ec*, ectopterygoid; *Euc*, Eustachian canal; *f*, frontal; *fm*, foramen magnum; *j*, jugal; *lu*, lumen; *m*, maxilla; *m3*, 7, maxillary tooth 3, 7; *n*, nasal; *np*, narial passage; *pl*, palatine; *pm*, premaxilla; *pm3*, 5, premaxillary tooth 3, 5; *po*, postorbital; *popr*, paroccipital process; *prf*, prefrontal; *pt*, pterygoid; *ptfl*, pterygoid flange; *q*, quadrate; *se*, septum; *sq*, squamosal; *v*, vomer.

tive size after reaching subadult size in *A. gomesii* (Price 1959; Hecht 1991). The opening is proportionately largest in *A. tsangatsangana* and appears to lack any smooth surface attributable to an antorbital fossa (Turner 2006). A prominent knob and ridge are situated on the lacrimal dorsal to the fossa and are continuous posteriorly with the edge of a large anterior palpebral. The lacrimal foramen is located ventral to this knob within the orbit.

The anterior and posterior *palpebrals* are missing in cranium MNN GAD19, exposing articular fossae on the lacrimal and *prefrontal* anteriorly and on the postorbital posteriorly (Figs. 14B, 15B). Disarticulated palpebrals have been discovered on the large block (Fig. 23). In *A. wegneri* the interdigitating prefrontal-frontal suture contrasts with the broad scarf joint described in *A. tsangatsangana* (Turner 2006). The prefrontal pillar is anteroposteriorly flattened and angles ventromedially and slightly posteriorly, tapering strongly from the skull roof to the palate.

The *frontal* and *parietal* are fused to their opposites and join each other by an interdigitating frontoparietal suture. The frontals have a distinct median crest, and the parietal skull table between the supratemporal fossae is noticeably narrower than in other species of *Araripesuchus*. In *A. wegneri* a parasagittal line extending along the orbital margin passes across the supratemporal fossa rather than along its lateral rim as in other species (Figs. 14B, 15B). The frontal enters the supratemporal fossa to a greater degree than in other species of *Araripesuchus*, reaching the inner margin of the fossa in dorsal view. The rim of the fossa in *A. wegneri* also has a marked anteromedial corner with parasagittal and transverse edges, whereas in other species the rim of the fossa is nearly uniformly curved. The posterior margin of the skull table in *A. wegneri* is scalloped to each side of the supraoccipital, differing from the nearly straight posterior margin in other species.

The *postorbital* is notched by an articular facet for a small posterior palpebral, as in other species of *Araripesuchus* and most stem crocodyliforms. The surface of the postorbital between this facet and the supratemporal fossa varies, remaining textured with pits in some species, such as *A. gomesii* (Price 1959) and *A. tsangatsangana* (Turner 2006), and smooth in others such as *A. patagonicus* (Ortega et al. 2000). In *A. wegneri* this surface is smooth and convex (Figs. 14B, 15B) rather than flat with a sharp medial and lateral rims as in many protosuchians and neosuchians.

The *squamosal* is distinctly triradiate in dorsal view in *A. wegneri* and all other species except *A. gomesii*. The difference lies in the length and orientation of the posterior process, which has more subdued pitting and is offset below the skull table. The posterior process appears to be both shorter and angled more steeply posteroventrally in *A. gomesii*, such that it appears to be of negligible length in dorsal view of the skull (Price 1959; Hecht 1991). The pitted dorsal surface of the squamosal in *A. wegneri* has an L-shaped fossa where the pitted texture is depressed, a condition more strongly expressed in *Simosuchus* (Buckley et al. 2000).

The anterior ramus of the *jugal* extends as a broad process as far anteriorly as the lacrimal, approaching the border of the antorbital fossa with a narrow fingerlike process. The anterior ramus is not as deep or extended anteriorly in either *A. patagonicus* (Ortega et al. 2000) or *A. tsangatsangana* (Turner 2006). The base of the smooth rod-shaped dorsal ramus, which is inset from the textured body of the jugal and pierced by a si-

Table 8. Dimensions (mm) of the skulls and postcranial bones of *Araripesuchus wegeneri* preserved in proximity on a block of matrix (MNN GAD20–22). Measurements are taken from the left side except as indicated. Ungual length is measured along longest chord from base to tip. Parentheses indicate estimated measurement. Abbreviations: C, cervical; D, dorsal.

Structure	Measurement	Length
Cranium	MNN GAD20, length (premaxilla to quadrate condyle)	111.6
	MNN GAD21, “ “	(122.0)
	MNN GAD22, “ “	(130.0)
Axial column (MNN GAD20)	Atlas to tip of tail length	(600.0)
	Dorsal vertebrae (D1–15) length	(190.0)
	Tail length	(300.0)
	Osteoderm pair (dorsal) at base of tail, width	34.2
Forelimb (MNN GAD21)	Radius length	50.7
	Radiale length	20.4
	Metacarpal 1 length	10.2
	Metacarpal 2 length	14.2
Manus ¹ (MNN GAD22)	Metacarpal 3 length	(15.8)
	Metacarpal 4 length	14.7
	Metacarpal 5 length	12.6
	Phalanx II-2 length	6.6
	Phalanx II-3 (ungual) length	10.2
	Phalanx III-1 length	6.4
	Phalanx III-2 length	4.5
	Phalanx III-3 length	4.8
	Phalanx III-4 (ungual) length	8.4
	Phalanx IV-1 length	6.9
	Phalanx IV-2 length	4.4
	Phalanx V-1 length	6.1
	Phalanx V-2 length	3.8
Pes (MNN GAD22)	Metatarsal 1 length	32.8
	Metatarsal 2 length	38.2
	Metatarsal 3 length	40.7
	Metatarsal 4 length	35.4
	Phalanx I-1 length	10.6
	Phalanx I-2 (ungual) length	9.4
	Phalanx II-1 length	12.4
	Phalanx II-2 length	7.7
	Phalanx II-3 (ungual) length	8.8
	Phalanx III-1 length	12.5
	Phalanx III-2 length	8.5
	Phalanx III-3 length	7.0
	Phalanx III-4 (ungual) length	7.2
	Phalanx IV-1 length	11.8
	Phalanx IV-2 length	6.5
	Phalanx IV-3 length	6.5

¹Right side.

phonal foramen, is situated on the posterior one-half of the jugal (Figs. 14A, 15A). The posterior ramus of the jugal is distinctive. As in *A. gomesii* but unlike other species, the ramus tapers to a point below the posterior corner of the laterotemporal fenestra rather than at mid-length along the infratemporal bar. Unique to *A. wegneri*, a marginal fossa with reduced texture is present along the dorsal margin of the posterior ramus.

The L-shaped *quadratojugal* has an inset articular facet for the posterior ramus of the jugal. The quadratojugal-quadrate contact adjacent to the condyles and along the shaft is an interdigitating suture. Texturing of the external surface of the quadratojugal is limited to the posteroventral corner, where the bone approaches, but does not contribute to, the articular surface for the lower jaw.

Palate. The configuration of the anterior palate in *A. wegneri* is unusual compared to that in *A. gomesii* (Price 1959) and other basal metasuchians. The premaxillary contribution is limited to the periphery of the anterior palate adjacent to the alveolar margin. Opposing premaxillae have very little contact on the palate. They join in the midline only anterior and posterior to an elliptical incisive foramen (Figs. 14C, 15C). Most of the palate between the premaxillary tooth rows is formed by the maxillae. A pit for reception of the tip of the dentary caniniform is present at the premaxilla-maxilla suture medial to the premaxilla-maxilla foramen. The tip of the dentary caniniform in this location can be seen in the articulated dentition of MNN GAD20 (Fig. 20B).

The configuration of the remainder of the palate, including the *palatine*, *ectopterygoid* and *pterygoid*, is quite similar to that in *A. gomesii* (Price 1959) and *A. tsangatsangana* (Turner 2006). The semicircular suborbital fenestra is larger than the adjacent choana, which is situated farther posteriorly on the palate, although not butted against the posterior transverse edge of the pterygoids (Figs. 14C, 15C). *A. patagonicus* is unusual in this regard, with the posterior margin of the choana positioned farther anteriorly than the posterior margin of the suborbital fenestra, although breakage may have artificially expanded the fenestra (Ortega et al. 2000). *A. wegneri* shares with *A. gomesii* the presence of a distinctive wedge-shaped flange on the pterygoid at the posterior margin of the palate (Figs. 14C, 15C, 16C, 17C), a process that is either very reduced or absent in other species of the genus.

Three palatal features differentiate *A. wegneri* from other species (Figs. 14C, 15C, 16C). The anterior margin of the choanae is V-shaped rather than transverse; there is a flat, strap-shaped border between the suborbital fenestra and choana rather than a narrow, ventrally directed edge; the choanal septum is narrow, its rounded ventral edge only slightly thickened posteriorly rather than developed as a horizontal flange.

The main shaft of the *quadrate* angles posteroventrally from the recessed otic region to the quadrate condyles, which are directed ventrally. In the otic region, there is a preotic siphonium, ventral to which is a marked fossa and posterior to which is a large opening housing the fenestra ovalis and confluent cranioquadrate passage (Fig. 16B). A sharp vertical crest on the quadrate contributes to the posterior skull margin, joining the paroccipital process with the rim of the medial condyle. In posterior view, a foramen aërum opens on the posterior aspect of the quadrate shaft just above the

medial condyle. The relatively flat quadrate condyles, which are well preserved on the left side, are separated by a marked V-shaped cleft.

Braincase. Poorly exposed in other species, the braincase in *A. wegeneri* is well preserved with visible sutures and foramina (Figs. 14C, 15C, 16B, 17C). The *supraoccipital* is exposed along the posterior margin of the skull table as a pitted subtriangular surface sutured to a notch between the fused parietals. A thin nuchal crest projects posteriorly and recedes ventrally at the contact with the exoccipitals.

Although the ventral portion of the occipital condyle on the *basioccipital* is weathered away, the hemisphere of the condyle is prominent and fully exposed in ventral view. The ventral prominence of the condyle is a key difference when compared to the condyle in an extant crocodylian. A ventrally deflected condyle characterizes notosuchians, such as *Anatosuchus* and *Simosuchus*, but is less common among other crocodylomorphs. In *Hamadasuchus*, for example, a comparable profile of the occipital condyle is achieved with the braincase held in posteroventral view (Larsson and Sues 2007: fig. 5B).

The remainder of the basioccipital angles anteroventrally at approximately 45°. In the midline moving anteriorly from the condyle, there is a small posterior Eustachian foramen, a wedge-shaped median crest, and a large anterior Eustachian foramen opening between the basioccipital and basisphenoid. The Eustachian foramen opens antero-dorsally into the pituitary fossa (Fig. 17C). The lateral edge of the basioccipital curls up against the low basal tubera to each side, between which is located a relatively small lateral Eustachian foramen.

In posterior view, the *otoccipital* (exoccipital + opisthotic) meets its opposite over the foramen magnum as a protruding rim, excluding the supraoccipital from its border. The rim, which provides an articular surface for the proatlas, overhangs the foramen magnum in *A. wegeneri*, a condition coincident with ventral deflection of the occipital condyle. In non-notosuchian crocodylomorphs such as *Hamadasuchus* (Larsson and Sues 2007), in contrast, the exoccipital rim projects posteriorly. The paroccipital processes project to each side, their central axis following a sigmoid curve.

The otoccipital forms the extreme dorsolateral edge on each side of the occipital condyle and then extends anteroventrally to the basioccipital, tapering to a point against a crest formed by the quadrate and basisphenoid. The anteroventral tip of the otoccipital is raised as a low, rugose basal tuber, which is held between the basioccipital, basisphenoid and quadrate. Four foramina open to each side of the occipital condyle for passage of the posterior cranial nerves and internal carotid artery. The carotid foramen is larger than the others and opens ventrally rather than ventrolaterally.

Exposure of the *basisphenoid* is very limited in *A. wegeneri*. The more extensive exposure shown in *A. patagonicus* (Ortega et al. 2000) may well be due to erosion of the ventral surface of the braincase. Turner described “large posteroventral exposure” of the basisphenoid in *A. tsangatsangana* (Turner 2006: 286), although this cannot be verified in images of the specimens. In *A. wegeneri* the basisphenoid is pinched between the pterygoids and quadrates anteriorly and the basioccipital and otoccipital posteriorly (Figs. 14C, 15C). The basisphenoid contributes to the medial portion of the more

posterior of two crests running anteromedially from the quadrates to the pterygoids. This paired posterior crest converges in the midline running across the center of the exposed surface of the basisphenoid.

Endocast. An endocast, generated from a computed-tomographic scan of cranium MNN GAD19 (Fig. 22), closely resembles the endocast of *Anatosuchus* (Fig. 10). Both have spade-shaped, dorsoventrally compressed cerebral hemispheres separated dorsally by a shallow sinus. In *Araripesuchus* there is also a median fossa separating the hemispheres ventrally (Fig. 22C).

The optic lobe is differentiated as a low swelling posterior to each cerebral hemisphere. In the cerebellar region, the sagittal sinus ascends to a height level with the cerebral hemispheres, creating a steeply angled pontine flexure resembling that in theropod dinosaurs (Hopson 1979; Larsson 2001). On the ventral side of the endocast, the exit for the optic nerves and a pendant pituitary fossa are visible (Fig. 22A, C).

Lower jaw. Except for the *dentary* (Fig. 18), the lower jaw has yet to be well exposed in any available specimens. The dentary in *A. wegneri* is unusual in several regards. No alveoli are visible in lateral view. The lateral alveolar margin is dorsally prominent as compared to its medial counterpart, which appears to be lacking entirely posterior to dentary tooth 10 (Figs. 18B, 20). The alveolar margin is sinuous in lateral view as in many crocodyliforms. The most prominent, convex portions of the alveolar margin house the largest teeth and oppose smaller teeth in the upper tooth row set in a dorsally concave alveolar margin (Fig. 20A). In lateral view, the alveolar margin adjacent to the postcaniniforms is smooth and bordered ventrally by a connected row of large neurovascular foramina (Fig. 18A, D).

The dentary symphysis is rugose and fairly shallow (Fig. 18B, D). The articular scar for the splenial covers the anterior end of Meckel's canal and then curves onto the dorsal aspect of the dentary between the tooth rows (Fig. 18B, C). As a result, the *splenial* appears to have formed most of the dorsal surface of the symphysis between the tooth rows posterior to the caniniform.

Dentition. There are 5 premaxillary, 14 maxillary, and 16 dentary teeth in the best preserved subadult and adult dentitions (MNN GAD19, GAD20). The teeth in *A. wegneri* are regionalized. For descriptive purposes, we identify upper and lower teeth as *incisiforms*, *caniniforms*, and *postcaniniforms*, although tooth form grades between these functional types.

Incisiforms have subconical crowns with a bulbous base separated from an expanded root by a gentle constriction. The crown tip is slightly recurved posterolingually, and the crown is asymmetrical with a longer mesial than distal carina. The carina is both smooth and unornamented or has apically inclined, relatively fine denticles numbering about 5–6 per mm. The crown surface of incisiforms in *A. wegneri* is ornamented with fine wrinkles toward its apex and very rounded ridges toward the crown base that are occasionally visible under high magnification of well preserved, unworn crowns.

Caniniforms are discordantly (20–50%) larger than adjacent teeth, their principal defining feature. Like the incisiforms, the caniniform teeth have a bulbous crown with a basal constriction, are asymmetrical with a longer mesial carina, may have either smooth or denticulate carinae, and have crown surfaces characterized by fine wrinkles and low rounded ridges.

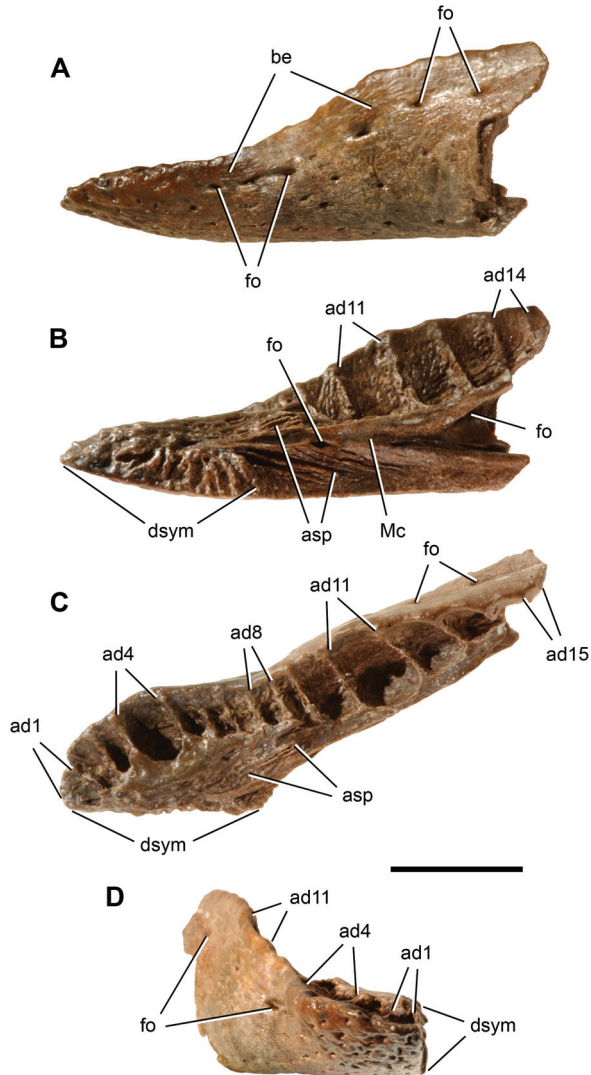


Figure 18. Right dentary of the crocodyliform *Araripesuchus wegneri*. Isolated, edentulous right dentary from a subadult (MNN GAD26). **A** Lateral view (reversed). **B** Medial view. **C** Dorsal view. **D** Anterior view. Scale bar equals 1 cm. Abbreviations: *ad1*, 4, 8, 11, 14, 15, alveolus for dentary tooth 1, 4, 8, 11, 14, 15; *asp*, articular surface for the splenial; *be*, buccal emargination; *dsym*, dentary symphysis; *fo*, foramen; *Mc*, Meckel's canal.

Postcaniniforms are located posterior to caniniform teeth. Crown form is quite variable, from tall pointed crowns that are asymmetrical with longer mesial carinae to squat symmetrical crowns that are longer mesiodistally than deep apicobasally. All have a marked constriction between crown and root, and all have denticulate mesial and distal carinae.

There are five *premaxillary teeth* in *A. wegneri*, the first four of which have the centroid of the tooth base or alveolus aligned in a straight row. The centroid of the small fifth premaxillary tooth (or its alveolus if missing) is inset slightly lingual to a line through the other teeth/alveoli. In palatal view, the straight portions of the premaxillary tooth rows converge anteriorly at an angle of 85° as in *A. gomesii* (Price 1959). A similar morphology appears to be preserved in *A. tsangatsangana* (Turner 2006). Although no specimen of *A. tsangatsangana* preserves the premaxillary tooth row in place, the anterior five dentary teeth are aligned in a straight row [12: fig. 41A]. *Libycosuchus* has a similar linear configuration of alveoli, although the tooth rows converge more abruptly at an angle of approximately 100° (Stromer 1914). The straight premaxillary tooth rows are reflected in the external margin of the premaxilla, which appears straight or slightly concave, rather than convex, in dorsal view of the cranium.

All but the first premaxillary tooth are preserved in both MNN GAD19 and GAD20 (Figs. 19A, 20B). All of the crowns are incisiform as described above. The first three alveoli are virtually identical in size in MNN GAD19, yet the second premaxillary tooth preserved on the left side is slightly smaller than the third premaxillary tooth preserved on the right side. It is probable, thus, that there is a continuous increase in crown size from pm1 to pm4 and that pm5 is the smallest of the premaxillary series.

Crown shape is remarkably similar in the premaxillary series and is asymmetrical in labial and apical views. In labial view, the longer mesial carina is convex, displacing the crown tip distally. The shorter distal carina is also convex in all but the large pm4, where it is straight. All of the premaxillary crowns have low vertical fluting and sharp, unornamented mesial and distal carinae. The lingual crown face is slightly less convex than its labial counterpart, and a shallow trough is present adjacent to both carinae on the lingual side of the crown (Figs. 19A, 20B). Given these asymmetries, it is possible to determine whether an isolated premaxillary crown is from left or right premaxillae.

The *maxillary teeth* can be divided into two anterior incisiforms (m1, m2), a caniniform (m3), and 11 postcaniniforms (m4–m14). All have finely denticulate carinae upon eruption (approximately 5–6 denticles per millimeter) and low fluting on both crown surfaces, as preserved in both MNN GAD19 and GAD20 (Figs. 20, 21). Fine denticles are present on the carinae of an erupting m1 crown in the mature individual MNN GAD19. Apical wear, however, has reduced or obliterated the denticles on other crowns in the same tooth row (Fig. 19B, C). The mesial and distal carinae of the caniniform (m3) in MNN GAD19 have been truncated by wear, giving the misleading appearance that the crown is recurved (Figs. 16A, 19A). An unworn m3 is partially exposed in MNN GAD20 and shows that the caniniform tooth in the upper jaw is not recurved but rather has an asymmetrical leaf shape in labial or lingual view (Fig. 20B).

Crown shape in the maxillary series changes rapidly from leaf-shaped in m1–3 to the squat proportions of the postcaniniforms (Fig. 21). The denticles in postcaniniforms are restricted to the apical margin, and there is often a low primary ridge leading to the apical denticle.

All of the *dentary teeth* have finely denticulate margins, although information is limited for d2 and absent for d1. The fourth dentary tooth is enlarged as a caniniform, which has a crown shape similar to that of pm4 and m3 in the upper tooth row; the longer mesial carina is convex whereas the distal carina is straight. Postcaniniform

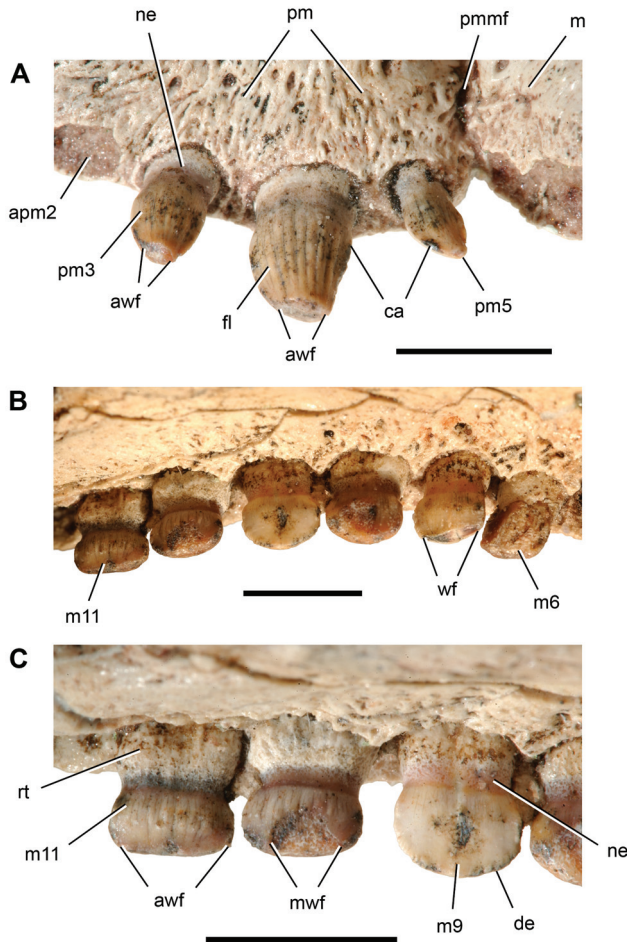


Figure 19. Worn dentition of the crocodyliform *Araripesuchus wegneri*. Detailed views of the dentition (MNN GAD19). **A** Right premaxillary teeth 3–5 in ventromedial view. **B** Left maxillary teeth 6–11 in ventromedial view. **C** Left maxillary teeth 9–11 in ventromedial view. Scale bars equal 5 mm. Abbreviations: *apm2*, alveolus for premaxillary tooth 2; *awf*, apical wear facet; *ca*, carina; *de*, denticle; *fl*, fluting; *m*, maxilla; *m6*, 9, 11, maxillary tooth 6, 9, 11; *muf*, medial wear facet; *ne*, neck; *pm*, premaxilla; *pm3*, 5, premaxillary tooth 3, 5; *pmmf*, premaxilla-maxilla foramen; *rt*, root; *uf*, wear facet.

crowns decrease in size to d7 followed by an increase in size to d11 and d12 (Fig. 20). The trough adjacent to the mesial carina on the lingual crown face is marked, giving the appearance that the mesial edge of the crown is curled lingually (Fig. 20C).

Three aspects of the dentition deserve special note. The first involves crown orientation along the tooth row. Many postcaniniform maxillary and dentary crowns

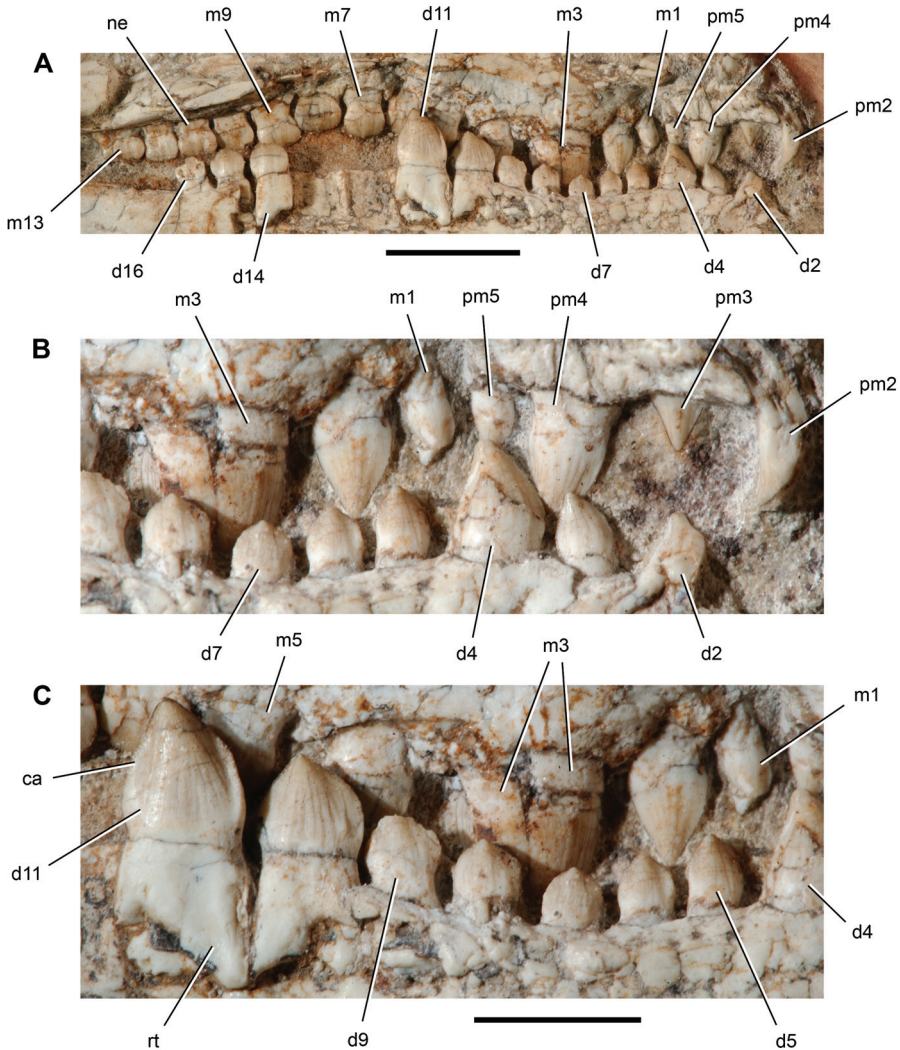


Figure 20. Unworn dentition of the crocodyliform *Araripesuchus wegneri*. Detailed views of the anterior and middle portions of the tooth rows (MNN GAD20). **A** Left tooth rows in medial view. **B** Anterior portion of left tooth rows in medial view. **C** Middle portion of left tooth rows in medial view. Scale bar equals 1 cm in A and 5 mm in B and C. Abbreviations: *ca*, carina; *d2*, 4, 5, 7, 9, 11, 14, 16, dentary tooth 2, 4, 5, 7, 9, 11, 14, 16; *m1*, 3, 5, 7, 9, 13, maxillary tooth 1, 3, 5, 7, 9, 13; *ne*, neck; *pm2*–5, premaxillary tooth 2–5; *rt*, root.

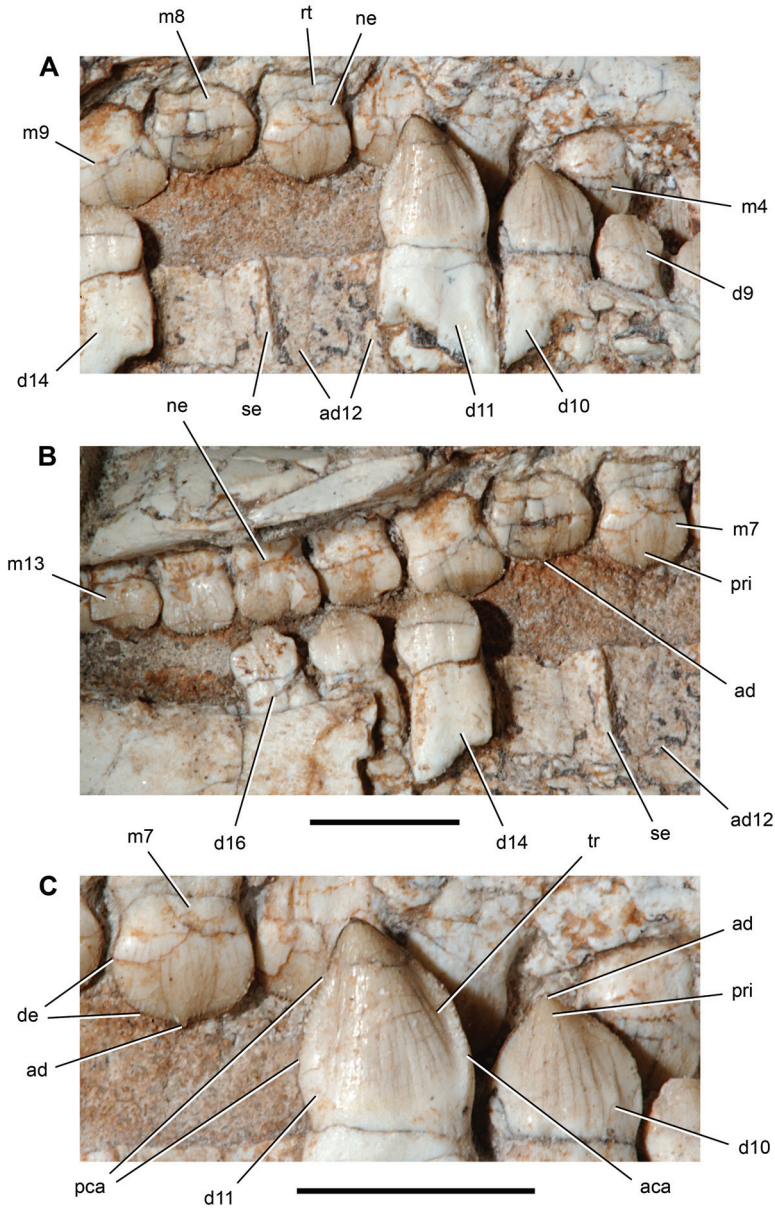


Figure 21. Unworn dentition of the crocodyliform *Araripesuchus wegneri*. Detailed views of the middle and posterior portions of the tooth rows (MNN GAD20). **A** Middle portion of left tooth rows in medial view. **B** Posterior portion of left tooth rows in medial view. **C** Close-up view of maxillary tooth 7 and dentary tooth 10 and 11 in medial view. Scale bar for A and B and scale bar for C equal 5 mm. Abbreviations: *aca*, anterior carina; *ad*, apical denticle; *ad12*, alveolus for dentary tooth 12; *d9–11*, *14*, *16*, dentary tooth 9–11, 14, 16; *de*, denticle; *m4*, *7–9*, *13*, maxillary tooth 4, 7–9, 13; *ne*, neck; *pca*, posterior carina; *pri*, primary ridge; *rt*, root; *se*, septum; *tr*, trough.

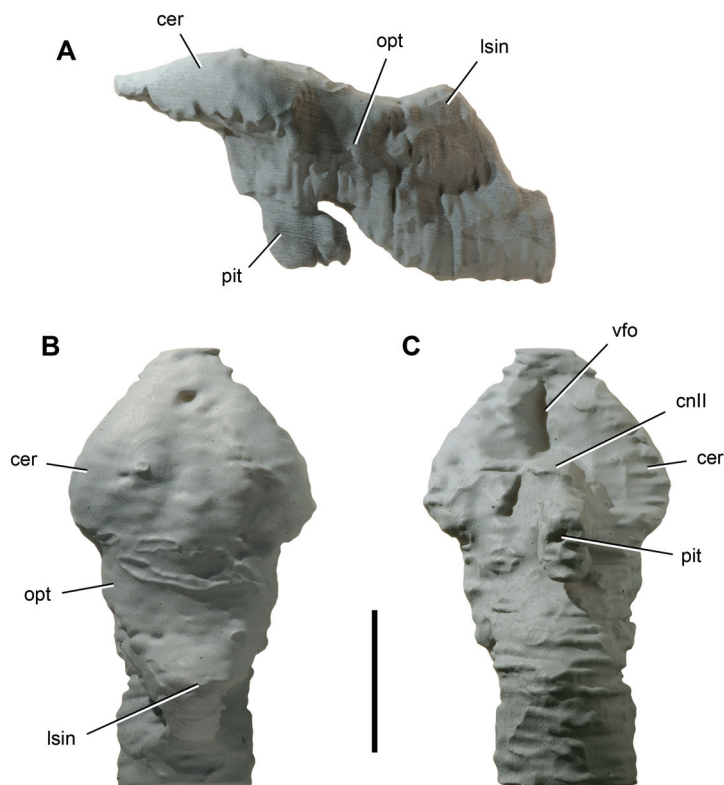


Figure 22. Endocast of the crocodyliform *Araripesuchus wegneri*. Endocast (UCRC PVC5) prototyped from a computed-tomography scan of skull MNN GAD19. The endocast lacks a portion of the pituitary fossa and right and left labyrinths. **A** Lateral view. **B** Dorsal view. **C** Ventral view. Scale bar equals 1 cm. Abbreviations: *cer*, cerebrum; *cnII*, cranial nerve II (optic nerve); *lsin*, longitudinal sinus; *opt*, optic lobe; *pit*, pituitary fossa; *vfo*, ventral fossa.

are canted mesiolingually (anteromedially) relative to the tooth row, creating an echelon arrangement reminiscent of the condition in basal sauropodomorph and ornithischian dinosaurs. This can be seen in m5–7 in MNN GAD19 and d9–11 in MNN GAD20 (Figs. 14C, 15C, 20C). Secondly, the postcaniniform maxillary teeth and mid- and distal dentary teeth are set into a trough with alveoli incompletely divided by bony septa. The maxillary trough is best seen in MNN GAD19, and the lingually open alveoli in the dentary series are best seen in MNN GAD20. Thirdly, blunt apical wear occurs throughout the dentition in MNN GAD19. The prevalence of blunt apical tooth wear, denticulate carinae, crown surfaces with fluting, *en echelon* crown orientation and the absence of recurved caniniforms suggest that *A. wegneri* may have been an opportunistic, or even an obligate, herbivore. A detailed study of occlusion and wear is warranted on the materials here described.

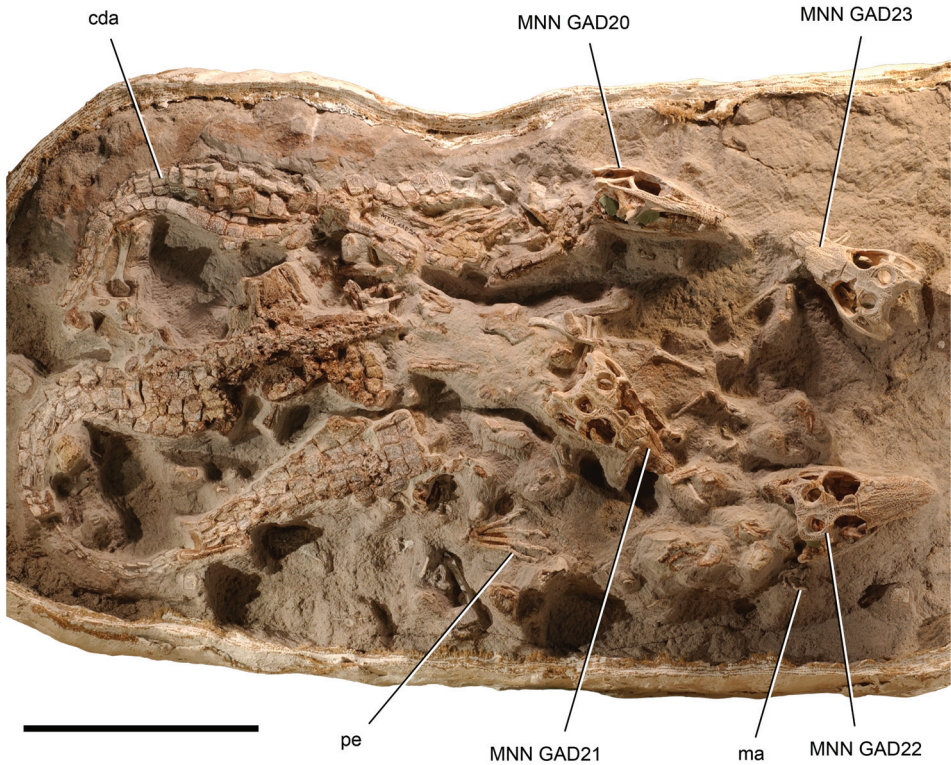


Figure 23. Block containing skeletons of the crocodyliform *Araripesuchus wegneri*. Three aligned and partially articulated skeletons (MNN GAD20–22) and a partial skull (MNN GAD23) in dorsal view. Weathered portions of the crania were restored based on MNN GAD19. Scale bar equals 20 cm. Abbreviations: *cda*, caudal dermal armor; *ma*, manus; *pe*, pes.

Axial skeleton. Portions of the axial column are preserved and differ little from that preserved in *A. gomesii* (Hecht 1991). The centra are amphicoelous. The thin sub-quadrate dorsal and caudal osteoderms have low parasagittal keels and no articular processes. The tail is surrounded by osteoderms, including paired dorsal osteoderms extending at least over the proximal two-thirds of the tail, a single lateral row in the proximal tail, and paired ventral osteoderm rows (Fig. 24).

Appendicular skeleton. The limbs are the best exposed portion of the appendicular skeleton. The humerus, radius and ulna in *A. wegneri* have straight and relatively slender shafts with proximal and distal articular surfaces consistent with upright posture (Fig. 25). In extant crocodylians with a habitual posture that is less erect, the humeral shaft has a sigmoidal axis and the distal condyles face anteriorly. The radiale, ulnare and

metacarpals (Figs. 25B, 26A), likewise, are proportionately elongate compared to those in extant crocodylians (Mook 1921).

Articulated forelimb elements in two individuals permit measurement of proportions within the forelimb of adult *Araripesuchus* for the first time (Table 6). Compared to extant crocodylians, distal forelimb segments in *A. wegneri* are longer relative to proximal segments. Thus the radius is longer relative to the humerus, and the radiale is longer relative to the radius in *A. wegneri* by a factor of between 10–15%. Comparison of the radiale and metacarpal three, however, is more striking. The radiale is more than 150% of metacarpal three length in *A. wegneri*, whereas

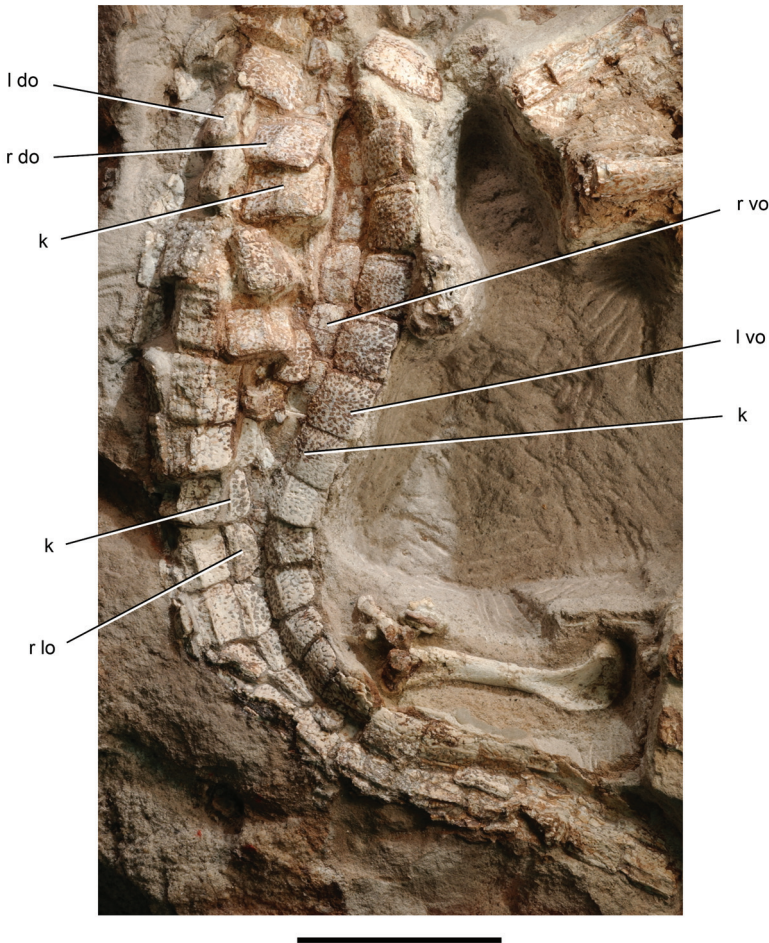


Figure 24. Caudal skeleton of the crocodyliform *Araripesuchus wegneri*. Flexed, articulated tail showing paired dorsal osteoderm rows in dorsal view, lateral osteoderm row in lateral view and ventral osteoderm rows in ventral view (MNN GAD20). Scale bar equals 5 cm. Abbreviations: *k*, keel; *l do*, left dorsal osteoderm; *l vo*, left ventral osteoderm; *r do*, right dorsal osteoderm; *r lo*, right lateral osteoderm; *r vo*, right ventral osteoderm.

the radiale is only about 75% the length of metacarpal three in extant crocodylians. In other words, the elongate proximal carpals in *A. wegneri* are approximately twice their length relative to the metacarpus in extant crocodylians. Relative lengthening of distal limb segments also suggests greater relative speed and a more upright limb posture. The proximal end of each metacarpal is flattened and expanded to enhance overlap, and the distal end is marked by pits that allow considerable extension of the proximal phalanges (Fig. 26A).

The long bones in the hind limb also have straight shafts. A calcaneum near skeleton MNN GAD22 (Fig. 23) has a deep calcaneal tuber that is only moderately laterally deflected. An articulated pes has straight, proportionately long metatarsals with flattened proximal shafts to enhance overlap and distal pits for extension of the proximal phalanges (Fig. 26B). These features, again, suggest that during terrestrial locomotion, limb posture in *A. wegneri* was more upright than in extant crocodylians.

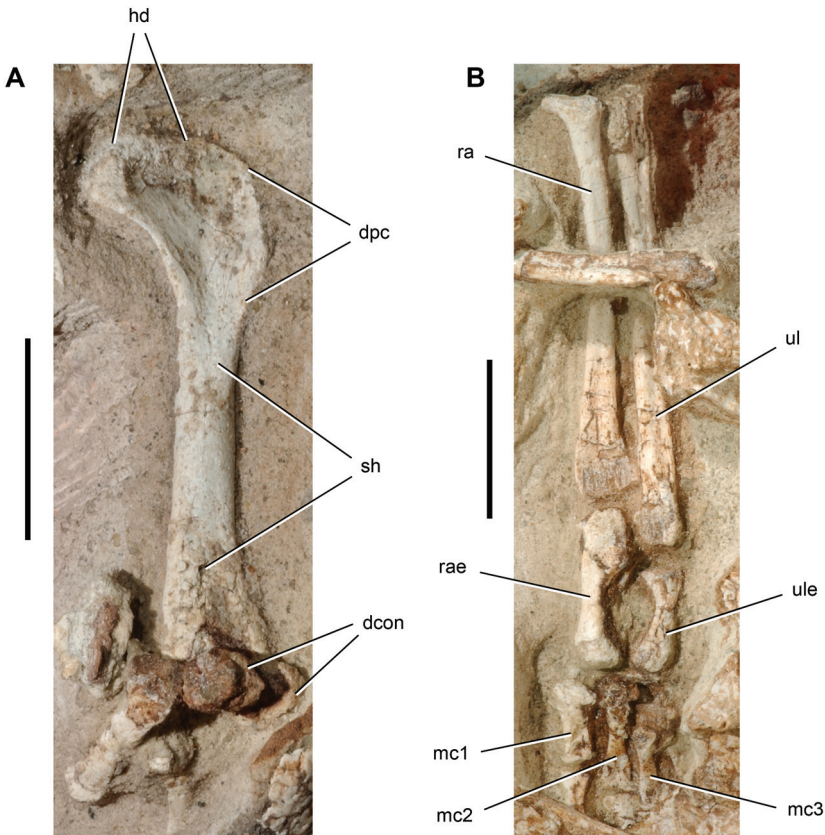


Figure 25. Forelimb bones of the crocodyliform *Araripesuchus wegneri*. **A** Left humerus in anterior view (MNN GAD20). **B** Partial right forelimb in anterior view (MNN GAD21). Scale bars equal 2 cm. Abbreviations: *dcon*, distal condyles; *dpc*, deltopectoral crest; *hd*, head; *mc1–3*, metacarpal 1–3; *ra*, radius; *rae*, radiale; *sh*, shaft; *ul*, ulna; *ule*, ulnare.

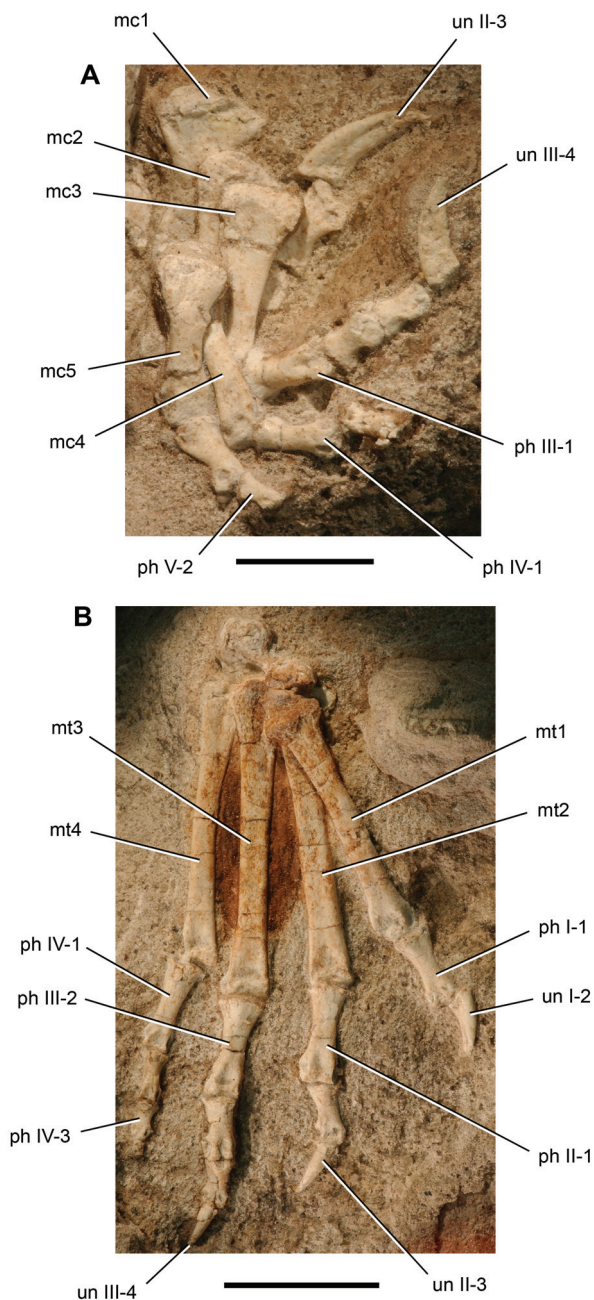


Figure 26. Manus and pes of the crocodyliiform *Araripesuchus wegneri*. **A** Right manus in dorsal view (MNN GAD22). **B** Right pes in dorsal view (MNN GAD22). Scale bar equals 1 cm in A and 2 cm in B. Abbreviations: *I–V*, digits I–V; *mc1–5*, metacarpal 1–5; *mt1–4*, metatarsal 1–4; *ph*, phalanx; *un*, ungual.

***Araripesuchus rattoides* sp. n.**

urn:lsid:zoobank.org:act:CF171699-D3FD-4B5C-909A-21C4412BCB0E

Figs. 27–30

Table 9

Etymology. *Rattus* (Latin); *-oides*, likeness (Latin). Named for the enlarged, procumbent first dentary tooth, which is reminiscent of the condition in many rodents.

Holotype. CMN 41893; right dentary preserving alveoli 1–14.

Referred material. UCRC PV3; anterior portion of left dentary preserving alveoli 1–8.

Type locality. Er Rachidia District (exact locality unknown), eastern Morocco (Fig. 1A, B). A referred specimen (UCRC PV3) was surface collected in 1990 in a small wash at Darelkarib (south of Erfoud).

Horizon. Kem Kem Beds; Upper Cretaceous (Cenomanian), ca. 95 Mya (Sereni et al. 1996). The referred specimen (UCRC PV3) appears to have come from the lower member (pers. commun. D. Dutheil).

Diagnosis. Small-bodied metasuchian (< 1 m) with an enlarged procumbent first dentary tooth that is set immediately adjacent to the midline; smaller procumbent second dentary tooth; a caniniform fourth dentary tooth that is particularly large (twice the basal dimensions of adjacent crowns); and a smooth anterior surface on the dentary symphyses with an oval fenestra opening into the first alveolus.

Dentary. The dentary of *A. rattoides* show a series of features that distinguishes it from the previously named species *A. wegneri* and from a contemporary unnamed species from Cenomanian beds in Niger that closely resembles *A. tsangatsangana* (Turner 2006). The skull in *A. rattoides* appears to be proportionately narrower than in *A. wegneri*, based on the angle of divergence of the dentary tooth row from the midline. In *A. wegneri*, the tooth row diverges at an angle between 20 and 25° from the midline (Fig. 18C), an angle matching the divergence of the upper tooth row (Figs. 14C, 15C). In *A. rattoides*, by contrast, the angle of divergence is approximately 10° (Fig. 27C), or less than half that in *A. wegneri*. The anterior end of the dentary in *A. rattoides* is proportionately deeper than in *A. wegneri* and other species of *Araripesuchus*. This difference is visible in both anterior and lateral view (Figs. 18A, D, 27A, D).

The orientation of the alveoli for teeth d1–11 is more procumbent in *A. rattoides*. The first and second alveoli project more strongly anteriorly than dorsally, a difference best appreciated in anterior view (Figs. 18D, 27D). Succeeding alveoli, including the caniniform (d4) and d5–11, are visible in lateral view (Fig. 27A), whereas they are hidden by the dorsal edge of the alveolar margin in *A. wegneri* (Fig. 18A). Despite the more pronounced anterior projection of the anteriormost pair of teeth, the symphyseal region below these teeth (Fig. 27A) is deeper than in *A. wegneri* (Fig. 18A) and in a larger contemporary of *A. wegneri* (Fig. 31A). Moreover, unlike these other species, the symphyseal articular surface of the dentary is not uniformly rugose in *A. rattoides* as it is in *A. wegneri* and its larger contemporary (Figs. 18B, 31B). The anterior portion is smooth and fenestrated, as seen in two specimens (Figs. 27B, 28C).

Tooth size is also distinctive in *A. rattoides* (Table 9). The first tooth is 75% the average diameter of the caniniform tooth (d4), which is already twice the diameter of adjacent crowns. In *A. wegneri* the first dentary tooth is small (Fig. 27C), and the caniniform is considerably less than twice as large as adjacent crowns (Fig. 20B).

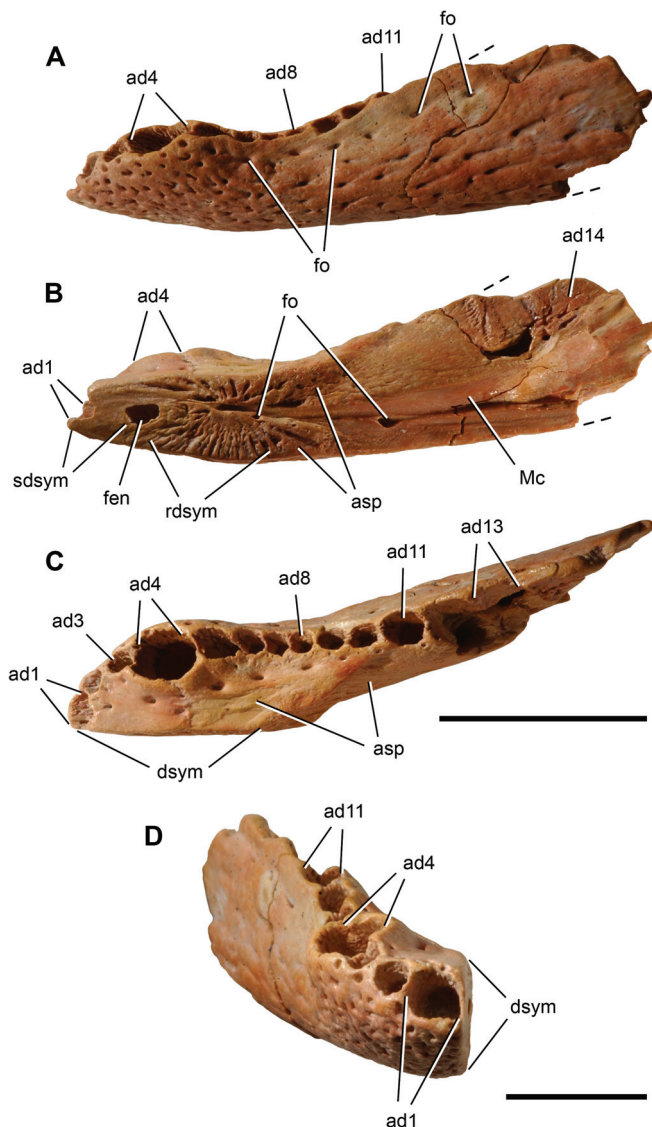


Figure 27. Right dentary of the crocodyliform *Araripesuchus rattoides* sp. n. Isolated right dentary lacking teeth (CMN 41893). **A** Lateral view (reversed). **B** Medial view. **C** Dorsal view. **D** Anterior view. Scale bars equal 2 cm in A–C and 1 cm in D. Abbreviations: *ad1*, 3, 4, 8, 11, 13, 14, alveolus for dentary tooth 1, 3, 4, 8, 11, 13, 14; *asp*, articular surface for the splenial; *dsym*, dentary symphysis; *fen*, fenestra; *fo*, foramen; *Mc*, Meckel's canal; *rdsym*, rough dentary symphysis; *sdsym*, smooth dentary symphysis.

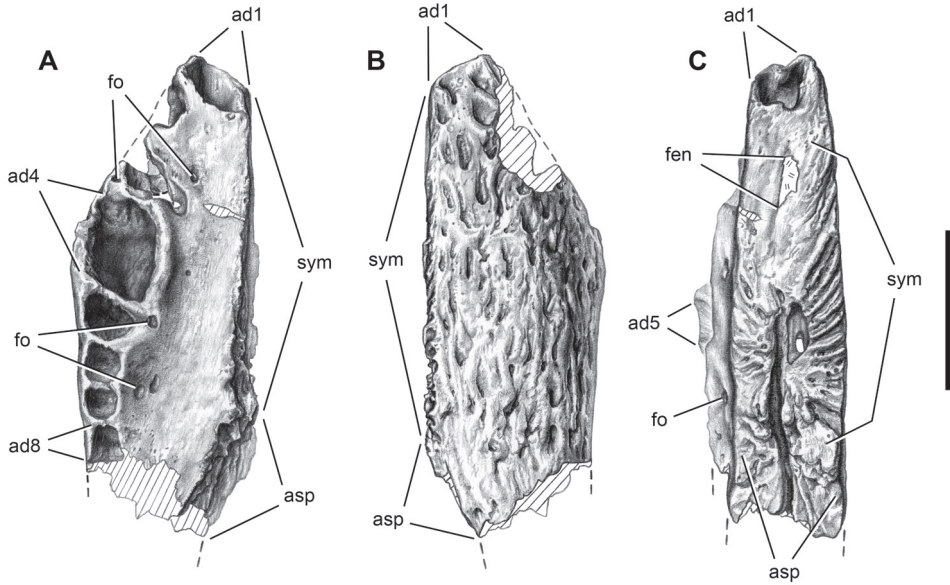


Figure 28. Left dentary of the crocodyliform *Araripesuchus rattoides* sp. n. Pencil drawing of isolated left dentary ramus lacking teeth (UCRC PV3). **A** Dorsal view. **B** Ventral view. **C** Medial view. Scale bar equals 1 cm. Parallel lines indicate broken bone surface. Abbreviations: *ad1*, 4, 5, 8, alveolus for dentary tooth 1, 4, 5, 8; *asp*, articular surface for the splenial; *fen*, fenestra; *fo*, foramen; *sym*, symphysis.

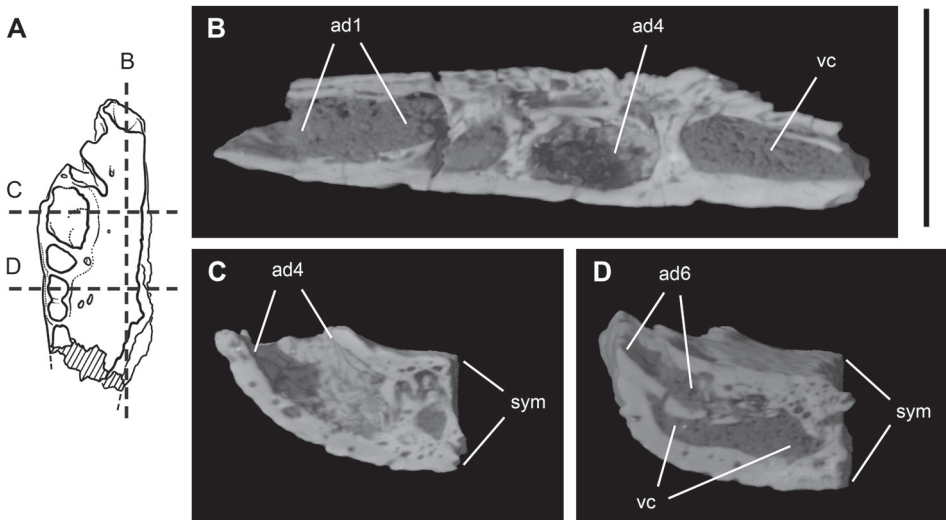


Figure 29. Computed-tomographic scan of the crocodyliform *Araripesuchus rattoides* sp. n. Isolated left dentary ramus lacking teeth (UCRC PV3). **A** Drawing in dorsal view showing the location of cross-sections (B-D). **B** Parasagittal section showing the size and orientation of the alveolus for dentary tooth 1. **C** Cross-section through the alveolus of the fourth dentary tooth. **D** Cross-section through the alveolus of the sixth dentary tooth. Scale bar for B-D equals 1 cm. Abbreviations: *ad1*, 4, 6, alveolus for dentary tooth 1, 4, 6; *sym*, symphysis; *vc*, vascular cavity.

Tooth number may have been slightly greater in *A. rattoides*. In *A. wegneri*, the largest postcaniniform teeth are d11 and d12 (Figs. 18B, 20A). In *A. rattoides* the largest postcaniniform dentary teeth are d12 and d13 (Fig. 27, Table 9).

Table 9. Dimensions (mm) of the alveoli in the holotype right dentary of *Araripesuchus rattoides* (CMN 41893). Width is labiolingual; length is mesiodistal. Parentheses indicate estimated measurement; dash indicates partially preserved alveolus, the dimension for which cannot be determined.

Alveolus	Width	Length	Comments
1	4.0	4.0	Enlarged incisiform tooth, subcircular alveolus
2	2.6	2.6	
3	2.4	2.4	Smallest incisiform tooth, subcircular alveolus
4	5.1	6.3	Caniniform tooth
5	3.0	3.5	
6	2.4	2.4	
7	1.9	2.0	Smallest tooth, subcircular alveolus
8	2.0	2.3	Second smallest tooth, subcircular alveolus
9	2.1	2.9	
10	2.3	3.3	
11	3.2	4.0	
12	(4.0)	5.0	
13	—	5.3	Largest tooth
14	—	3.8	
15	—	—	

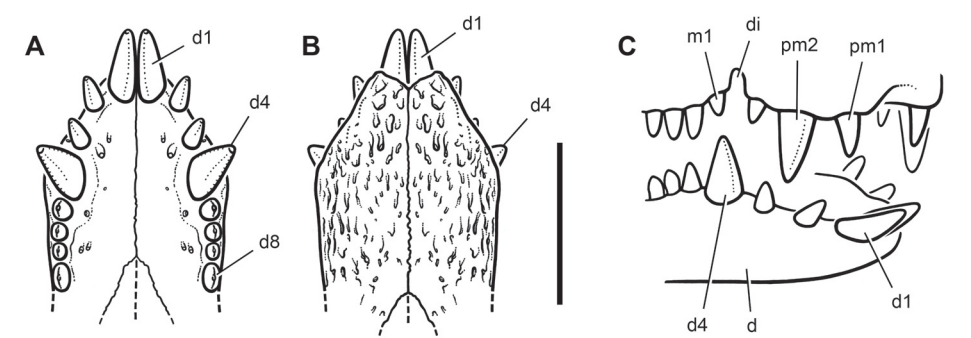


Figure 30. Reconstruction of the dentition of the crocodyliform *Araripesuchus rattoides* sp. n. Anterior dentition restored based on the size and orientation of the alveoli in CMN 41893 and UCRC PV3. **A** Dorsal view. **B** Ventral view. **C** Anterolateral view with premaxillary and anterior maxillary dentition restored to match those in the dentary. Given the presence of large, adjacent first dentary teeth, there may have been a median diastema between the premaxillary teeth and one or two fewer teeth in each premaxillary tooth row. Scale bar equals 2 cm in A and B. Abbreviations: *d1*, 4, 8, dentary tooth 1, 4, 8; *d*, dentary; *di*, diastema; *m1*, maxillary tooth 1; *pm1*, 2, premaxillary tooth 1, 2.

Other features in *A. rattoides* confirm its status as a species of *Araripesuchus*. Both *A. rattoides* and *A. wegneri* have an unusual anterior extension of the articular scar for the splenial located dorsal to the symphysis on the subhorizontal palatal surface. This articular extension of the splenial, which is located medial to the alveoli for d4–6 (Fig. 27C), is continuous posteriorly with the more typical vertical splenial attachment scar dorsal to Meckel's canal. *A. wegneri* shows a similar articular extension of the splenial (Fig. 18C). The alveoli posterior to d11, in addition, are open medially with alveolar septa poorly developed as low rounded ridges (Fig. 27B, C). A similar condition is present in *A. wegneri* (Fig. 18B) and some other species (Fig. 31C) (Pol and Apesteguía 2005).

***Araripesuchus* sp.**

Fig. 31

Material. MNN GAD27; isolated left dentary lacking teeth.

Type locality. Gadoufaoua, Agadez District, Niger Republic (more precise locality unknown) (Fig. 1A, C).

Horizon. Elrhaz Formation, Tegama Series; Lower Cretaceous (Aptian-Albian), ca. 110 Mya (Taquet 1976).

Discussion. With the notable exception of MNN GAD27, all of the cranial remains of *Araripesuchus* recovered from the Elrhaz Formation pertain to subadult or adult individuals with skull lengths between 10–15 cm. MNN GAD27, a left dentary lacking teeth with preserved crowns (Fig. 31), is approximately twice the length of the specimens described above for *A. wegneri* and *A. rattoides* and would pertain to a skull approximately 25–30 cm long.

In addition to its large size, the number of postcaniniform alveoli is greater than in other specimens. Probably at least three additional postcaniniform teeth are present. The largest teeth in the dentary of *A. wegneri* are between alveoli 10 and 13. In this larger dentary, the postcaniniform alveoli increase in size markedly starting with alveolus 13, suggesting that the comparable range for the largest dentary teeth would be alveoli 13–16.

Finally, the dorsal surface of dentary medial to the postcaniniform series (Fig. 31C) is flat, horizontal, and devoid of the accessory splenial articular scar observed in *A. wegneri* (Fig. 18B) and *A. rattoides* (Fig. 27B). In medial view, for example, no part of the nonarticular symphyseal surface medial to the tooth row is exposed, in contrast to the other African species (Figs. 27B, 28C, 31B).

The differences between this specimen and the others suggest the presence of a second, larger species of *Araripesuchus* in the Elrhaz Formation. A similar circumstance was recently proposed for fossil material recovered from the La Buitrera locality in the Candeleros Formation in Argentina (Pol and Apesteguía 2005). There, a second larger species similar in size to MNN GAD27 occurs as a contemporary of a more common smaller species of *Araripesuchus* (*A. buitreraensis*) with a skull length of under 15 cm. On the other hand, increased tooth number and better defined or developed features

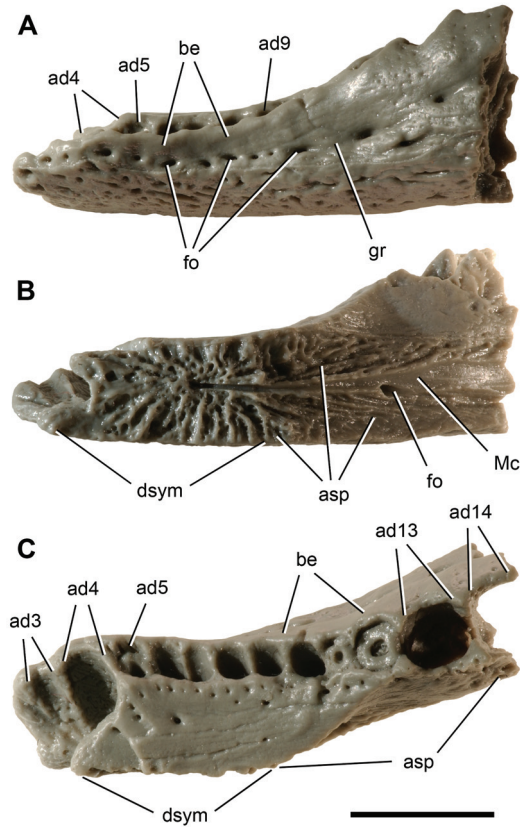


Figure 31. Left dentary of the crocodyliform *Araripesuchus* sp. Cast (UCRC PVC7) of an isolated, edentulous left dentary (MNN GAD27). **A** Lateral view. **B** Medial view (reversed). **C** Dorsal view (reversed). Scale bar equals 1 cm. Abbreviations: *ad3–5, 9, 13, 14*, alveolus for dentary tooth 3–5, 9, 13, 14; *asp*, articular surface for the splenial; *be*, buccal emargination; *dsym*, dentary symphysis; *fo*, foramen; *gr*, groove; *Mc*, Meckel's canal.

may manifest themselves in particularly large individuals within a species. We are inclined to regard MNN GAD27 as a distinct species but await confirmation from more complete remains before establishing formal taxonomic recognition.

Mahajangasuchidae fam. n.

urn:lsid:zoobank.org:act:6C28D343-821D-4CF6-B293-F12EDBB59B15

Diagnosis. Mid- to large-sized (~4–6 m) metasuchians with fused nasals, lacrimal-nasal contact absent, postorbital bearing an oval laterally facing fossa that may have served for articulation with the posterior palpebral, squamosal and parietal form a

hornlike posterodorsal process, steeply arched ventral jugal margin with a ventrolateral fossa at apex, ectopterygoid vertical and flush at jugal contact rather than arching medially, jaw articulation below posterior tooth row, pterygoid choanal septum with anterior footplate for palatine, pterygoid choanal septum with ventral edge expanded to approximately 40% of septum length, and pterygoid choanal wall invaginated dorsal to posterior margin of palate, deep mandibular symphysis oriented at approximately 45° anterodorsally, dorsolateral ridge on surangular, and maxillary tooth row terminates anterior to orbit.

Etymology. Named on the basis of *Mahajangasuchus insignis* (Buckley and Brochu 1999), the first described member of the clade. New fossil finds continue to expand basal metasuchian diversity, although interrelationships are poorly established. Establishing this stem-based taxon for *Mahajangasuchus*, *Kaprosuchus* and taxa closer to them than to several other metasuchians establishes a well known anchor among basal metasuchians, to which other taxa may eventually be assigned.

Phylogenetic definition. The most inclusive clade containing *Mahajangasuchus insignis* Buckley and Brochu 1999 but not *Notosuchus terrestris* Woodward 1896, *Simosuchus clarki* Buckley et al. 2000, *Araripesuchus gomesii* Price 1959, *Baurusuchus pachecoi* Price 1945, *Peirosaurus torminni* Price 1955, *Goniopholis crassidens* Owen 1842, *Pholidosaurus schaubbergensis* Meyer 1841, *Crocodylus niloticus* (Laurenti 1768).

Discussion. *Kaprosuchus saharicus* represents a distinctive new crocodyliform distinguished by numerous cranial autapomorphies. Derived characters shared with other crocodyliforms are limited, although a suite of features listed in the familial diagnosis above links *K. saharicus* to the unusual crocodyliform, *Mahajangasuchus insignis*, from the Upper Cretaceous of Madagascar (Buckley and Brochu 1999; Turner and Buckley 2008). These are described in more detail below (see Phylogenetic relationships).

***Kaprosuchus* gen. n.**

urn:lsid:zoobank.org:act:B8927ECE-E826-45CD-8A04-540F9E4BFE1C

Etymology. *Kapros*, boar (Greek); *souchos*, crocodile (Greek). Named for the extreme length of its three opposing pairs of caniniform teeth.

Type Species. *Kaprosuchus saharicus*.

Diagnosis. Same as for type species *K. saharicus*.

***Kaprosuchus saharicus* sp. n.**

urn:lsid:zoobank.org:act:1951A16E-5AD8-4959-AB6B-666D02B22049

Figs. 32–36

Tables 10, 11

Etymology. *Sahara*, Sahara Desert; *-icus*, belonging to (Greek). Named for the region where the holotype was discovered.

Holotype. MNN IGU12; nearly complete skull missing only portions of the right postorbital, squamosal and the middle one-third of the braincase.

Type locality. Iguidi (west of In Abangharit), Agadez District, Niger Republic (N 17° 56', E 5° 37') (Fig. 1A).

Horizon. Echkar Formation, Tegama Series; Upper Cretaceous (Cenomanian), ca. 95 Mya (Taquet 1976). In association with the crocodyliform *Laganosuchus thau-mastos*, the abelisaurid *Rugops primus*, the spinosaurid *Spinosaurus* sp., the carcharodontosaurid *Carcharodontosaurus iguidensis*, an unnamed rebbachisaurid and titanosaurian sauropods.

Diagnosis. Mid-sized (~6 m) neosuchian with the cranium characterized by parasagittal premaxillary rugosities separated by smooth margins near the midline and along the ventral alveolar margin; median keel formed along interpremaxillary suture; circumnarial fossa absent external to the rim of the external nares; rim of external nares telescoped above snout and internarial bar; premaxillary medial process forms posterior margin of the narial rim; nasal forms all of the internarial bar; lacrimal anterior ramus extends anterior to the antorbital fossa; jugal notch for surangular shifted strongly dorsomedially; fossa on jugal dorsal to coronoid process; supratemporal bar with parasagittal orientation; rugose, posterodorsally projecting squamosal-parietal horn; pneumatic spaces within the supratemporal fossa project into the base of the squamosal-parietal horn; anterior palate transversely convex and posterior palate transversely concave; choanal fossa subquadrate; choanal septum expanded ventrally with lenticular shape; and suborbital fossa transversely narrow and facing laterally.

Diagnostic features of the lower jaws include a dentary symphysis with long axis canted posteroventrally at 45° from the horizontal; surangular attachment process immediately posterior to the mandibular flange; angular ventral margin everted; hypertrophied retroarticular process (equaling quadrate length and three times the width of the quadrate condyles); retroarticular process with lateral ridge; axis of retroarticular process diverges posterolaterally; and the retroarticular ramus of the angular expands transversely toward the distal extremity of the process.

Diagnostic features of the dentition include hypertrophied premaxillary, maxillary and dentary caniniforms extending dorsal and ventral to the maxilla and dentary, respectively; nearly straight, labiolingually compressed crowns; pm1 rotated so that the lingual crown surface faces posterolaterally to oppose d1 caniniform; small noncaniniform maxillary teeth; d1 and d2 project dorsally into premaxillary pits, d1 enlarged relative to d2; and d3 (rather than d4) constitutes the lower caniniform.

Dorsal skull roof. The cranium of *Kaprosuchus* presents a unique morphological hybrid that combines aspects of two of the cranial forms commonly encountered among crocodylomorphs (Langston 1973; Brochu 2001). The snout has generalized proportions with a dorsally opening naris. Normally the teeth in this skull form are subconical and of moderate length, and the posterior skull of moderate depth. In *Kaprosuchus*, by contrast, the generalized snout is paired with hypertrophied, labiolingually compressed caniniforms and a posterior skull with deep proportions (Figs. 32–34).

The external nares are telescoped dorsally with a sharp rim (Fig. 35A). In profile (Figs. 33A, 34A), the snout ascends as it joins the orbital rim and skull table, beyond which the squamosal horns project at a conspicuous angle (Fig. 36A). The antorbital fenestra is narrow but elongate and partially surrounded by a fossa (Fig. 35B). Despite the dorsoventrally flattened snout, the subcircular orbits open laterally more than vertically and are angled anteriorly, suggesting that there may have been overlap in the visual fields (Fig. 36A). The supra- and laterotemporal fenestrae are relatively small, reflective of the relatively short skull table (Figs. 33B, 34B).

Most of the cranial surface has linear sculpting, with subcircular pitting predominant only on the frontals. Two aspects of surface texture require special comment. The anterior surface of the premaxilla has a raised rugose texture with several neurovascular openings (Figs. 35A, 36). The second unusual feature is branching impressed vessel tracts, a pair of which emerge from the anterior end of the antorbital fenestra (Figs. 33B, 34B). The more posterior of these tracts bifurcates distally, with one sub-branch curving ventrally to the alveolar margin by maxillary tooth 7 and a second sub-branch curving posteriorly onto the anterior end the jugal. The more anterior of these tracts courses anteriorly along the snout margin, with a pair of sub-branches curving to the alveolar margin by the diastema and by the posterior margin of the third maxillary caniniform (Figs. 33A, 34A).

The *premaxilla* forms the broad snout end (Figs. 33, 34, 35A, 36A). Most of the external surface of the bone has a rugose texture that is sharply delimited by smooth margins along the interpremaxillary suture medially and along the alveolar margin ventrally. As a result, the paired rugosity strongly resembles a well-trimmed “mous-



Figure 32. Skull of the crocodyliform *Kaprosuchus saharicus* gen. n. sp. n. Articulated cranium and lower jaws in anterolateral view (MNN IGU12). Scale bar equals 10 cm.

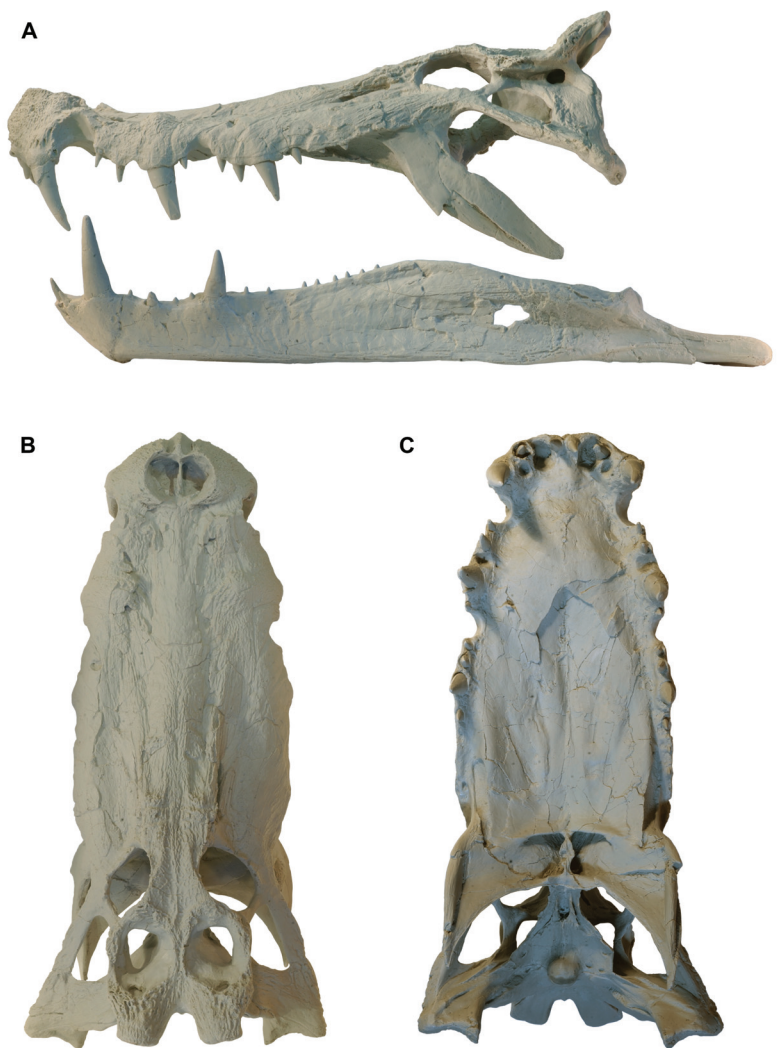


Figure 33. Skull of the crocodyliform *Kaprosuchus sabaricus* gen. n. sp. n. Cast (UCRC PVC8) of cranium and lower jaws (MNN IGU12), which were separated from a cast of the skull (which remains in one piece). Left maxillary teeth 1 and 8 were missing and are based on the corresponding right maxillary teeth. Dentary teeth 9–16 cannot be seen as a result of the adduction of the jaws but were visualized and then reconstructed on the basis of a computed-tomographic scan. A portion of the right side of the skull table is not preserved and is a reflection from the left side. Most of the occiput is not preserved and has been reconstructed. **A** Cranium and lower jaws in left lateral view. **B** Cranium in dorsal view. **C** Cranium in ventral view. Scale bar equals 20 cm.

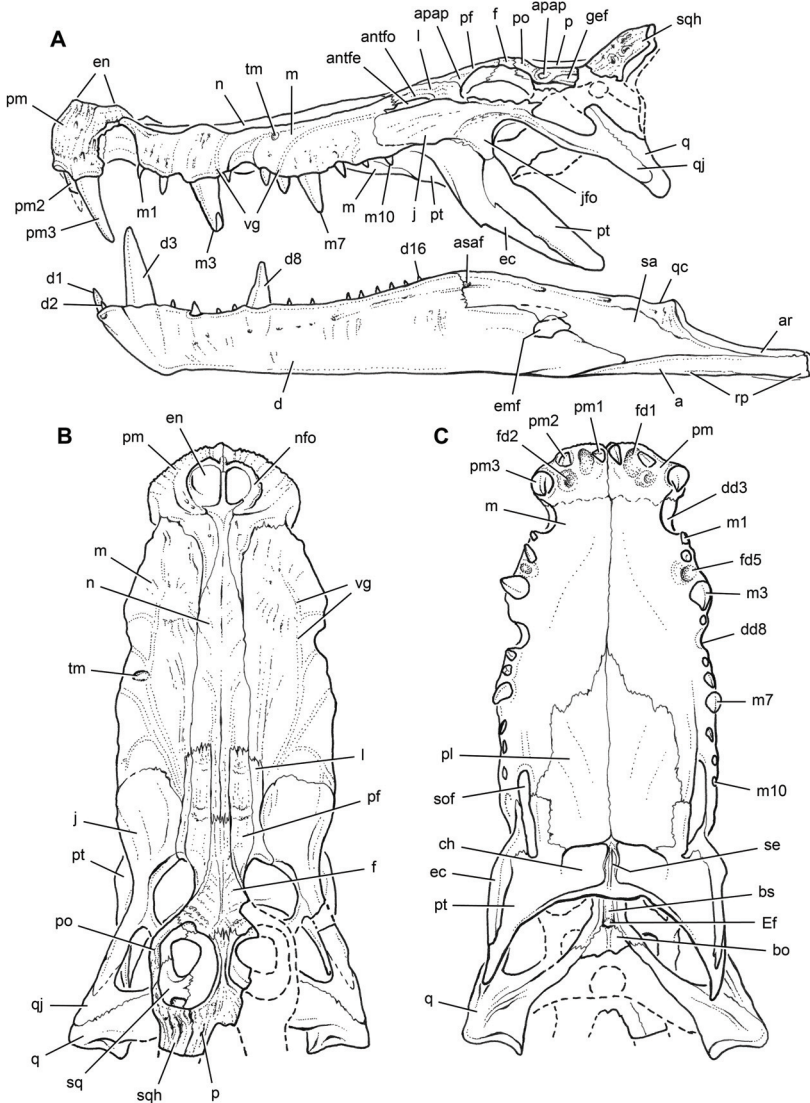


Figure 34. Skull of the crocodyliform *Kaposuchus sabaricus* gen. n. sp. n. Drawings matching the cranium and lower jaws (MNN IGU12) in Fig. 33. **A** Cranium and lower jaws in left lateral view. **B** Cranium in dorsal view. **C** Cranium in ventral view. Dashed line indicates missing bone or tooth crown. Scale bar equals 20 cm. Abbreviations: *a*, angular; *antfe*, antorbital fenestra; *antfo*, antorbital fossa; *apap*, articular surface for palpebral; *ar*, articular; *asaf*, anterior surangular foramen; *bo*, basioccipital; *bs*, basisphenoid; *ch*, choana; *d*, dentary; *d1*–3, 8, 16, dentary tooth 1–3, 8, 16; *dd3*, 8, diastema for dentary tooth *d3*, *d8*; *ec*, ectopterygoid; *Ef*, Eustachian foramen; *emf*, external mandibular fenestra; *en*, external naris; *f*, frontal; *fd1*, 2, 5, fossa for dentary tooth 1, 2, 5; *gef*, groove for ear flap; *j*, jugal; *jfo*, jugal fossa; *l*, lacrimal; *m*, maxilla; *m1*, 3, 7, 10, maxillary tooth 1, 3, 7, 10; *n*, nasal; *nfo*, narial fossa; *p*, parietal; *pf*, prefrontal; *pl*, palatine; *pm*, premaxilla; *pm1*–3, premaxillary tooth 1–3; *po*, postorbital; *pt*, pterygoid; *q*, quadrate; *qc*, quadrate cotylus; *qj*, quadratojugal; *rp*, retroarticular process; *sa*, surangular; *se*, septum; *sof*, suborbital fenestra; *sq*, squamosal; *sqh*, squamosal horn; *tm*, tooth mark; *vg*, vascular groove.

Table 10. Dimensions (mm) of the skull of *Kaprosuchus saharicus* (MNN IGU12). Paired structures measured on left side except as indicated. Parentheses indicate estimated measurement.

Structure	Measurement	Length
Dorsal skull roof	Cranium, maximum length (premaxilla to quadrate condyle)	507.0
	Cranium, width across posterior tip of squamosals	(112.0)
	Cranium, width across quadrate condyles	213.8
	Snout, maximum transverse width	179.4
	Snout, minimum transverse width (at notch for dentary canine)	105.1
	External naris, anteroposterior length	36.9
	External naris, maximum transverse width	55.2
	Antorbital fossa length	(73.0)
	Antorbital fenestra length	38.5 ¹
	Antorbital fenestra, maximum height	9.7 ¹
	Interorbital skull roof, minimum width	37.0
	Orbital anteroposterior diameter	59.6
	Orbital dorsoventral diameter	47.6
	Jugal orbital ramus, depth at mid-length	26.1
	Jugal lower temporal bar, minimum depth	14.5
	Postorbital bar, minimum anteroposterior diameter	7.4
	Laterotemporal fenestra length	59.7
	Laterotemporal fenestra depth	(28.5) ¹
	Supratemporal fossa, anteroposterior length	60.9
	Supratemporal fossa, transverse width	44.1
Palate	Quadrate shaft length	(107.0)
	Quadrate condyles, transverse width	52.6
	Pterygoid mandibular processes, maximum transverse width	177.8
	Choana, maximum anteroposterior length	35.5
Lower jaw	Lower jaw, maximum length (to end of retroarticular process)	603.0
	Lower jaw, anterior end, transverse width	105.6
	Lower jaw, mid-section end, transverse width	20.9
	Lower jaw, retroarticular process distal tips, transverse width	238.0
	Symphysis (dentary and splenial)	81.3
	External mandibular fenestra, length	39.0
	External mandibular fenestra, depth	16.1
	Retroarticular process, length	122.7
	Retroarticular process, transverse width at mid-length	32.5

¹Measurement from right side.

tache” in anterior view (Fig. 36A). The edges of the rugosity are elevated above the body of the premaxilla, suggesting that the rugosity is a product of secondary growth. This surface likely supported a keratinous shield of some kind, as is often the case for rugose, elevated, vascularized bone among extant amniotes.

The alveolar margin of the premaxilla is rounded and gently scalloped between the premaxillary teeth. the alveolar margin descends toward the large alveolus of the caniniform pm3. In the midline, the interpremaxillary suture lies in a trough near the alveolar margin but projects as a crest between the rugosities (Fig. 36A). The rim of the external naris is gently everted (Fig. 36A). In dorsal view, swollen premaxillary processes extend the elevated rim to the posterior side of the external naris (Fig. 35A). The posterior ramus of the premaxilla meets the maxilla along a raised suture. The medial margin of the ramus approaches the midline, reducing the nasals to a narrow fused median strut (Figs. 33B, 34B).

The medial two-thirds of each *maxilla* is oriented horizontally whereas the lateral one-third is oriented vertically. In lateral view, the anterior end of the maxilla is deeply notched to accommodate a large caniniform d3 (Figs. 33A, 34A). A large dorsal bulge is present over the caniniform m3 to accommodate its root (Fig. 36B). Three distinct ridges are present on the dorsal aspect of the maxilla. The first curves posteromedially from the notch for the caniniform d3 to the maxilla-nasal suture; the second curves from the alveolar bulge over the caniniform m3 to the maxilla-nasal suture; and the third arises along the dorsal margin of the antorbital fenestra. The second and third ridges join posterodorsally to form a V-shaped junction on the prefrontal, which is located dorsal to the posterior end of the antorbital fenestra. The posterior rami of the maxilla diverge. The posteroventral ramus maintains a horizontal orientation, whereas the posterodorsal ramus ascends at 45° toward the orbital rim.

The *nasal* is elongate, transversely arched, and fused to its opposite anteriorly and along its mid-section (Figs. 33A, 34A). The nasals form all but the anteriormost extremity of the internarial bar. The nasals contact the frontals along a transverse interdigitating suture. The nasal-maxilla suture has a fine saw-tooth pattern, with projections on the nasal pointed anterolaterally.

The *prefrontal* has anterior, posterior and ventral rami. The subrectangular anterior ramus is the longest, butting at its anterior extremity against a notch in the nasals along a slightly elevated squamous suture. At mid-length along this ramus, there is a raised, rugose V-shaped ridge, proximal to which is an arcuate groove. The central body of the prefrontal is inset for attachment of an anterior palpebral (Fig. 35B). The tapered posterior end of the subtriangular posterior process is inset into frontal along the orbital rim, which is gently everted. Its dorsal surface is recessed before meeting the frontal medially along a raised suture (Fig. 35B). The ventral ramus must have tapered strongly in width, angling toward the midline, where the base of the “pillar” is preserved. It expands anteroposteriorly to form a solid buttress to the palatine on the palate.

The central body of the *lacrimal* is subquadrate, from which extend a long anterior and a short ventral ramus. Nearly all of this bone is oriented in a vertical plane. The orbital margin is beveled, presenting a smooth surface in lateral view (Fig. 35B). The dorsal edge of the anterior ramus is everted and rugose, joining the prefrontal along a ridge dorsal to the antorbital fenestra. The lacrimal forms the C-shaped posterior margin of this fenestra, contributing to its ventral margin and half of its dorsal margin. The lacrimal also forms most of the antorbital fossa, which is located on the dorsal side of the fenestra (Fig. 35B).

The *frontal* is fused to its opposite. The composite element is diamond-shaped in dorsal view, with interdigitating nasal and parietal sutures anteriorly and posteriorly. The fused interfrontal suture is raised into a low sagittal crest (Figs. 33B, 34B). The orbital margin is slightly everted (Figs. 33A, 34A). The frontal is excluded from entering

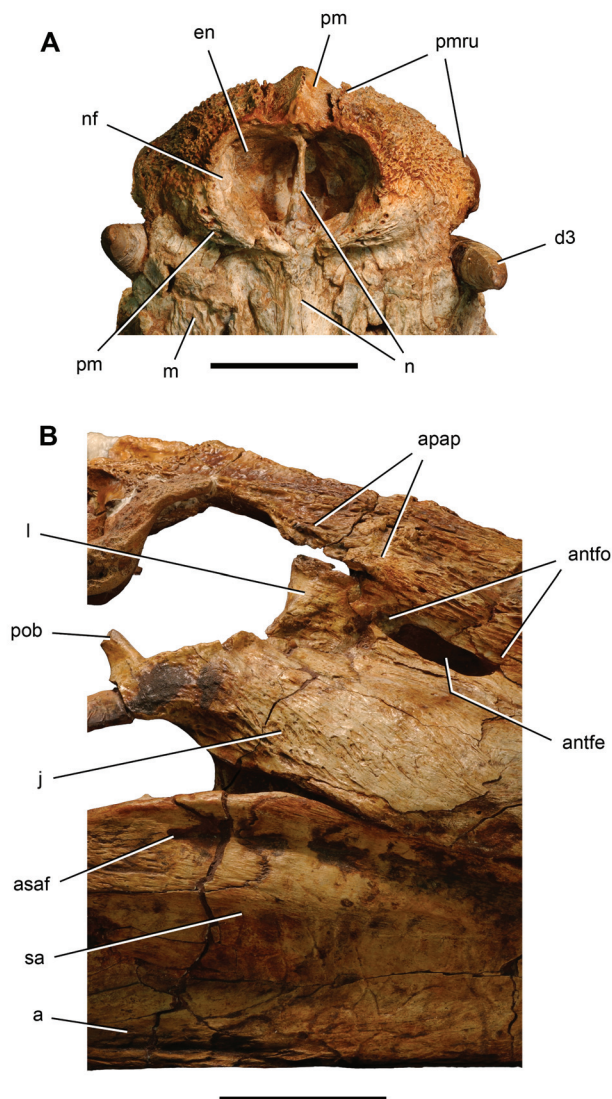


Figure 35. Skull of the crocodyliform *Kaprosuchus saharicus* gen. n. sp. n. Detailed views of the external nares and orbital region (MNN IGU12). **A** Snout end in dorsal view. **B** Orbital, antorbital, and coronoid regions of the skull in right lateral view. Scale bars equal 5 cm. Abbreviations: *a*, angular; *antfe*, antorbital fenestra; *antfo*, antorbital fossa; *apap*, articular surface for the palpebral; *asaf*, anterior surangular foramen; *d3*, dentary tooth 3; *en*, external naris; *j*, jugal; *l*, lacrimal; *m*, maxilla; *n*, nasal; *nf*, narial fossa; *pm*, premaxilla; *pmru*, premaxillary rugosity; *pob*, postorbital bar (jugal portion); *sa*, surangular.

the supratemporal fossa by the parietal and postorbital, the latter contacting the frontal along an interdigitating suture.

The *parietal* is fused to its opposite forming a very narrow skull table between the supratemporal fossae (Figs. 33B, 34B). That surface is rugose, depressed in the midline, and raised into a sharp edge along the medial rim of the supratemporal fossa, closely resembling the condition in *Mahajangasuchus* (Turner and Buckley 2008). The posterior edge of the parietals overhangs the occiput forming a posterior cranial margin that would have extended at least 1 cm beyond the occiput. The posterolateral portions of the parietals extend even further posterodorsally to form the medial portion of the base of the squamosal horn. That interdigitating parietal-squamosal suture passes anterolaterally along the medial margin of the enlarged foramen within the fossa. The ventral contact with the supraoccipital has a pneumatic recess, suggesting that the mastoid antrum in the supraoccipital likely passed dorsally into the parietal.

The triradiate *postorbital* forms the posterior margin of the orbit, anterolateral margin of the supratemporal fenestra, and anterior margin of the laterotemporal fenestra. The medial process is broad, its posterior one-third devoted to the smooth margin of the supratemporal fossa. The subtriangular posterior process is deeply notched laterally for the anterior process of the squamosal. The ventral process is inset and continuous posteriorly within the auditory fossa.

The tetraradiate *squamosal* has anterior, medial, posterior and posterodorsal rami, although only the medial and posterodorsal rami are preserved. The medial ramus forms most of the posterior margin of the supratemporal fenestra and surrounds the enlarged pneumatized opening to the posttemporal canal. The novel posterodorsal ramus is an elaboration of the posterior margin of the skull table (Fig. 32). It extends posterodorsally from the skull table at least two centimeters posterior to the occiput and has a markedly pitted and rugose surface. Broken along its distal edge, the process may have been longer and/or continued in keratin. Even at its preserved length, it is particularly prominent in anterior view of the skull (Fig. 36A). Other crocodylians have been reported with squamosal horns, the most exaggerated occurring in "*Crocodylus*" *robustus* (Brochu 2006). In this case and other crocodylids, the horn is an elaboration of the lateral edge of the squamosal rather than the posterior margin, and there is no contribution from the parietal.

The *jugal* has anterior, dorsal and posterior rami and forms the slightly everted ventral margin of the orbit. The anterior ramus is tongue-shaped and particularly broad, whereas the posterior ramus is strap-shaped. Both are oriented so they are more broadly exposed in dorsal than lateral views (Figs. 33A, B, 34A, B), as in *Mahajangasuchus* (Turner and Buckley 2008). Furthermore, as in *Mahajangasuchus*, the anterior and posterior rami are separated by a deep embayment, such that in lateral view the ventral margin of the anterior ramus is angled posterodorsally whereas that of the posterior ramus angles posteroventrally (Figs. 33A, 34A). Distinctive fossae are also present on each ramus, facing laterally on the anterior ramus and ventrally on the posterior ramus, again as in *Mahajangasuchus* (Turner and Buckley 2008).

The V-shaped *quadratojugal* forms a broad plate at the posterior corner of the laterotemporal fenestra. The anterior ramus and the anterior one-half of the dorsal

ramus are textured. The quadratojugal extends toward the lateral quadrate condyle, wrapping onto its ventral side, but does not participate in the jaw articulation. The quadratojugal-quadrate suture is visible near the jaw articulation but fuses as it passes anterodorsally. The dorsal contacts of the quadratojugal are not preserved.

Palate. The premaxillary palate is exposed only near the alveolar margin, where there are located two deep fossae, which accommodate the crowns of the first and second dentary teeth. The first dentary tooth is larger than the second, and the fossa on the premaxilla is correspondingly very large, its anterior margin extending between pm1 and pm2 to reach the anterior margin of the premaxilla (Figs. 33C, 34C). A second smaller fossa for the smaller d2 is located posterior to pm2. Although uncommon, an enlarged anteriorly placed fossa on the premaxillary palate separating pm1 and pm2 occurs in some extant crocodylians such as *Osteolaemus* (Iordansky 1983). *Mahajangasuchus* has an enlarged d1 (Buckley and Brochu 1999) and apparently has a premaxillary palate with a similarly positioned enlarged fossa (Turner and Buckley 2008). The palatal shelves of the maxillae contact along their length and form a broad, U-shaped secondary palate that appears to curve ventrally from the premaxillary palate (Figs. 33C, 34C).

The *palatine* forms most of the broad posterior one-half of the secondary palate (Figs. 33C, 34C). A slender process extends between the maxillae anteriorly. Posteriorly, the palatine forms the straight, nearly transverse anterior margin of the choana. Laterally, the palatine expands but does not reach the narrow suborbital fenestra, separated from that opening on both sides of the palate by a narrow contact between the maxilla and pterygoid. This unusual condition is absent in *Anatosuchus* (Figs. 5C, 6C), *Araripesuchus* (Figs. 14C, 15C), *Mahajangasuchus* (Turner and Buckley 2008) and may be unique among crocodyliforms. The suborbital fenestrae are shifted to the lateral edge of the palate. Because the lateral margin formed by the maxilla and ectopterygoid is shifted dorsally, the fenestra opens laterally as much as ventrally and is nearly obscured in ventral view (Figs. 33C, 34C). In this regard, *Kaprosuchus* is clearly derived and quite distinct from the aforementioned crocodyliforms (Turner and Buckley 2008).

The *pterygoid*, fused to its opposite, has a broad palatal ramus that forms the remainder of the border of the choana and extends laterally over the palatines to border the suborbital fenestra. The lateral border of the choana is flat and lacks a discrete edge (Figs. 33C, 34C). At the anterolateral corner of the choana, the pterygoid has a short medial process that supports the palatine. The choanal septum is strut-shaped anteriorly and posteriorly but has an expanded ventral margin centrally. Lenticular fossae are present on either side of a thin median septum. The posterior rim of the choana is sturdy and rod-shaped without any processes. The choanal fossa is invaginated under this rim. The pterygoids extend laterally and posteriorly, so the posterior margin of the palate is deeply U-shaped, unlike the less embayed margin in *Anatosuchus* (Figs. 5, 6), *Araripesuchus* (Figs. 14C, 15C), and *Mahajangasuchus* (Turner and Buckley 2008) but similar to the deeply embayed posterior margin of the palate in baurusuchids such as *Stratiotosuchus*.

The *ectopterygoid* twists into a vertical plane, anteriorly, forming the lateral edge of the suborbital fenestra. Posteriorly, the ectopterygoid extends as the swollen lateral margin of the pterygoid flanges.

The *quadrate* angles posteroventrally to the jaw articulation in lateral view (Figs. 33A, 34B). The condyles are broad and transversely oriented, the lateral condyle larger and more convex. A subcircular fossa is present dorsal to the condyles. A foramen on the medial edge of the fossa just dorsal to the medial condyle is identified as the opening of the siphoneal foramen.

Braincase. The parasphenoid and posterior two thirds of the braincase are not preserved. The ventral portion of the *basioccipital* and *basisphenoid* are present, their ventral surface inclined anteroventrally at approximately 45°. A low median crest is present on the basioccipital, anterior to which is a large Eustachian foramen. The basisphenoid has limited ventral exposure between the pterygoids and basioccipital, as in *Anatosuchus* and *Araripesuchus*. Two crests are present on the basisphenoid to either side of the Eustachian opening (Figs. 33C, 34C).

Lower jaw. The jaws are shut with prominent crowns fitted snugly into notches in the opposing jaw margin (Fig. 32). Separation of the jaws would have risked damage to the teeth and alveolar margins. The skull was subjected to a computed-tomographic scan to locate small dentary crowns covered from view by the maxilla, and then a cast of the skull was cut apart with hidden teeth restored (Figs. 33A, 34A).

Unlike the sculpted bones of the cranium, most of the external surface of the lower jaw is lightly textured. Only the symphyseal margin and posterior one-quarter of the lower jaws are sculpted.

The *dentary* is dorsoventrally deep with a nearly vertical lateral surface marked by shallow vertical undulations (Figs. 33A, 34A). Posteriorly, in the region of the coronoid process, the depth of the dentary exceeds that of the dorsal skull roof, as in *Mahajangasuchus* (Buckley and Brochu 1999; Turner and Buckley 2008). As in that genus, the prominence of the coronoid process is accommodated by a marked embayment in the jugal. Anteriorly, the symphysis is robust, deep, and angled posteroventrally at approximately 45°. In ventral view, the symphysis is U-shaped. An interdigitating interdental suture did not allow movement at the symphysis. The alveoli of the enlarged caniniform third dentary tooth bulges laterally, as the dentary curves posteriorly. Ventrally, the crypt for the root of this tooth bulges to each side of the symphysis.

Posteriorly, the dentary tapers in depth from the coronoid process. The dentary-surangular suture is L-shaped. It descends vertically from the coronoid process, and then continues horizontally toward the external mandibular fenestra. At the fenestra, the dentary is split into dorsal and ventral rami, which form most of the boundary of this opening (Figs. 33A, 34A). *Mahajangasuchus* apparently does not have a comparable dentary process ventral to the fenestra. In *Anatosuchus* and *Araripesuchus* a short process is present, but it does not border the fenestra (Figs. 5, 6, 14, 15). In *Kaprosuchus* the dentary is a remarkably long element, extending posteriorly to a point nearly ventral to the quadrate cotylus.

A thin medial process of the *splénial* meets its opposite on the posteroventral edge of the symphysis. At the base of the process lies a large oval foramen between the splénial and dentary. The remainder of the splénial contributes to the ventral margin of the lower jaw and forms a thin vertical plate on the medial aspect of the dentary.

The *surangular* forms the posterior one-half of the coronoid process, from which exits a large anterior surangular foramen. A pointed bone spur, presumably a prominent tendon attachment, is located on the dorsomedial edge of both the left and right surangular. The upper one-half of the surangular flares laterally near the glenoid, posterior to which it tapers to the tip of the very long retroarticular process. The surangular forms the lateral portion of the articular cup of the glenoid. There is no articular contact between the surangular and quadratojugal (Figs. 33A, 34A).

The ventral margin of the *angular* ventral to the external mandibular fenestra is deflected laterally. The angular forms the ventral margin of the external mandibular fenestra and extends along the lateral aspect of the hypertrophied retroarticular process. The *articular* forms the majority of the glenoid and the body of the nearly straight retroarticular process. The articular is exposed along the medial aspect of the process and faces dorsomedially, as in *Anatosuchus* and *Araripesuchus*. The *prearticular* sheathes the ventral aspect of the retroarticular process.

Dentition. The dentition of *Kaprosuchus* is noteworthy for the hypertrophied caniniform teeth in the premaxillae, maxillae and dentaries, which project above and below the skull (Fig. 32). All exposed crowns are labiolingually compressed and have smooth mesial and distal carinae. There are only three *premaxillary teeth*. Pm1 is the smallest, its crown rotated laterally so that its lingual crown surface more directly opposes the more laterally situated d1 (Fig. 36). As a result, the pm1 crowns appear to diverge in anterior view of the premaxilla (Fig. 36A). The larger pm2 is rotated in the opposite direction, so that its lingual crown surface is canted posteromedially. The carinae on both pm1 and pm2 are displaced lingually, giving these teeth an incisiform shape. The caniniform pm3 is rotated so its lingual crown surface opposes the bend in the mandibular ramus, and the axis of the crown is deflected posteroventrally (Fig. 36A, B). A substantial gap is needed before the tips of opposing premaxillary and anterior dentary caniniforms clear one another (Figs. 33A, 34A).

There are 10 *maxillary teeth* in the heterodont right maxillary tooth row, which is completely exposed. The first maxillary tooth projects anteroventrally, canted toward the large dentary caniniform. It is the most slender tooth in the maxillary series. The larger second maxillary tooth projects ventrally and is separated from the third maxillary tooth by a fossa for the fifth dentary tooth. The presence of this fossa, is the reason the alveolar margin between m2 and m3 is deeply festooned (Figs. 33A, 34A, 36B). The large caniniform m3, which is directed ventrally, is followed by m4, one of the smallest teeth in the series. M4 and m5 straddle a large dentary caniniform, with m4 canted posteroventrally toward that tooth. M6 is transitional in size to m7, the posterior smaller maxillary caniniform, which is directed posteroventrally. M8–10 form a trailing series of increasingly smaller teeth that are directed more strongly posteroventrally.

There are probably 16 *dentary teeth*. D1–3, d5, and d8 are exposed, and the remaining smaller teeth were visualized in a computed-tomographic scan. The first and second dentary teeth are incisiform only in that their carinae appear to be shifted more strongly lingually. D1 is more than twice the size of d2. The fully erupted crown on the right side has a basal diameter of approximately 1 cm and a length of approximately 3 cm, which is subequal to that of caniniform m7. D1, the crown of which is accommodated by a large diameter and deep premaxillary fossa, is regarded here as a caniniform.

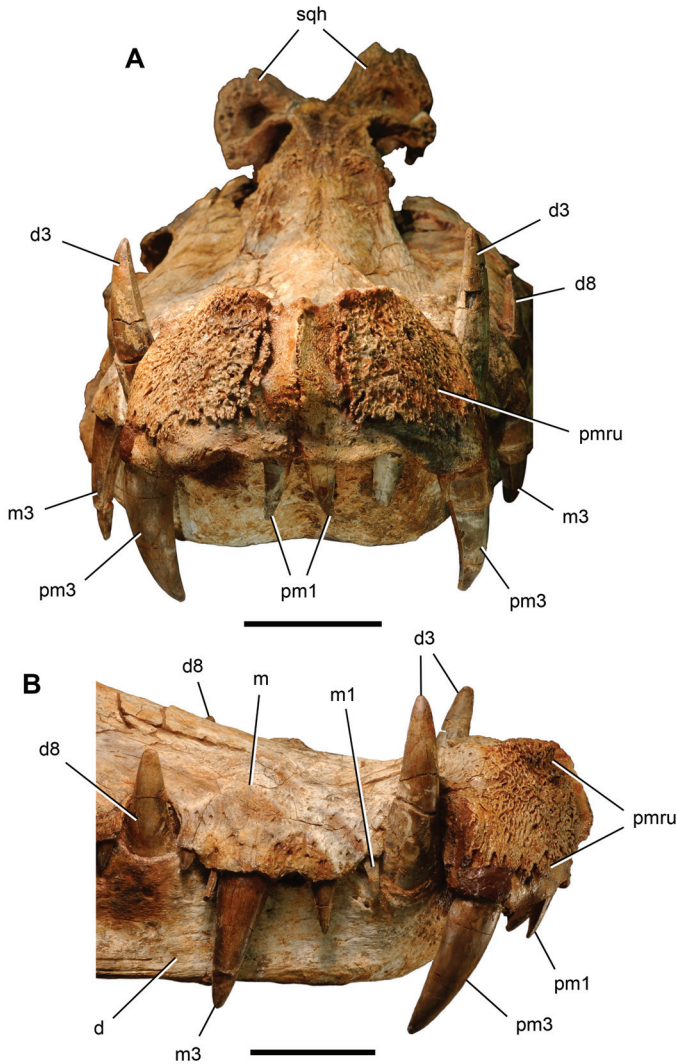


Figure 36. Snout of the crocodyliform *Kaprosuchus sabaricus* gen. n. sp. n. Detailed views of the snout and dentition (MNN IGU12). **A** Premaxillary dentition in anterior view. **B** Upper and lower dentitions in right lateral view. Scale bars equal 5 cm. Abbreviations: *d*, dentary; *d3*, 8, dentary tooth 3, 8; *m*, maxilla; *m1*, 3, maxillary tooth 1, 3; *pm1*, 3, premaxillary tooth 1, 3; *pmru*, premaxillary rugosity; *sqh*, squamosal horn.

Table 11. Dimensions (mm) of crowns in the jaws of *Kaprosuchus saharicus* (MNN IGU12). Measurements from the right side except for premaxillary crowns 2 and 3 and maxillary crowns 8–10. Parentheses indicate estimated measurement. Asterisks indicate caniniform crowns. Abbreviations: *d*, dentary; *m*, maxillary; *pm*, premaxillary.

Tooth Number	Crown height	Mesiodistal width
d1	(34.7)	14.4
d2	7.4	7.8
d3*	65.3	24.5
d8*	41.3	19.2
pm1	22.6	9.4
pm2	(44.1)	12.6
pm3*	58.8	20.0
m1	12.4	7.4
m2	23.1	10.6
m3*	51.5	19.7
m4	8.2	5.8
m5	13.4	8.0
m6	16.3	9.3
m7	33.2	17.3
m8	14.4	8.4
m9	4.4	5.8
m10	4.2	6.3

D3 is the largest dentary caniniform and is canted slightly anterodorsally. D8 is slightly larger than caniniform d1 and is canted slightly posterodorsally.

Stomatosuchidae Stromer, 1925

Revised diagnosis. Mid- to large-sized (~4–8 m) metasuchians with elongate cranial proportions (jaw length from the jaw articulation approximately five times maximum width); U-shaped lower jaws with very gently bowed dentary rami in horizontal and vertical planes; extremely slender dentary ramus (jaw length from the glenoid approximately 30 times depth of jaw at mid-length); dentary ramus with minimum depth at tooth positions d5 and d6; coronoid process transversely broad with horizontal dorsal surface (maximum width approximately 85% maximum height); external mandibular fenestra very reduced or closed; splenial symphysis absent.

Phylogenetic definition. The most inclusive clade containing *Stomatosuchus inermis* Stromer 1925 but not *Notosuchus terrestris* Woodward 1896, *Simosuchus clarki* Buckley et al. 2000, *Araripesuchus gomesii* Price 1959, *Baurusuchus pachecoi* Price 1945, *Peirosaurus torminni* Price 1955, *Crocodylus niloticus* (Laurenti 1768).

Discussion. In 1925 Stromer described a most unusual crocodyliform from the early Late Cretaceous (Cenomanian) Bahariya Formation of Egypt (Stromer 1925). *Stomatosuchus inermis* has an elongate, flattened “duck-faced” cranium nearly two meters in length, and U-shaped lower jaws that are extremely slender (Fig. 2). The relatively smooth cranium has dorsally directed orbits situated posteriorly and about 30 relatively small, closely spaced teeth in the anterior one-half of the upper jaw (Fig. 2A, F). Only the alveoli are preserved, which are oval with the larger alveoli averaging about 1.5 cm in maximum length (Stromer 1925). Posteriorly, the alveoli decrease in size and merge to form a groove at mid-length along the upper jaw (Stromer 1925; Nopcsa 1926).

The coronoid process of the lower jaw is low and transversely broad (Fig. 2C), and the dentary ramus is straight in dorsal and lateral views (Fig. 2B, C), before the jaw curves abruptly toward the symphysis (Stromer 1925). The symphysis is not preserved, and so there is no evidence to justify later remarks that the symphysis was particularly weak or “moveable” (Steel 1973). The external mandibular fenestra is apparently closed (Fig. 2B, G). The retroarticular process is well developed, relatively short, and projects posteriorly. In both medial and dorsal views, the process is subrectangular and does not taper distally.

The holotype and only known specimen of *Stomatosuchus* was destroyed in World War II, and no additional material of this taxon has ever been discovered. With only the brief accounts by Stromer (Stromer 1925, 1936) and Nopcsa (1926), the taxon has remained enigmatic. *Stomatosuchus* is closest in general form to *Mourasuchus* (= *Nettosuchus*), a “nettosuchid” alligatoroid of Miocene age from Columbia (Langston 1965). *Mourasuchus* also has an extremely low, “duck-faced” cranium, dorsally facing posteriorly positioned orbits, and extremely slender, U-shaped lower jaws. The lower jaw, furthermore, resembles new stomatosuchid material described below in having a dentary with a festooned alveolar margin and slightly enlarged first dentary tooth. Recent phylogenetic work has confirmed the position of *Mourasuchus* as a close relative of *Purussaurus* among alligatorids (Aguilera et al. 2006).

More detailed comparisons, however, show that *Stomatosuchus* and *Mourasuchus* are not closely related and share only general features related to their extreme platyrostral “duck-faced” condition (see Phylogenetic relationships). The lower jaws in *Stomatosuchus* are less strongly bowed transversely and dorsoventrally, the splenial nearly reaches the symphysis rather than terminating near mid-length along the dentary ramus, the coronoid process is very broad transversely rather than only moderately expanded, and the external mandibular fenestra is closed or nearly closed (Fig. 2B, C) rather than large. The posterior end of the lower jaw in *Stomatosuchus* has a rounded rather than cupped glenoid (Fig. 2C), and the retroarticular process extends directly posteriorly rather than curving dorsally as in *Mourasuchus* and extant crocodylians (Fig. 2B).

Discovery of new material related to *Stomatosuchus* provides a long-awaited opportunity to learn more about this enigmatic African taxon. The most informative specimen is a mandible from Cenomanian-age beds in a region called Iguidi in Niger (Figs. 1A, 37). These lower jaws were found a short distance from the skull of *Kaprosuchus*, a

contemporary inhabitant of the waterways. A closely related species, known only from anterior dentary fragments, is described from the Cenomanian-age Kem Kem Beds in Morocco (Figs. 1A, B, 42).

***Laganosuchus* gen. n.**

urn:lsid:zoobank.org:act:E23D26F4-42BB-4D63-9E75-FF1F8A4E73D3

Etymology. *Laganon*, pancake (Greek); *souchos*, crocodile (Greek). Named for the shallow depth of its skull.

Type species. *Laganosuchus thaumastos*.

Diagnosis. Mid-sized (~4–6 m) stomatosuchid with spaced teeth and an undulating, or festooned, alveolar margin; spike-shaped crowns that lack recurvature; crowns flattened buccolingually with sharp unornamented mesial and distal carinae; d1 enlarged (subequal to d4 caniniform); postcaniniform teeth (d5–24) gradually decrease in size; Meckel's canal developed as a very narrow, sharply delimited groove on the anterior one-half of the dentary.

***Laganosuchus thaumastos* sp. n.**

urn:lsid:zoobank.org:act:B9B7ACB2-A32A-4190-810E-F93ADE61C245

Figs. 37–41

Tables 12, 13

Etymology. *Thaumastos*, astonishing (Greek). Named for the remarkably slender depth of its lower jaws and its straight spike-shaped teeth.

Holotype. MNN IGU13; nearly complete lower jaws missing only the left retro-articular process (Fig. 37).

Type locality. Iguidi (west of In Abangharit), Agadez District, Niger Republic (N 17° 56', E 5° 38') (Fig. 1A).

Horizon. Echkar Formation, Tegama Series; Upper Cretaceous (Cenomanian), ca. 95 Mya (Taquet 1976). Found in association with the crocodyliiform *Kaprosuchus saharicus*, abelisaurid *Rugops primus*, spinosaurid *Spinosaurus* sp., carcharodontosaurid *Carcharodontosaurus iguidensis*, an unnamed rebbachisaurid, and titanosaurian sauropods.

Diagnosis. Metasuchian characterized by alveoli for dentary teeth 1–10 with a depressed labial rim that exposes the upper portion of the alveolus in labial view; slightly procumbent d1 and d2 teeth; two pairs of twinned dentary teeth with conjoined alveolar margins among postcaniniforms; and splenial anterior end split into a pair of short flanges.

Lower jaw. The lower jaws of *Laganosuchus thauma* and *Stomatosuchus inermis* are remarkably slender and elongate and the symphysis extremely reduced compared to any extant crocodylian (Fig. 37). The lower jaws of *Laganosuchus* measure 0.84 m in length (Table 12) and probably pertain to a crocodyliiform four-to-six meters in body

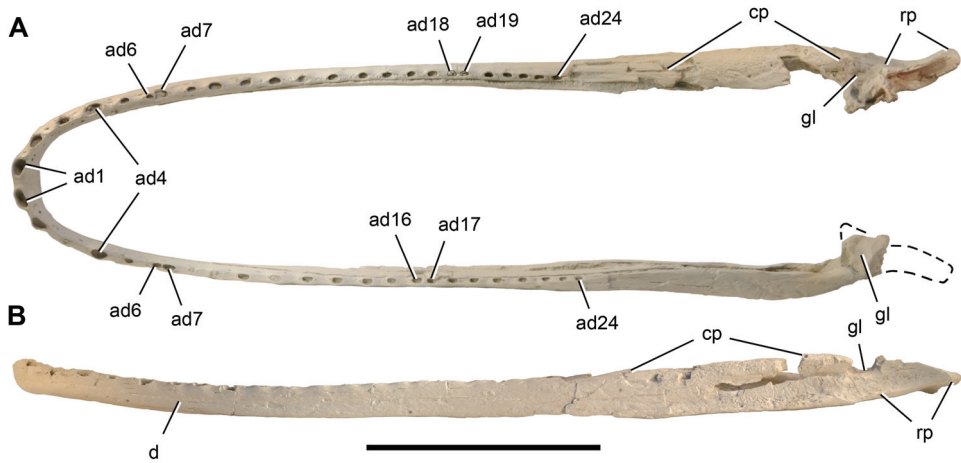


Figure 37. Lower jaws of the crocodyliform *Laganosuchus thaumastos* gen. n. sp. n. Cast (UCRC PVC9) of lower jaws (MNN IGU13). **A** Dorsal view. **B** Left lateral view (reversed). Scale bar equals 20 cm. Dashed line indicates missing bone. Abbreviations: *ad1*, 4, 6, 7, 16–19, 24, alveolus for dentary tooth 1, 4, 6, 7, 16–19, 24; *cp*, coronoid process; *d*, dentary; *gl*, glenoid; *rp*, retroarticular process.

Table 12. Dimensions (mm) of the lower jaw of *Laganosuchus thaumastos* (MNN IGU13). Measurements of paired structures taken from right side. Parentheses indicate estimated measurement.

Structure	Measurement	Length
Lower Jaw	Maximum length	838.0
	Dentigerous ramus length	490.0
	Functional length (anterior end to midpoint of glenoid)	750.0
	Transverse width at anterior end (across alveoli 4)	(140.0)
	Transverse width at mid-length (across alveoli 14)	(200.0)
	Transverse width at coronoid process	(233.0)
	Transverse width at posterior end of retroarticular process	(240.0)
	Coronoid process, transverse width	30.7
	External mandibular fenestra, length	(50.0)
	External mandibular fenestra, height at midpoint	5.7
	Retroarticular process, length	70.3
	Retroarticular process, maximum transverse width	33.2
	Retroarticular process, maximum depth	24.2
Dentary	Symphysis, dorsoventral height	(31.0)
	Symphysis, maximum anteroposterior width	22.2
	Ramus between alveolus 2 and 3, dorsoventral height	25.2
	Ramus between alveolus 5 and 6, dorsoventral height	22.6
	Ramus between alveolus 10 and 11, dorsoventral height	26.1
	Ramus between alveolus 15 and 16, dorsoventral height	29.3
	Ramus between alveolus 20 and 21, dorsoventral height	33.2
Splénial	Ramus between alveolus 24, dorsoventral height	37.5
	Anterior end, depth	15.7

length. The jaws of *Stomatosuchus* are 250% that of *Laganosuchus*, or approximately 2.1 m long. This is comparable to the length of the strongly built, robustly joined lower jaws in the largest individuals of *Sarcosuchus* (Sereno et al. 2001), the largest well documented crocodylomorph.

In dorsal view the mandible in *Laganosuchus* is U-shaped (Fig. 37A). Each side is gently bowed, with curvature toward the symphysis increasing at about the seventh alveolus. In lateral view the ventral margin of the lower jaw is also gently curved as in *Stomatosuchus* (Fig. 37B).

The *dentary* is most slender in the region of alveolus five and six (Table 12). At the symphysis, the dentary joins its opposite, an articulation that appears to have been fused in the holotype. The broken ventral margin at the symphysis appears to have been thickened dorsoventrally, forming a low chin (Fig. 38D). The internal (labial)

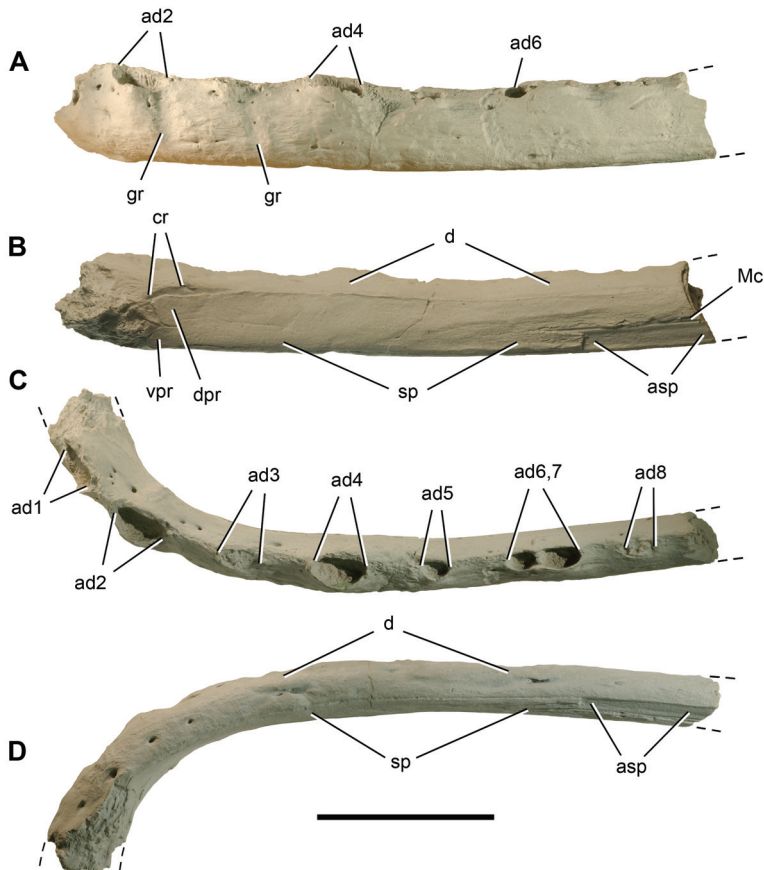


Figure 38. Lower jaws of the crocodyliform *Laganosuchus thaumastos* gen. n. sp. n. Cast (UCRC PVC9) of the anterior portion of the left dentary and splenial (MNN IGU13). **A** Left lateral view. **B** Medial view (reversed). **C** Dorsal view. **D** Ventral view. Scale bar equals 5 cm. Abbreviations: *ad1–8*, alveolus for dentary tooth 1–8; *asp*, articular surface for the splenial; *cr*, crest; *d*, dentary; *dpr*, dorsal process; *gr*, groove (for upper teeth); *Mc*, Meckel's canal; *sp*, splenial; *vpr*, ventral process.

aspect of the dentary near the symphysis is convex with a discrete crest running along the dorsal edge of the splenial (Fig. 38B).

At mid-length the dentary has an elliptical cross-section. The dorsal, festooned, alveolar margin is transversely broader than the ventral margin. In medial view, a very narrow neurovascular groove is exposed where the splenial has broken away (Fig. 38B). In lateral view the dentary splits into two posterior rami below alveoli 22 and 23. The dorsal ramus, which is the longer of the pair, twists onto the dorsal side of the coronoid process. There it extends posteriorly as a tongue-shaped process that overlaps the surangular. This relation is unusual compared to extant crocodylians, as the surangular typically extends anteriorly, overlapping the dentary and approaching the posterior-most tooth. The subtriangular ventral ramus is short, the angular lapping it medially and extending anteriorly between the dentary and splenial.

The *splenial* is a very thin sheet of bone that extends toward, but does not participate in, the symphysis (Fig. 38B). The distal end of the splenial is bifurcated, with Meckel's canal terminating in the notch between the processes. In the anterior one-half of the dentary, Meckel's canal is developed as a narrow incised groove lapped medially by the splenial (Fig. 38B). Externally, the symphyseal ramus of the dentary is marked by two rows of neurovascular foramina, one extending near the ventral margin in lateral view (Fig. 38A) and the other visible only in ventral view (Fig. 38D).

The posterior end of the lower jaw is characterized by a rugose, low, and transversely broad coronoid process, below which is a strongly reduced, slit-shaped external mandibular fenestra (Figs. 39, 40). In medial view, the remarkably small adductor fossa

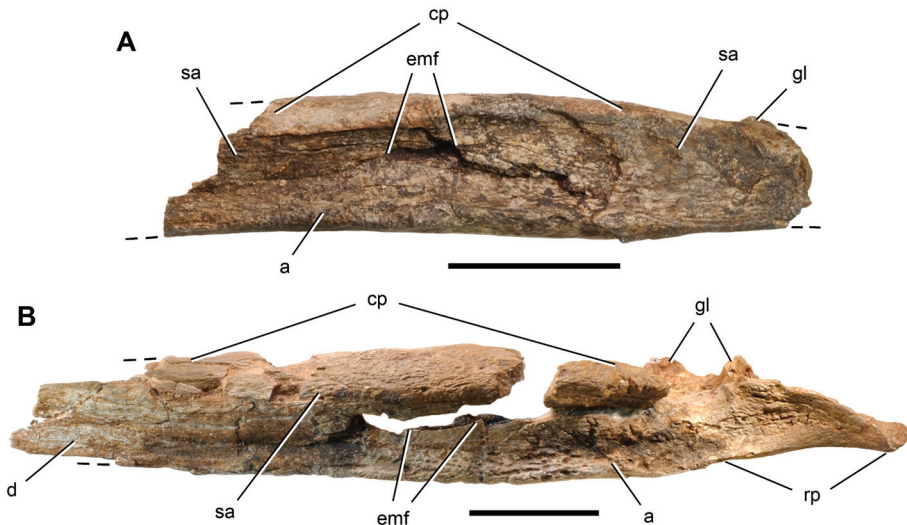


Figure 39. Lower jaws of the crocodyliform *Laganosuchus thaumastos* gen. n. sp. n. Posterior portion of the lower jaws (MNN IGU13). **A** Left lateral view. **B** Right lateral view (reversed). Scale bars equal 5 cm. Abbreviations: *a*, angular; *cp*, coronoid process; *d*, dentary; *emf*, external mandibular fenestra; *gl*, glenoid; *rp*, retroarticular process; *sa*, surangular.

is located immediately anterior to the glenoid. As seen on the left side (Fig. 40A), the articular surface of the glenoid is saddle-shaped, convex along an anterolateral-posteromedial axis and concave along an anteromedial-posterolateral axis (Fig. 40A). The right side is concave with irregular edges and shows signs of bone pathology.

The retroarticular process, preserved only on the right side (Figs. 39B, 40B), has a triangular cross-section with sides that are concave. Thin posterior rami of the angular and prearticular completely overlap the articular on lateral and medial sides. The articular forms all of the dorsomedial face of the process, which is canted at an angle of approximately 45° (Fig. 40B).

Dentition. There are 24 alveoli in each dentary with some variation in the position of two pairs of twinned alveoli. On both sides, the alveoli for tooth d6 and d7 are joined,

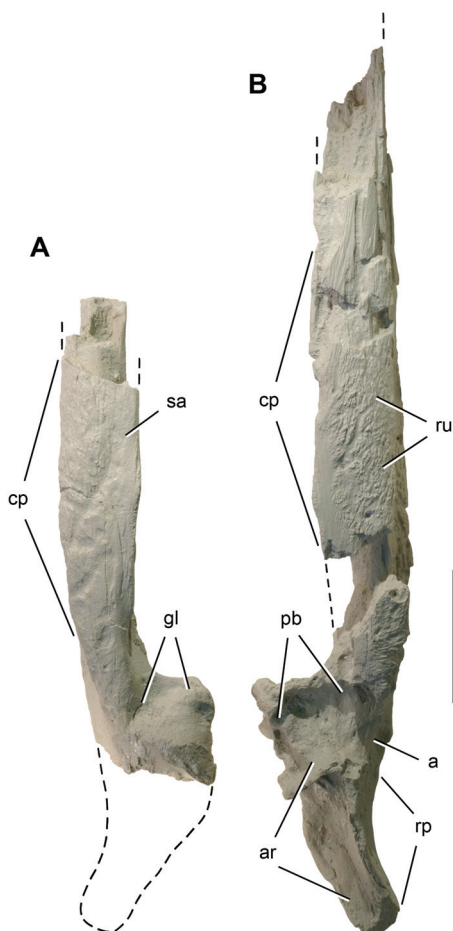


Figure 40. Lower jaws of the crocodyliform *Laganosuchus thaumastos* gen. n. sp. n. Cast (UCRC PVC9) of the posterior portion of the lower jaws (MNN IGU13). **A** Left side in dorsal view. **B** Right side in dorsal view. Dashed line indicates missing bone. Scale bar equals 5 cm. Abbreviations: *a*, angular; *ar*, articular; *gl*, glenoid; *cp*, coronoid process; *pb*, pathologic bone; *rp*, retroarticular process; *ru*, rugosities; *sa*, surangular.

Table 13. Dimensions (mm) of the 24 alveoli and replacing tooth (d11; crown height 14.3 mm) in the right dentary of *Laganosuchus thaumastos* (MNN IGU13). Parentheses indicate estimated measurement.

Alveolus or tooth Number	Mesiodistal length	Buccolingual width
1	15.5	9.4
2	12.4	6.7
3	8.7	5.1
4	14.9	7.6
5	8.4	4.5
6	5.7	3.9
7	11.1	6.4
8	7.6	4.2
9	11.2	5.9
10	10.5	(5.9)
11	10.7	5.9
12	11.3	5.5
13	10.2	5.3
14	8.7	5.2
15	9.6	4.8
16	8.3	5.1
17	9.1	5.0
18	8.6	4.5
19	8.6	4.5
20	8.7	4.5
21	8.4	4.5
22	8.4	4.6
23	8.5	4.3
24	8.4	4.4

the former is the smaller of the pair (Fig. 37A). A similar twinning, although less complete and involving alveoli of comparable size, occurs between alveoli of d16 and d17 on the left side and d17 and d18 on the right side.

The alveolus for d1 is the largest in the tooth row and slightly larger than d4, commonly enlarged as a caniniform among crocodyliforms, and d2 (Table 13). The alveoli of d1 and d2 are canted labially and probably projected anterior to the rim of the opposing premaxilla. The alveolus for d3 is small (Fig. 38C). In lateral view, this alveolus is flanked mesially and distally by canted troughs that accommodated crowns of the opposing maxillary series (Fig. 38A). The dorsal margin between alveoli is developed as a ridge that becomes rounded posterior to d7. Festooning of the alveolar margin involves elevation of the rim of each alveolus with concave embayment of the lateral aspect of the interalveolar margin. The resulting undulating alveolar margin doubtless accommodated the interdigitation of opposing crowns.

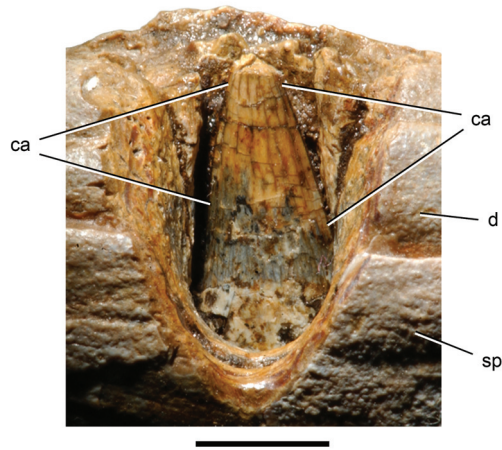


Figure 41. Tooth of the crocodyliform *Laganosuchus thaumastos* gen. n. sp. n. Medial view of the replacement crown in the eleventh alveolus of the right dentary (MNN IGU13). Scale bar equals 5 mm. Abbreviations: *ca*, carina; *d*, dentary; *sp*, splenial.

Several broken crowns remain in place, their crown bases tightly fitted to their respective alveoli. In cross-section, these crowns are oval with a large central lumen. We exposed replacement teeth in several crypts (Fig. 41). The crowns are spike-shaped in lateral view, lacking recurvature or any apparent asymmetry. They are oval in cross-section at their base, above which they become transversely compressed with sharp, unornamented mesial and distal carinae. There is no ornamentation of the crown surface.

The spike-shaped crowns remove any doubt that *Laganosuchus* was an active predator (Fig. 41). Because the spaced, oval alveoli resemble in size and shape those described in the anterior half of the maxilla of *Stomatosuchus*, it is possible that the latter genus had maxillary crowns of similar form (Stromer 1925). The alveolar margin of the dentary in *Stomatosuchus* was depicted as smooth, lacking large alveoli or a festooned margin (Fig. 2B, C), although Stromer (1925) questioned its state of preservation.

Both genera would have fed on fish in a very different manner than extant crocodylians, given the mechanical limitations of such a slender, hoop-shaped mandible, unexpanded cross-section at the symphysis, posteriorly positioned coronoid process, and short span available between the coronoid process and supratemporal region for the adductor musculature. Bite forces would have been limited. Stomatosuchids may best be interpreted as sit-and-wait predators in shallow water, closing their interdigitating spike-shaped dentition on unsuspecting prey that wandered within the U-shaped perimeter of their long jaws.

***Laganosuchus maghrebensis* sp. n.**

urn:lsid:zoobank.org:act:E5BCEEAD-DFEF-4EF6-AA62-110EF91FCD0F

Fig. 42

Table 14

Etymology. *Maghreb*, western (Arabic); *-ensis* (Latin), from. Named for the area where the holotype was discovered in the Kem Kem Beds of southeastern Morocco.

Holotype. UCRC PV2; anterior portion of the left dentary preserving four alveoli and one replacement tooth in the anteriormost tooth position (Fig. 42).

Referred material. CMN 50838, anterior left dentary fragment preserving the symphyseal end and alveoli 1–3.

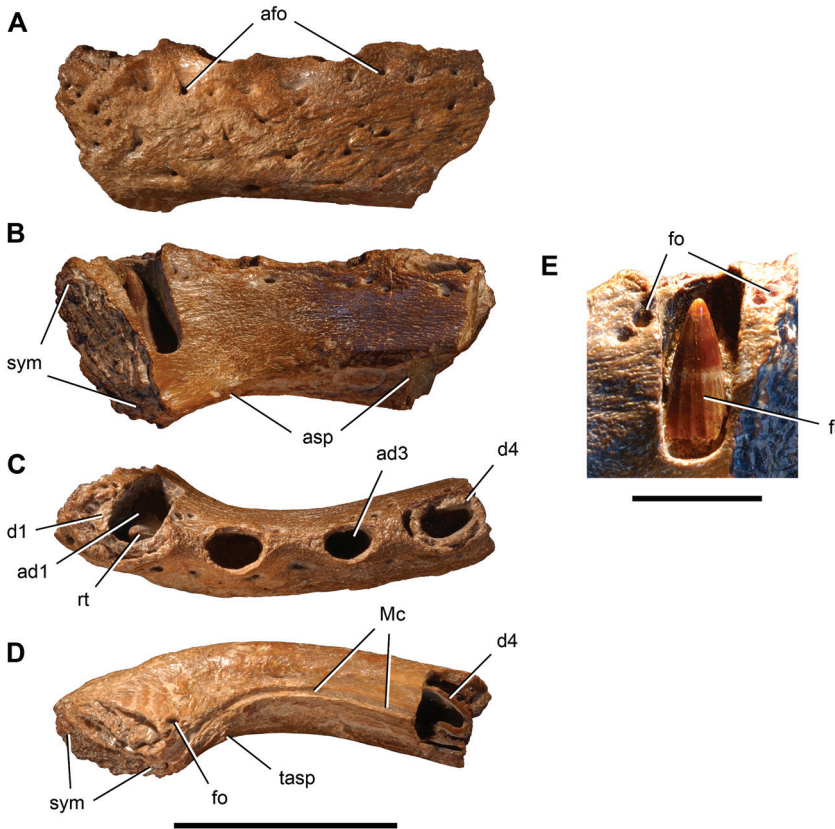


Figure 42. Dentary fragment of the crocodyliform *Laganosuchus maghrebensis* gen. n. sp. n. Anterior end of the left dentary (UCRC PV2). **A** Left lateral view. **B** Medial view (reversed). **C** Dorsal view. **D** Ventral view. **E** Replacement tooth in first dentary alveolus in lingual view. Scale bar in A-D equals 3 cm; scale bar in E equals 1 cm. Abbreviations: *ad1*, 3, alveolus for dentary tooth 1, 3; *afo*, alveolar foramina; *asp*, articular surface for the splenial; *d1*, 4, dentary tooth 1, 4; *fl*, fluting; *fo*, foramen; *Mc*, Meckel's canal; *rt*, replacement tooth; *sym*, symphysis; *tasp*, tip of the articular surface for the splenial.

Type locality. Er Rachidia District, Morocco (exact locality unknown). The referred specimen (CMN 50838) probably was found south of Erfoud (Fig. 1A, B).

Horizon. Kem Kem Beds, upper member; Upper Cretaceous (Cenomanian), ca. 95 Mya (Sereno et al. 1996).

Diagnosis. Metasuchian with a narrow, well defined groove on the ventral aspect of the anterior dentary immediately lateral to the splenial that arcs to the posterior aspect of the symphysis; shallow, anteriorly tapering trough on the anterior dentary just lateral to the more sharply defined groove.

Dentary. The anterior portion of the dentary is preserved in two specimens of *Laganosuchus maghrebensis*. The very rugose dentary symphysis suggests that it may have fused with maturity, and that its size, which is somewhat smaller than *Laganosuchus thaumastos*, may not be significant.

The more complete specimen (Fig. 42A-D) shows a remarkable similarity to *Laganosuchus thaumastos*. Both have slender U-shaped lower jaws with the symphysis restricted to the dentary, festooned alveoli with enlarged first and second teeth, and a sharply incised Meckel’s canal developed as a narrow groove. The teeth are also spike-shaped without recurvature or marginal ornamentation.

Several differences, however, establish *L. maghrebensis* as a distinct species. The dentary is narrower near the symphysis (Fig. 42C), lacking the internal crest that thickens the dentary in *L. thaumastos* (Fig. 38B). The anterior alveoli in *L. maghrebensis* are not procumbent or exposed in lateral view as in *L. thaumastos*. Likewise, an articular scar for the splenial in *L. maghrebensis* shows that its anterior end tapers to a narrow tip along the ventral margin (Fig. 42B) in contrast to the bifurcated flanges in *L. thaumas-*

Table 14. Dimensions (mm) of the anterior end of the right dentary of *Laganosuchus maghrebensis* (UCRC PV2).

Structure	Measurement	Length
Dentary	Symphysis, dorsoventral height	25.5
	Symphysis, maximum anteroposterior width	14.6
	Dentary ramus between alveolus 2 and 3, dorsoventral height	19.1
	Dentary ramus between alveolus 2 and 3,transverse width	11.4
Alveolus 1	Maximum mesiodistal length	10.1
	Maximum labiolingual width	6.4
Alveolus 2	Maximum mesiodistal length	7.3
	Maximum labiolingual width	5.0
Alveolus 3	Maximum mesiodistal length	6.4
	Maximum labiolingual width	4.0
Alveolus 4	Maximum mesiodistal length	11.9
	Maximum labiolingual width	5.7
Crown d1	Replacement crown, height	12.2
	Replacement crown, mesiodistal width of base	5.3

tos (Fig. 38B). The incised groove representing Meckel's canal is located on the ventral, rather than lingual, aspect of the dentary (Fig. 42D).

Although crown size in the two species is very similar, the alveolus of the caniniform tooth (d4) is slightly larger than comparable measurements for d1 (Table 14), the reverse of the condition in *Laganosuchus thaumastos* (Table 13). *L. maghrebenensis*, in addition, shows low fluting on the lingual aspect of the crown of the first dentary tooth (Fig. 42E). A comparable crown, however is not available at the anterior end of the dentary series in *L. thaumastos*.

Discussion

Phylogenetic relationships

Phylogenetic analysis of 252 characters for 43 taxa of crocodyliforms (Fig. 43) maintains a familiar structure to many cladistic analyses since that of Clark (1994). We used maximum parsimony with the heuristic search option with fifty random runs to avoid heuristic islands (Fig. 43; see also Appendix: Character list, Character-state matrix, Apomorphy list). Using the protosuchian *Orthosuchus stormbergi* as an outgroup, 4 minimum-length trees were recovered, each with a tree length of 986 steps, consistency index of 0.34, retention index of 0.64, and a rescaled consistency index of 0.22.

The strict consensus yields a relatively well-resolved topology with *Hsisosuchus* and *Thalattosuchia* as successive basal sister taxa to other crocodyliforms, as in several analyses (Buckley and Brochu 1999; Buckley et al. 2000; Sereno et al. 2001, 2003; Turner 2006; Larsson and Sues 2007) (Fig. 43A). The position of *Thalattosuchia*, however, is intimately tied to the weighting of "longirostrine" characters. Several analyses position *Thalattosuchia* near longirostrine neosuchians outside *Crocodylia* (Price 1955; Ortega et al. 2000; Pol 2005; Pol and Apesteguia 2005; Zaher et al. 2006; Fiorelli and Calvo 2008; Turner and Buckley 2008; Pol and Gasparini 2009). Here the basal position of *Thalattosuchia* within *Crocodyliformes* is reasonably supported, with 12 extra steps required to move *Thalattosuchia* outside *Pholidosauridae*.

In nearly all analyses including ours (Fig. 43), *Metasuchia* is split into *Notosuchia*, a clade containing an increasingly diverse assemblage of predominantly small-bodied taxa with differentiated dentitions, and *Neosuchia*, a clade with includes basal taxa such as *peirosaurids*, *pholidosaurids*, and *Crocodylia*.

The monophyly of the genus *Araripesuchus* and its position within *Metasuchia* has been controversial; the generic assignment of *A. wegeneri* has been questioned (Ortega et al. 2000) and supported (Pol and Apesteguia 2005; Turner 2006; Turner and Buckley 2008), and *Araripesuchus* has been placed at the base of either *Notosuchia* (Sereno et al. 2001, 2003; Turner and Buckley 2008; Fiorelli and Calvo 2008) or *Neosuchia* (Buckley and Brochu 1999; Buckley et al. 2000; Ortega et al. 2000; Pol 2005; Turner 2006; Pol and Gasparini 2009).

Bootstrap analysis of 2000 replicates (Fig. 43B) underscores the weakness of character support for many of the nodes in the strict consensus tree, in particular at the base of Metasuchia and within Notosuchia (Fig. 43A). Homoplasy is rampant (consistency index = 0.34), missing data is a real limitation for many taxa, and character state ordering and character correlation have major effects on the preferred trees. *Anatosuchus rattoides* and *Laganosuchus thaumastos*, two very incompletely known taxa, were removed from this analysis to shorten computational time.

Much of the character data that we have assembled from our own analyses and from those in the literature, furthermore, must be reevaluated, because fundamental questions have arisen recently over how morphological characters are best constructed, scored and ordered (Sereno 2007). More than a dozen phylogenetic analyses have been performed by different researchers in the last decade, with little or no tangible comparison of character selection or character scoring. Without this comparative analysis, it is difficult to pin down the underlying causes for differing phylogenetic results (Sereno 2009). In this light we set aside lengthy discussion of the merits of our particular phylogenetic results (Fig. 43; Appendix: Apomorphy list) to concentrate on the more particular ramifications of these results for the taxa described in this report.

***Anatosuchus minor*.** In both trees *Anatosuchus minor* is placed within Notosuchia, and several characters are consistent with this position (Fig. 43). *Anatosuchus* shares all the characters with Notosuchia that are also present in *Araripesuchus* as discussed below. One exception concerns the orientation of the distal quadrate shaft in lateral view (character 155: see Appendix: Character list).

Anatosuchus was initially allied with *Comahuesuchus* on the basis of characters that have turned out to represent artifacts preservation, such as a broad median diastema between the premaxillary tooth rows (Sereno et al. 2003). *Anatosuchus* (Figs. 5A, 6A) and *Simosuchus* (Buckley et al. 2000), by contrast, have a unique condition among crocodyli-forms, in which the distal quadrate shaft angles anteroventrally. Coding and scoring the orientation and form of the distal shaft of the quadrate, however, are challenging tasks with more than a single interpretation (characters 151–155: see Appendix: Character list).

Other synapomorphies supporting a close relationship between *Anatosuchus* and the Madagascan genus *Simosuchus* include the broad, squared anterior end of the snout (characters 3, 4; see Appendix: Character list). (Figs. 5A, B, 6A, B). The snout is so broad in both genera that the premaxilla-maxilla suture is exposed in anterior, rather than lateral, view of the cranium. In addition, both taxa have transversely broad mandibular rami sheathed by the splenial in ventral view (Figs. 5C, 6C, 9B) and tooth rows with more uniform crowns that lack a lower caniniform (character 182; see Appendix: Character list).

Although the bootstrap analysis breaks down some of the structure within Notosuchia (Fig. 43B), it takes 10 extra steps to position *Anatosuchus* and *Simosuchus* next to the notosuchians *Notosuchus* and *Baurusuchus*.

***Araripesuchus wegneri*.** The well preserved material of *Araripesuchus wegneri* demonstrates its close relationship to other species of *Araripesuchus*, although the mono-

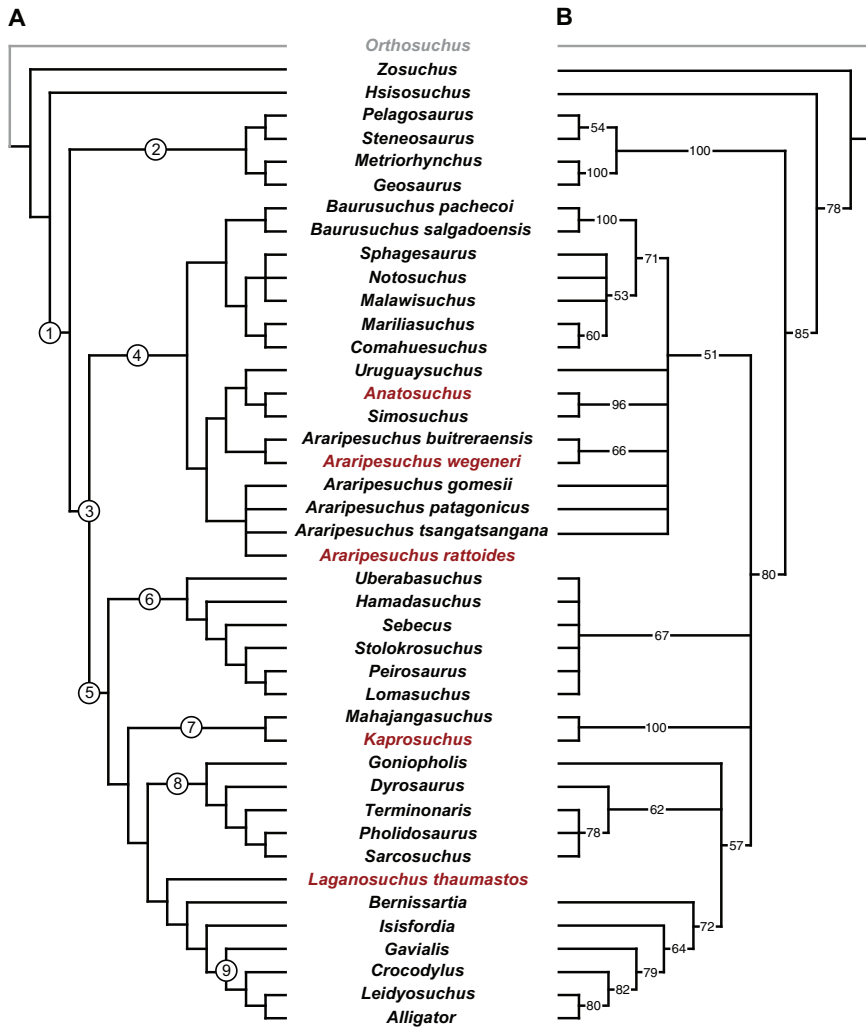


Figure 43. Phylogeny of stem crocodyliforms. Maximum parsimony and bootstrap analysis of representative stem crocodyliforms scored for 252 characters using the protosuchian *Orthosuchus* as an outgroup. Taxon names in red highlight those species described here. The character list, character-state matrix, and apomorphy list (for one of the minimum-length trees) are available in the Appendix. **A** Strict consensus tree based on 4 minimum-length trees (TL = 986, consistency index = 0.34; retention index = 0.64) from maximum-parsimony analysis using PAUP* (Swofford 1998) of all 42 ingroup crocodyliforms, which places *Hsisosuchus* and *Thalattosuchia* at the base of *Crocodyliformes*, recognizes a diverse *Notosuchia* including *Anatosuchus* and *Araripesuchus*, and positions several taxa including *Kaprosuchus* and *Laganosuchus* within *Neosuchia*. **B** 50%-majority-rule consensus tree based on 2000 bootstrap replicate parsimony analyses on 40 ingroup crocodyliforms (excluding for computational efficiency the poorly known taxa *Araripesuchus rattoides* and *Laganosuchus thaumastos*). The bootstrap result recognizes less structure at the base of *Metasuchia* and within *Notosuchia*. Taxon names (circled numbers) are positioned on nodes and stems to reflect their node- and stem-based phylogenetic definitions, respectively (Sereno 2005; Larsson and Sues 2007). Abbreviations: 1, Mesoeucrocodylia; 2, *Thalattosuchia*; 3, *Metasuchia*; 4, *Notosuchia*; 5, *Neosuchia*; 6, *Sebecia*; 7, *Mahajangasuchidae*; 8, *Pholidosauridae*; 9, *Crocodylia*.

phyly of the genus remains at issue (Fig. 43A). None of the most parsimonious trees unambiguously recovers a monophyletic *Araripesuchus*. Resolution of their relationships to each other and other notosuchians, however, is hampered by the fragmentary nature or subadult status of available material for species such as *A. rattoides*, *A. patagonicus* and *A. buitrerensis* and the realization that *Uruguaysuchus* (Rusconi 1933) is closer to *Araripesuchus* in cranial and dental morphology than was previously realized.

As a result, only a few additional characters can split the genus despite the characters we cited in support of a monophyletic *Araripesuchus* (e.g., premaxilla external surface smooth with ornamentation limited to the distal end of the ascending ramus; two neurovascular foramina posterior to the narial fossa; premaxillary tooth row straight; maxillary postcaniniform alveolar margin dorsally arched; characters 82, 83, 97, 106; see Appendix: Character list). In the present analysis, a frontal sagittal crest, the relative length of particular processes of the jugal and quadratojugal, and the presence of quadratojugal ornamentation unite *A. buitrerensis* and *A. wegneri* with *Uruguaysuchus* and closest relatives (Fig. 43A; characters 28, 38, 52, 53; Appendix: Character list), although that group is unstable (Fig. 43B). *A. wegneri* and *A. buitrerensis* share four synapomorphies including a rounded anterior palatine ramus and deep posterior pterygoid process (characters 124, 130; see Appendix: Apomorphy list). These characters however, are not preserved in several other *Araripesuchus* species. Finally, it should be noted that paralogy of the genus is not strongly supported either; the genus can be united with two additional steps.

Only more detailed character documentation at the base of Notosuchia will resolve the relationships within and immediately outside the putative genus *Araripesuchus*. The skull of *Araripesuchus wegneri* has proven to be fertile ground for new characters, such as the peculiar sinus that inflates the premaxilla (Fig. 17A, premaxillary lumen). The dentition, likewise, exhibits unusual features with respect to crown shape, orientation, ornamentation and the lingual deflection of some carinae. The postcranial skeleton, moreover, could be a source of additional character data.

A few synapomorphies place the various species of *Araripesuchus* within Notosuchia (Fig. 43; see Appendix: Apomorphy list), their removal requiring six additional steps. The most notable concern the jaw joint and osteoderms. Notosuchia and all species of *Araripesuchus* share a ventrally oriented quadrate near the jaw joint in both lateral and posterior views. The quadrate condyles so oriented are aligned transversely and are orthogonal to the sagittal plane of the skull. The medial quadrate condyle is flat and angles ventromedially below the lateral condyle, forming a medial brace to the jaw joint, as is well seen in *Anatosuchus* (Fig. 8). In most other crocodyliforms, the condyles are canted posteromedially in ventral view with less disparity between medial and lateral condyles, as in *Hamadasuchus* (Larsson and Sues 2007). The orthogonal orientation of the jaw joint may be associated with dental morphology of these crocodyliforms, which includes a variety of crown shapes for isognathous occlusion in both dorsoventral (Figs. 20, 21) and propalinal directions (Lecuna and Pol 2008). The distal quadrate of Notosuchia, including all species of *Araripesuchus*, is thick in cross-section with distinct posterolateral and posteromedial surfaces, in contrast to the anteroposteriorly compressed quadrate shaft in other crocodyliforms.

The paravertebral osteoderms in notosuchians including *Araripesuchus* and *Anatosuchus* lack any development of an anteriorly projecting process that interlocks and stabilizes the lateral margin of the paravertebral shield, as described in basal crocodylomorphs (Crush 1984; Wu and Chatterjee 1993; Clark et al. 2000), protosuchians (Colbert and Mook 1951), *Goniopholis* (Salisbury et al. 1999), and pholidosaurids (Serenio et al. 2001). This process is also lacking in the basal crocodyliform *Hsisosuchus* (Li et al. 1994), the basal neosuchian *Mahajangasuchus* (Buckley and Brochu 1999), and eusuchians and their immediate outgroups (Gans 1980; Ross and Mayer 1984; Salisbury et al. 2006). The process was likely lost several times in the evolution of Crocodyliformes (character 248; Appendix: Character list).

***Araripesuchus rattoides*.** With scores available for only 13 characters (approximately 1%) on the limited material available for this species, it is surprising that it joins a cluster with other species of *Araripesuchus* (Fig. 43A). Its position is not very stable, and the taxon could not be included in the bootstrap analysis. It owes its alliance with the *Uruguaysuchus*-*Araripesuchus* cluster to the trough-shaped surface on the mandibular symphysis (character 180) and a complex character describing the orientation of the dorsal edge of the dentary (character 190; Appendix: Character list). Although several other aspects of the dentary and only known bone of *A. rattoides* are similar to other species of *Araripesuchus*, we await more material of this interesting taxon to test its relationships more effectively.

***Kaprosuchus saharicus*.** *Kaprosuchus saharicus* is positioned with *Mahajangasuchus* among neosuchians in an initial analysis (Fig. 43A), although an unambiguous relationship between these genera and Neosuchia is not resolved in the bootstrap consensus tree (Fig. 43B). Several characters, nevertheless, support a special relationship with the squat-skulled *Mahajangasuchus insignis* from Madagascar, as described below, and the position of Mahajangasauridae as neosuchians positioned just outside pholidosaurids and more derived neosuchians. It takes 6 and 12 extra steps, respectively, to place Mahajangasauridae at the base of Sebecia or as sister taxon to Piosauridae.

Characters supporting Mahajangasauridae include obliteration of all but the posterior portion of the internasal suture (Figs. 33B, 34B; *M. insignis* (Turner and Buckley 2008)). Nasal fusion is very rare in other crocodyliforms (e.g., *Dyrosaurus*). The postorbital (Figs. 33A, 34A) has an unusual rugose, external articular fossa, presumably for the posterior palpebral, that faces laterally in *K. saharicus* and *M. insignis* (Figs. 33A, 34A). In other crocodylomorphs such as *Anatosuchus* (Fig. 7D) and *Araripesuchus* (Fig. 16B), this articular facet faces anteriorly or dorsally. The external rim of the squamosal is turned dorsally in a hornlike projection. In *K. saharicus* (Figs. 33A, 34A) this projection is much better developed and involves the posterior edge of the squamosal rather than the lateral edge, as in *M. insignis* (Turner and Buckley 2008) and a few later crocodylians (Brochu 2006).

The ventral margin of the jugal is distinctive in both *K. saharicus* (Figs. 33A, 34A) and *M. insignis* (Turner and Buckley 2008). The posterior ramus is angled strongly posteroventrally, which positions the jaw joint below the posterior maxillary teeth.

There is an arched apex where the posterior and anterior rami meet. A distinctive rugose and elliptical fossa is present along the ventral margin below the orbit (Fig. 35B).

Several derived aspects of the posterior palate also link *K. saharicus* and *M. insignis*. The ectopterygoid descends vertically from its contact with the jugal and is inset only slightly from the lateral margin of the jugal in *K. saharicus* (Figs. 33A, 34A) and *M. insignis* (Turner and Buckley 2008). In ventral view of the cranium, the posterior ramus of the jugal is obscured by the ectopterygoid and pterygoid (Figs. 33C, 34C). In other crocodyliforms, the ectopterygoid arches medially from its contact with the jugal, the space accommodating the coronoid process of the lower jaw, as in *Araripesuchus* (Figs. 14A, C, 15A, C). Other shared features are located in the choanae. The choanal septum flares anteriorly to form an articular foot for the palatine (Figs. 33C, 34C). The foot is more developed in *M. insignis* (Turner and Buckley 2008) than in *K. saharicus* (Figs. 33C, 34C). The ventral margin of the choanal septum is transversely expanded to about 40% the length of the septum. Transverse expansion of the ventral edge of the septum does occur elsewhere among crocodyliforms, such as in *Araripesuchus gomesii* (Turner 2006), but not to the same degree. Lastly, the choanal passage is invaginated into the posterior palate, hollowing a space dorsal to the posterior rim of the palate in both *K. saharicus* (Figs. 33C, 34C) and *M. insignis* (Turner and Buckley 2008).

The mandible also supports a phylogenetic link between *K. saharicus* and *M. insignis*. The symphysis in both is relatively deep and oriented along an anterodorsal axis. The symphysis of *K. saharicus* is markedly longer than that of *M. insignis*, but the peculiar symphyseal orientation is shared. The surangular in each taxon projects laterally over the external mandibular fenestra and adjacent to the articular cotyle for the lower jaw, forming a robust lateral shelf. A similar dorsolateral mandibular shelf is present in *Baurusuchus*, which may reflect similar biomechanical properties. The coronoid region of the mandible is deep and angled in lateral view in *K. saharicus* and *M. insignis*. This angle is associated with the steeply angled jugal and contributes to the extremely tall mandibles of these taxa.

Finally, the maxillary tooth row terminates anterior to the orbit in both *K. saharicus* and *M. insignis*, both of which emphasize the anterior end of the dentition over the posterior end.

***Laganosuchus thaumastos*.** The nearly complete lower jaws of *Laganosuchus thaumastos* (Fig. 37) provide a new perspective on *Stomatosuchus inermis* (Stromer 1925, 1936; Nopcsa 1926) (Fig. 2). *Laganosuchus* and *Stomatosuchus* share a number of derived features suggesting their close relationship, not least of which are the extremely elongate cranial proportions, in which jaw length is approximately five times maximum width. The very slender proportions of the lower jaw, which is 30 times its depth at mid-length, are also diagnostic.

The lower jaws have nearly straight, parallel-sided rami and a narrow symphysis, features which distinguish stomatosuchids from other slender-jawed, “duck-faced” crocodylomorphs, such as the Miocene alligatoroid *Mourasuchus* (= *Nettosuchus*) (Langston 1965, 1966; Bocquentin-Villanueva 1984). Although Langston noted that the transverse bowing might be an artifact of preservation in *Mourasuchus* (as the max-

illary tooth row suggests), the arc of its long axis in lateral view seems natural, a curve that is not present in stomatosuchids [65]. The most slender depth of each dentary in stomatosuchids occurs near the fifth and sixth tooth positions (Fig. 2B, 3B), whereas in *Mourasuchus* the anterior end of the dentary is uniform in depth (Langston 1965).

In stomatosuchids the coronoid process is very low and transversely broad (maximum width approximately 85% maximum height), and the external mandibular fenestra very small or closed. In *Mourasuchus* the coronoid region is dorsally convex with a transverse width about 50% of its maximum depth, and the external mandibular fenestra is quite large (Langston 1965). Finally, the very thin splenial in *Laganosuchus* extends toward, but does not quite contact, its opposite in the midline (Fig. 38B), whereas in *Mourasuchus* and most extant crocodylians the splenial tapers to a point on the lateral side of the skull at a significant distance from the symphysis (Jollie 1962; Langston 1965; Iordansky 1973).

The jaw articulation and retroarticular process look distinctly primitive in stomatosuchids [Figs. 2B, C, 39B, 40B] compared to *Mourasuchus* (Langston 1965). Both have a saddle-shaped (transversely convex, anteroposteriorly concave) glenoid, but in *Mourasuchus* anterior and posterior rims bound the articular surface. In stomatosuchids, likewise, the retroarticular process projects posteriorly, its dorsal surface ventral to the glenoid. In *Mourasuchus*, in contrast, the retroarticular process is the culmination of the posterodorsally curving ventral margin of the angular, which elevates the retroarticular process so that its surface is above the glenoid as in extant crocodylians (Jollie 1962; Langston 1965; Iordansky 1973).

A single, poorly preserved vertebral centrum and neural arch were described by Stromer (Price 1959), the centrum tentatively identified as pertaining to a middle cervical vertebra and figured in anterior view (Fig. 2D). Stromer remarked that it appeared to be procoelous as in eusuchians, although he admitted that his orientation of the vertebra and possibly its association with the skull are uncertain. Perhaps on this basis, Steel (1973) and Brochu (2001) tentatively placed *Stomatosuchus* within Eusuchia. The vertebra, however, is unusual compared to the condition in Eusuchia or among immediate eusuchian outgroups. As Stromer noted, there is no trace of a hypapophysis ventrally, even though such a process is prominently developed in cervicals among eusuchian outgroups such as *Isisfordia* (Salisbury et al. 2006), in which the posterior centrum face is only slightly convex. Secondly, the body of the centrum is remarkably short. The posterior convexity, according to Stromer, measures nearly 60% (3.3 cm) of the length of the remainder of the centrum (5.7 cm), which is much greater than the proportion between the convex centrum face and body in *Isisfordia* (10%) (Salisbury et al. 2006) or that common to extant crocodylians (40%) (Mook 1921). Given the uncertainties surrounding the association of this centrum and its interpretation, we regard the vertebral evidence in *Stomatosuchus* as problematical.

Evidence from the cranium is equally uncertain. The only information available for the cranium is a single, unlabeled lithographic drawing in ventral view (Fig. 2A), a few remarks that sometimes differ on the dorsal skull roof by Stromer (1925) and Nopcsa (1926), and a reconstruction of the skull in lateral and dorsal views by Stromer (1936)

that attempts to resolve these differences (Fig. 2F, G). One important area of the cranium is the posterior portion of the palate. The lack of preserved detail, the asymmetry of the fossae in the available lithographic drawing, and the absence of a detailed description or specific interpretation by those who saw it first-hand render its interpretation questionable. We regard as unknown the form and position of the internal nares in *Stomatosuchus*.

The form of the lower jaw in several regards is different and primitive compared to the functionally similar alligatoroid genus *Mourasuchus*. The anterior extension of the splenial, poorly raised edges of the glenoid, and depressed position of the retroarticular process do not resemble the condition in eusuchians. The eusuchian dentary, in addition, splits posteriorly to form both dorsal and ventral margins of the external mandibular fenestra, a condition present in *Kaprosuchus* (Figs. 33A, 34A). In *Laganosuchus*, in contrast, the bone is not split posteriorly and contributes only to the dorsal margin of the external mandibular fenestra. Notosuchians, such as *Anatosuchus* (Figs. 5A, 6A), often show an intermediate condition, in which the posterior dentary is forked but the ventral process is much smaller and does not contribute to the ventral margin of the mandibular fenestra (Ortega et al. 2000; Buckley et al. 2000; Turner 2006).

With scores available for only 34 characters (approximately 13%) based on the limited material available for this species, *Laganosuchus* is positioned outside a clade consisting of Eusuchia and closest outgroups (Fig. 43A), although only two additional steps are required to position *Laganosuchus* in many other positions on the cladogram. The absence of the splenial from the mandibular symphysis (character 188), the short, straight retroarticular process (character 208), and a few others unite Eusuchia and closest relatives to the exclusion of *Laganosuchus*, providing some support for our tentative conclusion that stomatosuchids do not lie within Crocodylia (Fig. 43A). We were forced to remove *Laganosuchus* from the bootstrap analysis due to computational limitations (Fig. 43B).

Endocranial volume

We used computed-tomographic scans of skulls of *Anatosuchus minor* (MNN GAD17), *Araripesuchus wegneri* (MNN GAD19) and extant *Alligator mississippiensis* to generate prototypes (Figs. 10, 11, 22) and to calculate endocranial volume. The endocasts for *A. minor* and *A. wegneri* are the first available for the more terrestrial, erect-limbed notosuchians. The endocasts are quite similar in shape and volume, although the ventral surface is rendered in more detail in the endocast for *A. wegneri*. Total endocranial volume in *A. wegneri* is estimated at 2218 mm³. *A. minor* probably had a very similar total endocranial volume; we calculate an absolute minimum estimate of 1964 mm³ based on dorsal and lateral surfaces of the endocast. Thus, endocranial volume is around 2000 mm³ in these similar-sized, small-bodied crocodyliforms. The forebrain in *A. minor* and *A. wegneri* probably filled the endocranial cavity, given the details discernable on the endocast such as the median sinus and optic lobes (Figs. 10, 22).

We estimated cerebral hemisphere volume from paired ellipsoids filling the cerebral endocranial space (Larsson et al. 2000; Larsson 2001). We made additional ap-

proximations of cerebral hemisphere volume, because the floor of the cerebral space may have been artificially lifted somewhat in *A. wegeneri* and is poorly resolved in the scan of *A. minor*. For example, we swapped the transverse radius of each ellipsoid for the dorsoventral radius, which are similar in extant crocodylians. These estimates have yielded a range of cerebral volumes for each species (Fig. 44B). As measured directly

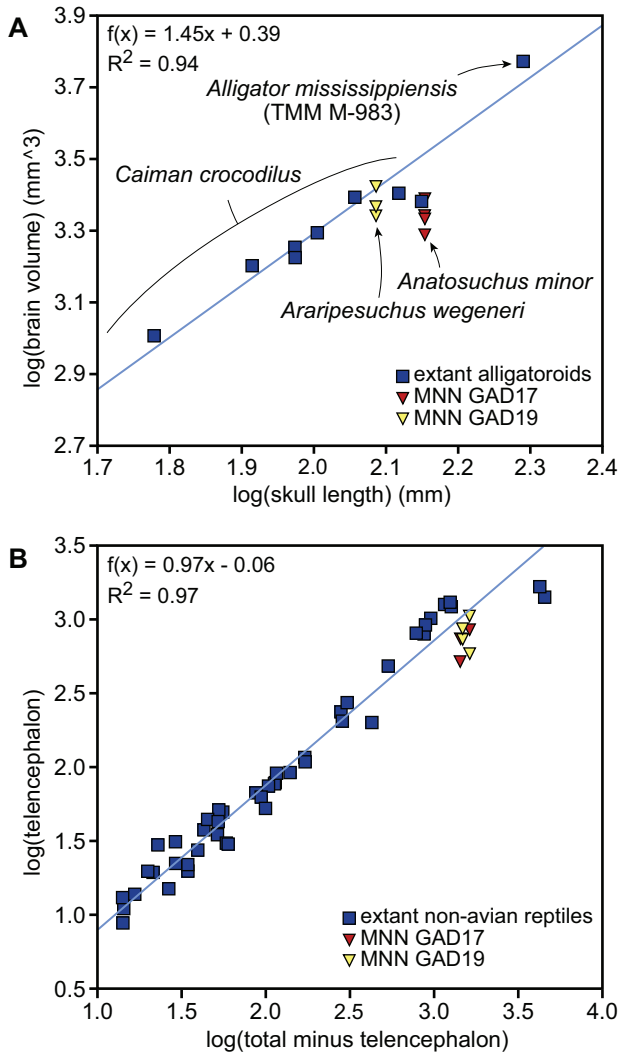


Figure 44. Bivariate plots of brain volume in *Anatosuchus minor* and *Araripesuchus wegeneri* compared to that in nonavian reptiles. **A** Brain volume as a function of skull length in *Anatosuchus minor*, *Araripesuchus wegeneri* and extant alligatoroids (Gans 1980). **B** Cerebral volume as a function of total endocranial volume in *Anatosuchus minor*, *Araripesuchus wegeneri* and extant nonavian reptiles (Platel 1976; Gans 1980). Blue squares are estimates from extant alligatoroids (top) and extant nonavian reptiles (bottom); red triangles are independent estimates (see text) based on the endocast of *Anatosuchus minor* (MNN GAD17); yellow triangles are independent estimates (see text) based on the endocast of *Araripesuchus wegeneri* (MNN GAD19).

from the endocranial volume, cerebral hemisphere volume in *A. wegeneri* is approximately 630 mm³ (mean of range of 528–732 mm³) and in *A. minor* is at least 561 mm³ (mean of range of 528–593 mm³). When swapping the transverse for the dorsal radius, the volumes increase slightly in *A. wegeneri* to 966 mm³ (mean of range of 875–1056 mm³) and in *A. minor* to at least 801 mm³ (mean of range of 747–854 mm³). In sum, cerebral volume is around 750 mm³ in these similar-sized, small-bodied crocodyliforms.

Endocranial volume as a function of skull length, when corrected for size, is not significantly different from that in modern crocodylians with comparable skull shapes (alligatorids) (Fig. 44A). Likewise, cerebral hemisphere volume as a function of the volume of the remaining endocranial space, corrected for size, is not significantly different from that in extant reptiles (Fig. 44B). Thus despite their broad, spade-shaped forebrains in dorsal view, the two small-bodied crocodyliforms, *A. minor* and *A. wegeneri*, exhibit absolute and proportional endocranial volumes that match those in extant crocodylians and other nonavian reptiles (Hopson 1979). Their forebrain shape in dorsal view resembles that of a juvenile *Caiman* with a skull length of 3 cm (Hopson 1979). The endocranial and forebrain volumes in these two notosuchians do not differ from the ranges observed in extant crocodylians, despite their upright posture and, quite possibly, more active lifestyle in terrestrial environments.

Trophic inferences

We attempt here to draw some tentative inferences regarding diet from the cranial and dental information now available for *Anatosuchus*, *Araripesuchus*, *Kaprosuchus* and *Laganosuchus*.

***Anatosuchus*.** *Anatosuchus* has one of the most specialized snouts among crocodylomorphs. The smooth narial fossa and adjacent smooth surface on the premaxilla suggests that it had a fleshy external naris that opened dorsally (Figs. 7A, B, 45A). On either side a series of large neurovascular foramina opens along a smooth and presumably fleshy anterior snout margin. The premaxillary teeth have increased in number to six probably in relation to the increased breadth of the snout.

The subcylindrical, lingually curved, smooth upper and lower crowns do not engage one another. Rather the U-shaped lower jaw fits in a gap within the upper jaw (Figs. 5, 6). In contrast to the contemporaneous *Araripesuchus wegeneri*, little apical wear and no wear facets are evident on the pointed crowns. At the center of the lower jaw is an edentulous, subrectangular bony projection that articulates against the premaxillary palate behind the mesial three premaxillary teeth (Fig. 45). The largest teeth are located at the corner of both upper and lower jaws, although unlike many notosuchians no discordantly enlarged caniniform teeth are present. The ventral margin of the dentary projects laterally and is highly vascularized.

We have depicted *Anatosuchus* as an upright notosuchian (Fig. 45) based on the straight-shafted bones of the forelimb, which has folded like an accordion alongside

the trunk in the most complete specimen (Fig. 12). *Anatosuchus* has a carnivorous dentition with hook-shaped crowns suitable for snaring frogs or small fish, a median mandibular process for crushing, and a snout end rife with elaborated olfactory and neurovascular structures. Armed with a particularly large manus and elongate flat-tipped manual unguals (Fig. 13B), *Anatosuchus* may have scratch-dug for soft invertebrates or sought amphibians or small fish in shallow or vegetated water.

***Araripesuchus*.** *Araripesuchus* has been described as “terrestrial” (Hecht 1991) and depicted eating insects (Turner 2006: fig. 99). According to Turner, the jaw joint in *A. tsangatsangana* would not allow the propalinal movement described as probable in *Notosuchus* and possibly other closely related notosuchians (Lecuona and Pol 2008). Little else has been posited regarding the potential jaw mechanics or diet of the speciose genus *Araripesuchus*.

All species of *Araripesuchus* had an upright posture, judging from the straight-shafted long bones (Fig. 25), angle and depth of the calcaneal heel, and the elongate proportions of the proximal carpals and metapodials (Figs. 25B, 26). *A. tsangatsangana* appears to have the most slender, elongate limbs, although an associated skeleton is not available. Based on the material available to us, *A. wegneri* grew as in extant crocodylians, starting as an agile longer-legged juvenile and becoming a proportionately shorter limbed adult (Fig. 46).

Diet doubtless shifted in the course of post-hatching growth as in extant crocodylians (Tucker et al. 1996). As an adult *A. wegneri* does not appear to have been a pure carnivore, as not one of the crowns is laterally compressed or recurved and none has serrate carinae. Upper and lower crowns, furthermore, do not interdigitate as is common among piscivores (Savitzky 1983). One premaxillary crown (pm4) owes its apparent recurvature to an elongate wear facet that has trimmed the posterior carina (Fig. 19A). A fresh premaxillary crown in the same position shows the convex distal margin of a leaf-shaped crown (Fig. 20B).

Premaxillary and maxillary crowns in an adult skull of *A. wegneri* show heavy apical wear that has blunted crown tips and truncated carinae (Fig. 19), obliterating the short apical ridge and inclined denticles that are present on the crowns of a subadult skull (Fig. 21A). This appears to be abrasive wear that has rounded and polished the crown apices. One maxillary crown in the middle of the tooth row, however, has a low-angle wear facet that truncates the lingual crown surface (Fig. 19C). This less polished, nearly flat wear facet must have been generated by tooth-to-tooth occlusion. The crowns in opposing tooth rows do not interdigitate for prey capture, but rather alternate in size, with an enlarged crown opposing an arched series of smaller crowns (Fig. 20). All of the dentary teeth and mid- and posterior maxillary teeth are denticulate, and both upper and lower crown surfaces are textured with low, rounded ridges or vertical wrinkles. A carnivore, particularly an insectivore, is more likely to maintain pointed smooth crowns for puncture or penetration.

Several outstanding features are manifest in the central portion of the dentition in *A. wegneri*. The largest dentary crowns have a mesial carina that curls medially (Fig.

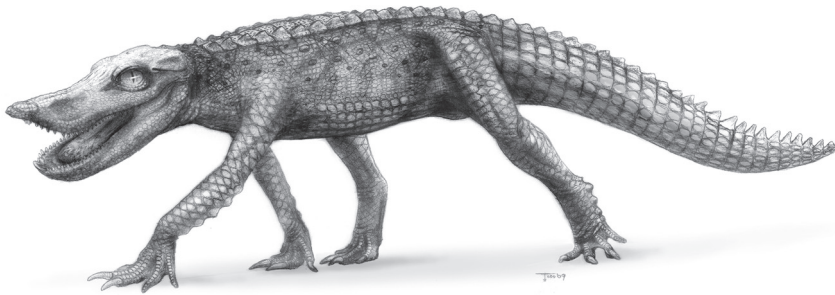


Figure 45. Flesh reconstruction of the crocodyliform *Anatosuchus minor*.

20C). These crowns and the smaller maxillary crowns show an en echelon orientation in which mesial crown edges are canted linguallly (Fig. 21), as in ornithischian and basal sauropodomorph dinosaurs (Crompton and Attridge 1986; Sereno 1997). The alveolar margin on the maxilla and dentary lateral to these teeth is smooth and bounded by a row of neurovascular foramina (Figs. 16A, 18A).

A. rattoides seems to have had a similar dentition except for procumbent lower incisors, which at present we know only from their alveoli. These enlarged anteriormost teeth are butted next to one another in the midline. The opposing premaxillary incisors may also have been procumbent or shortened, or there may have been a median diastema between the premaxillary tooth rows (Figs. 30C, 45B).

The two species of *Araripesuchus* described in this report may well have been herbivores or, at least, omnivores, given the evidence summarized regarding crown orientation, form, ornamentation and wear and the presence of smooth buccal margins on the maxilla and dentary. The diversity of species within this genus has been perplexing but may be related in some way to their dietary specialization.

Kaprosuchus. *Kaprosuchus* has sharp-edged hypertrophied, relatively straight caniniform teeth set in matching pairs along the sturdy, powerfully muscled jaws. The long retroarticular process suggests rapid opening of the substantial gape required for the opposing caniniforms to clear one another (Figs. 33A, 34A). The size differential within the dentition is very atypical for a crocodyliforms, most of which have fluted, subconical, recurved crowns for aquatic predation.

The fused nasals suggest that the anterior snout margin was reinforced for compression generated by a powerful bite (Fig. 36). Dorsally opening external nares can be interpreted as an aquatic adaptation for sequestering the head during predation. In *Kaprosuchus*, however, the upturned, telescoped external nares appear to be removed from the anterior margin of the snout as protection against impact with prey. The anterior snout margin is thickened and covered with unusual rugosities, which may have served as a platform for a protective keratin sheath (Fig. 35).

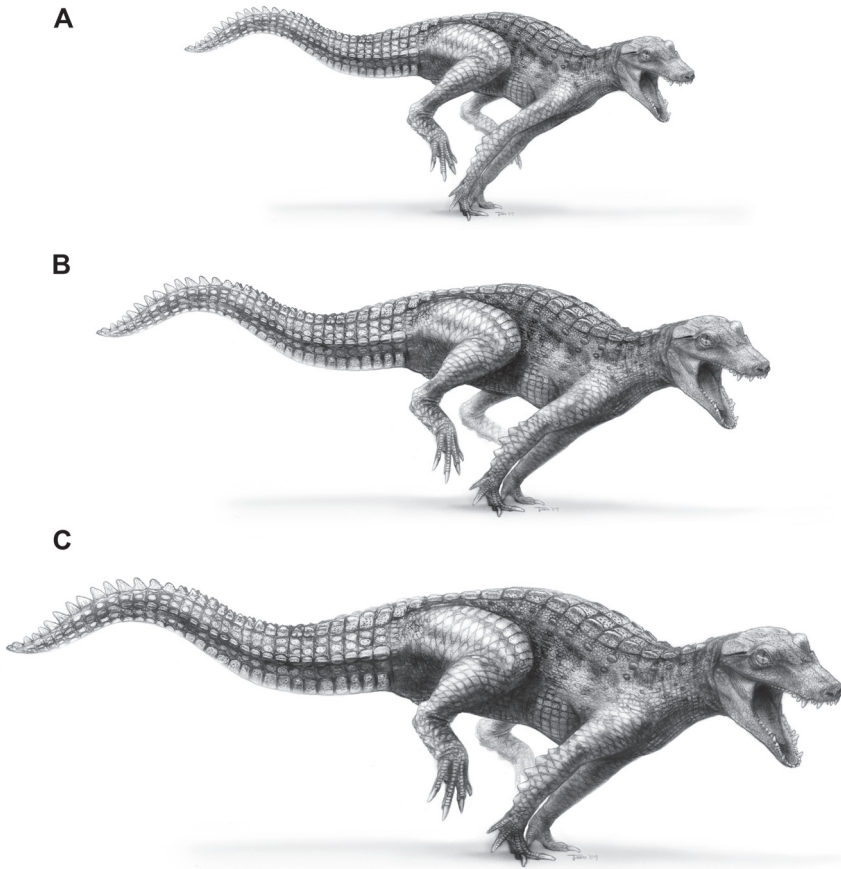


Figure 46. Flesh reconstruction of three growth stages in the crocodyliform *Araripesuchus wegeneri*.

Flesh reconstruction shows upright limb posture and an osteoderm-sheathed tail with convergent proximal keels and median distal paddle. The pose depicted is the forelimb support phase of a symmetrical bounding gallop, the gait pattern observed in *Crocodylus johnstoni* and juveniles of other species within the genus. The flesh reconstructions are based on specimens, in which we measured (or estimated) “trunk length” (= length of the dorsosacral column), “forelimb length” (= sum of humerus, radius, radiale, and metacarpal 3 lengths), and “hind limb length” (= sum of femur, tibia, and metatarsal 3 lengths). **A** Juvenile (~48 cm or 60% adult length) with proportions based on a juvenile specimen of *Araripesuchus gomesii* (AMNH 45550; Hecht 1991), in which forelimb and hind limb length comprise 68% and 98%, respectively, of trunk length. **B** Subadult (~66 cm or 80% adult length) with proportions based on a subadult specimen of *Araripesuchus wegeneri* (MNN GAD20) (Fig. 23). **C** Adult (~81 cm) with proportions based on an adult skeleton (MNN GAD21) (Fig. 23), in which forelimb and hind limb length comprise 50% and 75%, respectively, of trunk length.

The squamosal horns are particularly prominent in anterior view of the skull, which differs from the few crocodyliforms that have raised or swollen the lateral edge of the squamosal (Brochu 2006). The central axis of the orbit, in addition, is directed laterally more than vertically, opposite to that in extant subaquatic crocodylians (Fig.

36A). The orbits thus do not appear to be designed for sequestering the head during aquatic predation. These features together suggest that adult *Kaprosuchus* was primarily, or possibly exclusively, a terrestrial rather than an aquatic predator. At present we have no remains of the postcranium.

***Laganosuchus*.** *Laganosuchus* has begun to lift the veil on its larger cousin *Stomatosuchus*, an enormous flat-skulled crocodyliform for which the only known skull was destroyed during World War II (Nothdurft et al. 2002). The presence of some kind of gular sac below the lower jaw in *Stomatosuchus* remains speculative (Fig. 2G) (Stromer 1925, 1936; Nopcsa 1926). Both genera have extremely slender, long U-shaped lower jaws with a very low, posteriorly positioned coronoid process and short retroarticular processes. The jaws could not have been adducted or abducted with great force. *Laganosuchus* has straight, spike-shaped teeth, the largest of which are slightly procumbent and located at the anterior end of the jaws. At present we have no reliably associated remains of the postcranium. We tentatively infer that stomatosuchids were aquatic low-lying, sit-and-wait predators.

Conclusions

Based on the new fossil material from Morocco and Niger, we draw the following conclusions:

(1) All described taxa in this report fall within Metasuchia. *Anatosuchus* and *Araripesuchus* are positioned within Notosuchia and *Kaprosuchus* and *Laganosuchus* within Neosuchia. *Laganosuchus*, which is clearly related to the enigmatic crocodyliform *Stomatosuchus inermis*, lies outside Eusuchia.

(2) Two of the Saharan crocodyliforms, *Anatosuchus* and *Kaprosuchus*, suggest a novel paleobiogeographic link between continental Africa and Madagascar. Substantial character evidence links them, respectively, with *Simosuchus* and *Mahajangasuchus* from Madagascar.

(3) Endocranial volume (total, forebrain) in *Anatosuchus minor* and *Araripesuchus wegeneri* is allometrically consistent with that in extant crocodylians. The notosuchian forebrain is dorsoventrally flattened and spade-shaped, most closely resembling that in hatchling crocodylians.

(4) Based on crown form, orientation, occlusion and wear, adult *Anatosuchus*, *Kaprosuchus* and *Laganosuchus* are interpreted as carnivores with diets centered, respectively, on small vertebrates/soft invertebrates, large terrestrial vertebrates such as dinosaurs, and aquatic vertebrates. *Araripesuchus wegeneri* and *Araripesuchus rattoides* are interpreted as potential herbivores with denticulate leaf-shaped-to-subcircular crowns that show marked tooth wear with age and procumbent incisors for digging, respectively.

(5) African crocodyliforms of mid- and early Late Cretaceous age appear to be as diverse in locomotor and trophic specializations as comparable-aged crocodyliforms on South America.

Acknowledgements

For execution of final drafts of technical figs. (Figs. 1–5, 7–14, 16–33, 35–42, 44) and graphic flesh reconstructions (Figs. 45, 46), we are indebted to C. Abraczinskas and T. Marshall, respectively. The remaining figs. were prepared by the authors (P. Sereno, Figs. 6, 15, 34; H. Larsson, Fig. 43). We are especially grateful for a detailed critique of the manuscript by D. Pol, H.-D. Sues and D. Unwin and for comments and assistance with specimens by R. Allain, D. Dutheil, and N. Ibrahim. We thank D. Bourgeois, E. Fitzgerald, T. Keillor, R. Masek, and R. Vodden for exquisite fossil preparation, molding and casting. We also thank W. Simpson, A. Resetar and S. Rieboldt for access to fossil and recent crocodyliform skeletal material at the Field Museum and K. Shepherd and M. Feuerstack for loan of material in their care at the Canadian Museum of Nature. For CT-scans of fossil material, we thank M. Colbert and J. Miasano of the University of Texas and C. Straus of the University of Chicago Hospitals. For discovery of the fossil material, we are indebted to D. Dutheil, members of the 1995 Expedition to Morocco, and members of the 1997 and 2000 Expeditions to Niger. We thank the National Geographic Society, Island Fund of the New York Community Trust, Whitten-Newman Foundation, Pritzker Foundation, and David and Lucile Packard Foundation for support of this research. We also thank B. Gado, O. Ide, and A. Maga of the Institut des Sciences Humaines (République du Niger) and Ministère des Mines (Royaume du Maroc) for permission to conduct paleontological fieldwork.

References

- Aguilera OA, Riff D, Bocquentin-Villanueva J (2006) A new giant *Purussaurus* (Crocodyliformes, Alligatoridae) from the Upper Miocene Urumaco Formation, Venezuela. *Journal of Systematic Palaeontology* 4: 221–232.
- Bocquentin-Villanueva J (1984) Un nuevo *Nettosuchidae* (Crocodylia, Eusuchia) proveniente de la Formación Urumaco (Mioceno Superior), Venezuela. *Ameghiniana* 21: 3–8.
- Brochu CA (2006) A new miniature horned crocodile from the Quaternary of Aldabra Atoll, western Indian Ocean. *Copeia* 2006: 149–158.
- Brochu CA (2001) Crocodylian snouts in space and time: phylogenetic approaches toward adaptive radiation. *American Zoologist* 41: 564–585.
- Broin F de Lapparent de, Taquet P (1966) Découverte d'un crocodile nouveau dans la Crétacé inférieur du Sahara. *Comptes Rendus de l'Académie des Sciences Paris* 262: 2326–2329.
- Broin F de Lapparent de (2002) *Elosuchus*, a new genus of crocodile from the Cretaceous of the North of Africa. *Comptes Rendus Palevol* 1: 275–275.25]
- Buckley GA, Brochu CA (1999) An enigmatic crocodile from the Upper Cretaceous of Madagascar. *Special Papers in Palaeontology* 60: 149–175.
- Buckley GA, Brochu CA, Krause DW, Pol D (2000) A pug-nosed crocodyliform from the Late Cretaceous of Madagascar. *Nature* 405: 941–944.

- Buffetaut E (1974) *Trematochampsia taqueti*, un crocodilien nouveau du Sénomien inférieur du Niger. Comptes Rendus de l'Académie des Sciences Paris, Séries D 279: 1749–1752.
- Buffetaut E (1976) Ostéologie et affinités de *Trematochampsia taqueti* (Crocodylia, Mesosuchia) du Sénomien inférieur d'In Beceten (République du Niger). Geobios 9: 143–198.
- Buffetaut E (1981) Die biogeographische Geschichte der Krokodilier, mit Beschreibung einer neuen Art, *Araripesuchus wegeneri*. Geologische Rundschau 70: 611–624.
- Buffetaut E (1994) A new crocodilian from the Cretaceous of southern Morocco. Comptes Rendus de l'Académie des Sciences Paris, Séries 2, Sciences de la Terre et des Planètes 319: 1563–1568.
- Buffetaut E, Rage J-C (1993) Fossil amphibians and reptiles and the Africa-South America connection. In: George W, Lavocat R (Eds) The Africa-South America Connection. Clarendon Press, Oxford, 87–99.
- Buffetaut E, Taquet P (1977) The giant crocodilian *Sarcosuchus* in the Early Cretaceous of Brazil and Niger. Palaeontology 20: 203–208.
- Buffetaut E, Taquet P (1979a) An early Cretaceous terrestrial crocodilian and the opening of the South Atlantic. Nature 280: 486–487.
- Buffetaut E, Taquet P (1979b) Un nouveau crocodilien mésosuchien dans le Campanien de Madagascar, *Trematochampsia oblita*, n. sp. Bulletin de la Société géologique de France 9: 143–198.
- Busbey AB (1994) The structural consequences of skull flattening in crocodilians. In: Thomson JJ (Ed) Functional Morphology in Vertebrate Paleontology. Cambridge University Press, Cambridge, 173–192.
- Candeiro CRA, Martinelli AG (2006) A review of paleogeographical and chronostratigraphical distribution of mesoeucrocodylian species from the upper Cretaceous beds from the Bauru (Brazil) and Neuquén (Argentina) groups, southern South America. Journal of South American Earth Sciences 22: 116–129.
- Candeiro CA, Martinelli AG, Avilla LS, Rich TH (2006) Tetrapods from the Upper Cretaceous (Turonian-Maastrichtian) Bauru Group of Brazil: a reappraisal. Cretaceous Research 27: 923–946.
- Carvalho IS, Ribeiro LCB, Avilla LS (2004) *Uberabasuchus terrificus* sp. n., a new Crocodylomorpha from the Bauru Basin (Upper Cretaceous). Gondwana Research 7: 975–1002.
- Carvalho IS (1994) *Candidodon*: um crocodilo com heterodontia (Notosuchia, Cretaceo Inferior-Brasil). Anais da Academia Brasileira de Ciências 66: 331–346.
- Chiappe LM (1988) A new trematochampsid crocodile from the Early Cretaceous of north-western Patagonia, Argentina and its palaeobiogeographical and phylogenetic implications. Cretaceous Research 9: 379–389.
- Chiasson RB (1962) Laboratory Anatomy of the Alligator. W. C. Brown Company Publishers, Dubuque, Iowa, 56 pp.
- Clark JM (1994) Patterns of evolution in Mesozoic Crocodyliformes. In: Fraser NC, Sues H-D (Eds) In the Shadow of the Dinosaurs: Early Mesozoic Tetrapods. Cambridge University Press, Cambridge, 84–97.
- Clark JM, Sues H-D, Berman DS (2000) A new specimen of *Hesperosuchus agilis* from the Upper Triassic of New Mexico and the interrelationships of basal crocodylomorph archosaurs. Journal of Vertebrate Paleontology 20: 683–704.
- Clark JM, Xu X, Forster CA, Wang Y (2004) A Middle Jurassic spheenosuchian from China and the origin of the crocodylian skull. Nature 430: 1021–1024.

- Colbert EH, Mook CC (1951) The ancestral crocodilian *Protosuchus*. Bulletin of the American Museum of Natural History 94: 143–182.
- Crompton AW, Attridge J (1986) Masticatory apparatus of the larger herbivores during Late Triassic and Early Jurassic times. In: Padian K (Ed) The Beginning of the Age of Dinosaurs: Faunal Change Across the Triassic-Jurassic Boundary. Cambridge University Press, London, 223–236.
- Crush PJ (1984) A late Upper Triassic sphenosuchid crocodilian from Wales. Palaeontology 27: 131–157.
- Fiorelli LE, Calvo JO (2008) New remains of *Notosuchus terrestris* Woodward, 1896 (Crocodyliformes: Mesoeucrocodylia) from the Late Cretaceous of Neuquén, Patagonia, Argentina. Arquivos do Museu Nacional Rio de Janeiro 66: 83–124.
- Gans C (1980) Allometric changes in the skull and brain of *Caiman crocodilus*. Journal of Herpetology 14: 297–301.
- Gasparini Z, Chiappe LM, Fernandez M (1991) A new Senonian peirosaurid (Crocodylomorpha) from Argentina and a synopsis of the South American Cretaceous crocodilians. Journal of Vertebrate Paleontology 11: 316–333.
- Gomani EM (1997) A crocodyliform from the Early Cretaceous dinosaur beds, northern Malawi. Journal of Vertebrate Paleontology 17: 280–294.
- Hecht M (1991) *Araripesuchus* Price, 1959. In: Maisey JG (Ed) Santana fossils: An illustrated atlas. T.F.H. Publications, Neptune, New Jersey, 342–347.
- Hopson JA (1979) Paleoneurology. In: Gans C (Ed.) Biology of the Reptilia. Academic Press, London, 39–146.
- Iordansky NN (1973) The skull of the Crocodilia. In: Gans C, Parsons TS (Eds) Biology of the Reptilia, vol. 4 Morphology. Academic Press, London and New York, 201–262.
- Jollie M (1962) Chordate Morphology. Reinhold, New York, 478 pp.
- Langston Jr. W (1965) Fossil crocodilians from Colombia and the Cenozoic history of the Crocodilia in South America. University of California Publications in Geological Sciences 52: 1–169.
- Langston Jr. W (1966) *Mourasuchus* Price, *Nettosuchus* Langston, and the Family Nettosuchidae (Reptilia: Crocodilia). Copeia 1966: 882–885.
- Langston Jr. W (1973) The crocodilian skull in historical perspective. In: Gans C (Ed) Biology of the Reptilia, 263–284.
- Larsson HC (2001) Endocranial anatomy of *Carcharodontosaurus saharicus* (Theropoda: Allosauroidae) and its implications for theropod brain evolution. In: Tanke DH, Carpenter K (Eds) Mesozoic Vertebrate Life. Indiana University Press, Bloomington, 19–33.
- Larsson HCE, Gado B (2000) A new Early Cretaceous crocodyliform from Niger. Neues Jahrbuch für Geologie und Paläontologie Abhandlungen 217: 131–142.
- Larsson HCE, Sereno PC, Wilson JA (2000) Forebrain enlargement among nonavian theropod dinosaurs. Journal of Vertebrate Paleontology 20: 615–618.
- Larsson HCE, Sidor CA (1999) Unusual crocodyliform teeth from the Late Cretaceous (Cenomanian) of southeastern Morocco. Journal of Vertebrate Paleontology 19: 398–401.
- Larsson HCE, Sues HD (2007) Cranial osteology and phylogenetic relationships of *Hamadrasuchus rebouli* (Crocodyliformes: Mesoeucrocodylia) from the Cretaceous of Morocco. Zoological Journal of the Linnean Society 149: 533–567.

- Lavocat R (1955) Découverte d'un crocodilien du genre *Thoracosaurus* dans le Crétacé supérieur d'Afrique. Bulletin du Muséum National d'Histoire Naturelle 27: 338–340.
- Lecuona A, Pol D (2008) Tooth morphology of *Notosuchus terrestris* (Notosuchia: Mesoeucrocodylia): New evidence and implications. Comptes Rendus Palevol 7: 407–417.
- Li J-L, Wu X-C, Li X-M (1994) New material of *Hsisosuchus chungkingensis* from Sichuan, China. Vertebra Palasiatica 32: 107–126.
- Marinho TS, Carvalho IS (2009) An armadillo-like sphagesaurid crocodyliform from the Late Cretaceous of Brazil. Journal of South American Earth Sciences 27: 36–41.
- Martinelli A (2003) New cranial remains of the bizarre notosuchid *Comahuesuchus brachybuccalis* (Archosauria, Crocodyliformes) from the Late Cretaceous of Río Negro Province (Argentina). Ameghiniana 40: 559–572.
- Montefeltro FC, Laurini CR, Langer MC (2009) Multicusped crocodyliform teeth from the Upper Cretaceous (São José do Rio Preto Formation, Bauru Group) of São Paulo, Brazil. Cretaceous Research 30: 1279–1286.
- Mook CC (1921) Notes on the postcranial skeleton in the Crocodilia. Bulletin of the American Museum of Natural History 44: 67–100.
- Nopcsa F (1926) Neue Beobachtungen an *Stomatosuchus*. Centralblatt für Mineralogie, Geologie und Paläontologie B 1926: 212–215.
- Nothdurft WE, Smith J, Lamanna MC, Lacovara KJ, Poole JC et al. (2002) The Lost Dinosaurs of Egypt. Random House, New York, 256 pp.
- O'Connor P, Sertich J, Stevens N, Gottfried M, Roberts E (2008) The evolution of mammal-like crocodyliforms (Crocodyliformes: Notosuchia) in Gondwana: New evidence from the Middle Cretaceous Galula Formation, Rukwa Rift basin, southwestern Tanzania. Journal of Vertebrate Paleontology 28: 122A.
- Ortega F, Gasparini Z, Buscalioni AD, Calvo JO (2000) A new species of *Araripesuchus* (Crocodylomorpha, Mesoeucrocodylia) from the Lower Cretaceous of Patagonia (Argentina). Journal of Vertebrate Paleontology 20: 57–76.
- Pol D, Apesteguía S (2005) New *Araripesuchus* remains from the early Late Cretaceous (Cenomanian-Turonian) of Patagonia. American Museum Novitates 3490: 1–38.
- Prasad GVR, Broin F de Lapparent de (2002) Late Cretaceous crocodile remains from Naskal (India): comparisons and biogeographic affinities. Annales de Paléontologie 88: 19–71.
- Platel R (1976) Analyse volumétrique comparée des principales subdivisions encéphaliques chez les reptiles sauriens. Journal für Hirnforschung 17: 513–537.
- Pol D (2005) Postcranial remains of *Notosuchus terrestris* Woodward (Archosauria: Crocodyliformes) from the Upper Cretaceous of Patagonia, Argentina. Ameghiniana 42: 21–38.
- Pol D, Gasparini Z (2009) Skull anatomy of *Dakosaurus andiniensis* (Thalattosuchia: Crocodylomorpha) and the phylogenetic position of Thalattosuchia. Journal of Systematic Palaeontology 7: 163–197.
- Price LI (1955) Novos crocodilídeos dos arenitos da Série Bauru. Cretáceo do Estado de Minas Gerais. Anais da Academia Brasileira de Ciências 27: 487–498.
- Price LI (1959) Sobre um crocodilídeo notosúquio do Cretáceo brasileiro. Boletim Divisão de Geologia e Mineralogia do Rio de Janeiro 188: 1–55.

- Rasmusson Simons EL, Buckley GA (2009) New material of “*Trematochampsia*” *oblita* (Crocodyliformes, Trematochampsidae) from the Late Cretaceous of Madagascar. *Journal of Vertebrate Paleontology* 29: 599–604.
- Roberts EM, O’Connor PM, Gottfried MD, Stevens N, Kapalima S et al. (2004) Revised stratigraphy and age of the Red Sandstone Group in the Rukwa Rift Basin, Tanzania. *Cretaceous Research* 25: 749–759.
- Ross FD, Mayer GC (1984) On the dorsal armor of the Crocodilia. In: Rhodin AGJ, Miyata K (Eds) *Advances in Herpetology and Evolutionary Biology*. Harvard University Press, Cambridge, 305–331.
- Rusconi C (1933) Sobre reptiles cretáceos del Uruguay (*Uruguaysuchus aznarezi*, n. gen. n. sp.) y sus relaciones con los notosúquidos de Patagonia. *Instituto de Geología y Perforaciones Boletín* 19: 1–64.
- Salisbury SW, Willis PMA, Peitz S, Sander PM (1999) The crocodilian *Goniopholis simus* from the Lower Cretaceous of north-western Germany. *Special Papers in Palaeontology* 60: 121–148.
- Salisbury SW, Molnar RE, Frey E, Willis P (2006) The origin of modern crocodyliforms: new evidence from the Cretaceous of Australia. *Proceeding of the Royal Society of London B* 273: 2439–2448.
- Savitzky AH (1983) Coadapted character complexes among snakes: fossoriality, piscivory, and durophagy. *American Zoologist* 23: 397–409.
- Sereno PC (1997) The origin and evolution of dinosaurs. *Annual Review of Earth and Planetary Sciences* 25: 435–489.
- Sereno PC (2005) The logical basis of phylogenetic taxonomy. *Systematic Biology* 54: 595–619.
- Sereno PC (2005) Stem Archosauria—*TaxonSearch*. Available: http://www.taxonsearch.org/dev/file_home.php. 2005 November 7.
- Sereno PC (2007) Logical basis for morphological characters in phylogenetics. *Cladistics* 23: 565–587.
- Sereno PC (2009) Comparative cladistics. *Cladistics*. 25:1–34.
- Sereno PC, Beck AL, Dutheil DB, Gado B, Larsson HCE et al. (1998) A long-snouted predatory dinosaur from Africa and the evolution of spinosaurids. *Science* 282: 1298–1302.
- Sereno PC, Beck AL, Dutheil DB, Larsson HC, Lyon GH et al. (1999) Cretaceous sauropods from the Sahara and the uneven rate of skeletal evolution among dinosaurs. *Science* 286: 1342–1347.
- Sereno PC, Brusatte SL (2008) Basal abelisaurid and carcharodontosaurid theropods from the Lower Cretaceous Elrhaz Formation of Niger. *Acta Palaeontol Pol* 53: 15–46.
- Sereno PC, Dutheil DB, Iarochene M, Larsson HCE, Lyon GH et al. (1996) Predatory dinosaurs from the Sahara and Late Cretaceous faunal differentiation. *Science* 272: 986–991.
- Sereno PC, Larsson HCE, Sidor CA, Gado B (2001) The giant crocodyliform *Sarcosuchus* from the Cretaceous of Africa. *Science* 294: 1516–1519.
- Sereno PC, McAllister S, Brusatte SL (2005) *TaxonSearch*: a relational database for suprageneric taxa and phylogenetic definitions. *PhyloInformatics* 8: 1–20.
- Sereno PC, Sidor CA, Larsson HCE, Gado B (2003) A new notosuchian from the Early Cretaceous of Niger. *Journal of Vertebrate Paleontology* 23: 477–482.
- Sereno, PC, Wilson JA, Witmer LM, Whitlock JA, Maga A et al. (2007) Structural extremes in a Cretaceous dinosaur. *PLoS ONE* 2: e1230.

- Steel R (1973) Crocodylia. Vol. 16. In: Handbuch der Paläoherpetologie, O. Kuhn (Ed), Gustav Fischer, Stuttgart-Portland, 1–116.
- Stromer E (1914) Ergebnisse der Forschungsreisen Prof. E. Stromers in den Wüsten Ägyptens. II. Wirbeltier-Reste der Baharije-Stufe (unterstes Cenoman). 1. Einleitung und 2. *Libysuchus*. Abhandlungen der Königlich Bayerischen Akademie der Wissenschaften, Mathematisch-Physikalische Klasse 27: 1–16.
- Stromer E (1925) Ergebnisse der Forschungsreisen Prof. E. Stromers in den Wüsten Ägyptens. II. Wirbeltier-Reste der Baharije-Stufe (unterstes Cenoman). 7. *Stomatosuchus inermis* Stromer, ein schwach bezahnter Krokodilier und 8. Ein Skelettrest des Pristiden *Onchopristis numidus* Huag sp. Abhandlungen der Königlich Bayerischen Akademie der Wissenschaften, Mathematisch-Physikalische Klasse 30: 1–22.
- Stromer E (1936) Ergebnisse der Forschungsreisen Prof. E. Stromers in den Wüsten Ägyptens. II. Wirbeltier-Reste der Baharije-Stufe (unterstes Cenoman). VII. Baharije-Kessel und -Stufe mit deren Fauna und Flora. Eine ergänzende Zusammenfassung. Abhandlungen der Königlich Bayerischen Akademie der Wissenschaften, Mathematisch-Physikalische Klasse 33: 1–102.
- Swofford D (1998) PAUP*. Phylogenetic Analysis Using Parsimony (*and Other Methods). Version 4.0. Version 4.0 ed. Sinauer Associates, Inc., Sunderland, Massachusetts.
- Taquet P (1976) Géologie et paléontologie du gisement de Gadoufaoua (Aptian du Niger). Cahiers de Paléontologie 1976: 1–191.
- Taquet P, Russell DA (1999) A massively-constructed iguanodont from Gadoufaoua, Lower Cretaceous of Niger. Annales de Paléontologie 85: 85–96.
- Tucker AD, Limpus CJ, McCallum HI, McDonald KR (1996) Ontogenetic dietary partitioning by *Crocodylus johnstoni* during the dry season. Copeia 1996: 978–988.
- Turner AH (2004) Crocodyliform biogeography during the Cretaceous: evidence of Gondwanan vicariance from biogeographical analysis. Proceedings of the Royal Society of London B 271: 2003–2009.
- Turner AH (2006) Osteology and phylogeny of a new species of *Araripesuchus* (Crocodyliformes: Mesoeucrocodylia) from the Late Cretaceous of Madagascar. Historical Biology 18: 255–369.
- Turner AH, Buckley GA (2008) *Mahajangasuchus insignis* (Crocodyliformes: Mesoeucrocodylia) cranial anatomy and new data on the origin of the eusuchian-style palate. Journal of Vertebrate Paleontology 28: 382–408.
- Wilson JA (2006) Anatomical nomenclature of fossil vertebrates: standardized terms or ‘lingua franca’? Journal of Vertebrate Paleontology 26: 511–518.
- Wilson JA, Gingerich PD (2001) New crocodyliform (Reptilia, Mesoeucrocodylia) from the Upper Cretaceous Pab Formation of Vitakri, Balochistan (Pakistan). Contributions of the Museum of Paleontology University of Michigan 30: 1–12.
- Wu X-C, Chatterjee S (1993) *Dibothrosuchus elaphros*, a crocodylomorph from the Lower Jurassic of China and the phylogeny of the Sphenosuchia. Journal of Vertebrate Paleontology 13: 58–89.
- Zaher H, Pol D, Carvalho AB, Riccomini C, Campos D et al. (2006) Redescription of the cranial morphology of *Mariliasuchus amarali*, and its phylogenetic affinities (Crocodyliformes, Notosuchia). American Museum Novitates 3512: 1–40.

Appendix

Character list

Characters and character states are listed for the 252 characters used in the phylogenetic analysis (Figure 43). The majority of the characters are taken or adapted from a series of previous publications with original authors cited accordingly (see References below). Five characters are introduced here and highlighted in red as “new characters” (characters 46, 83, 132, 178, 182). Forty-one characters are ordered, because the successive states logically include preceding states (characters 5, 8, 18, 21, 32, 33, 36, 44, 48, 49, 51, 52, 67, 69, 79, 80, 87, 89, 106, 121, 126, 127, 131, 132, 134, 135, 142, 147, 158, 160, 169, 185, 210, 216, 220, 223, 230, 246, 248, 251, 252).

1. External surface of dorsal cranial bones (adapted from Clark [1994: character 1])
 - 0 relatively smooth
 - 1 slightly grooved
 - 2 heavily ornamented with deep pits and grooves
2. Snout lateral expansion at orbits (adapted from Clark [1994: character 2])
 - 0 gradual
 - 1 abrupt
3. Snout length (anterior margin of orbits to rostrum) relative to remainder of skull (modified from Wu et al. [1997: character 4])
 - 0 equal or longer
 - 1 shorter
4. Snout cross-section dimensions (adapted from Clark [1994: character 3])
 - 0 higher than wide
 - 1 equally high as wide
 - 2 wider than high
5. Antorbital fenestra size relative to orbit (modified by Larsson and Sues [2007: character 72] from Clark [1994: character 67])
 - 0 about half
 - 1 smaller than half but present
 - 2 only an external fossa (may have a tiny fenestra)
 - 3 absent
6. Shape of antorbital fossa (Gasparini et al. [2006: character 246])
 - 0 subcircular or subtriangular
 - 1 elongated, low, and oriented obliquely
7. Anteroposterior length of supratemporal fenestrae (modified by Larsson and Sues [2007: character 21] from Clark [1994: character 68])
 - 0 equal to or shorter than orbits
 - 1 much longer than orbits
8. Nasal extension dorsally into external nares (modified from Clark [1994: character 13] by Larsson [2000])

- 0 absent by maxilla – maxilla contact
- 1 absent by premaxilla – premaxilla contact
- 2 none but contacts external nares
- 3 present and less than 50 percent
- 4 present and 50 percent or more but not completely
- 9. Dorsal surface of rostrum (adapted from Brochu [1997: character 101])
 - 0 curves smoothly
 - 1 bears medial boss
- 10. Nasal-nasal suture (Gasparini et al. [2006: character 257])
 - 0 unfused
 - 1 partially or completely fused
- 11. Nasal, posterior tip (Ortega et al. [2000: character 24])
 - 0 converge at sagittal plane
 - 1 separated by an anterior sagittal projection of frontals
- 12. Posterolateral region of nasals (Pol and Apesteguia [2005: character 223])
 - 0 flat surface facing dorsally
 - 1 lateral region deflected ventrally, forming part of the lateral surface of the snout
- 13. Immediate preorbital region cross section (Larsson [2000])
 - 0 squared
 - 1 gently curved
- 14. Prefrontal and lacrimal orbital margin (Larsson [2000])
 - 0 flat
 - 1 dorsally upturned to telescope orbit
- 15. Prefrontals anterior to orbits (modified from Gomani [1997: character 4])
 - 0 elongated, parasagittal orientation
 - 1 short, broad, and oriented anterolaterally
- 16. Orbital margin of prefrontal (Larsson [2000: character 6])
 - 0 confluent with orbit
 - 1 projects laterally
- 17. Prefrontal and lacrimal border to orbit (Gasparini et al. [2006: character 256])
 - 0 flat, confluent to snout surface
 - 1 invaginated, forming elevated rims
- 18. Depression on prefrontal for a palpebral element (Larsson [2000])
 - 0 absent
 - 1 thin groove
 - 2 deep groove terminating anteriorly in a deep fossa
- 19. Transverse external prefrontal-frontal ridge (Larsson [2000])
 - 0 absent
 - 1 present and complete over prefrontals and frontals
- 20. Prefrontal descending process (modified from Clark [1994: character 15])
 - 0 no palatine contact
 - 1 cylindrical or thin anteroposterior suture with palatine
 - 2 transversely broad suture with palatine

21. Lacrimal-nasal contact (modified from Clark [1994: character 11]; Brochu [1997: character 93])
 - 0 broad
 - 1 partially separated by posterior process of maxilla
 - 2 absent (maxilla separates lacrimal and nasal)
22. External lacrimal shape (modified from Brochu [1997: character 106])
 - 0 longer than broad
 - 1 nearly as broad as long
23. Total lacrimal length relative to total prefrontal (adapted from Norell [1988: character 7]; Brochu [1997: character 117])
 - 0 longer
 - 1 subequal
 - 2 shorter
24. Anterior ramus of frontals relative to anterior ramus of prefrontals (Larsson [2000])
 - 0 posterior
 - 1 anterior
25. Ventral half of lacrimal (Zaher et al. [2006: character 193])
 - 0 extends posteroventrally to widely contact jugal
 - 1 tapering posteroventrally to not or only slightly contact jugal
26. Frontal – frontal contact (adapted from Clark [1994: character 21])
 - 0 paired
 - 1 fused
27. Width of frontals between orbits relative to mid-length width across nasals (modified from Clark [1994: character 20])
 - 0 narrow (similar to width of nasals)
 - 1 broad (about twice the width of nasals)
28. Dorsal surface of frontal and parietal (Clark [1994: character 22])
 - 0 flat
 - 1 with sagittal ridge
29. Frontal orbital margin (Larsson [2000])
 - 0 flat
 - 1 dorsally upturned
30. Frontoparietal suture entry into supratemporal fenestra (modified from Clark [1994: character 23]; Brochu [1997: character 81])
 - 0 deep, preventing broad postorbital (or postfrontal) – parietal contact
 - 1 no entry, broad postorbital (or postfrontal) – parietal contact
31. Palpebrals (modified from Clark [1994: character 65])
 - 0 absent
 - 1 one small present
 - 2 one or multiple present and largely covering the dorsal surface of the orbit

32. Dermal bone overhang about the supratemporal fenestra (Larsson [2000])
 - 0 absent
 - 1 present only medially
 - 2 present about all but the anteromedial corner (fossa)
33. Medial borders of supratemporal fenestrae (Larsson [2000])
 - 0 separated by a broad sculptured region
 - 1 separated by a thin sculpted region
 - 2 contact to form a low sagittal crest
34. Medial dorsal edges of supratemporal fenestrae (Larsson [2000])
 - 0 flat
 - 1 raised
35. Posterior extent of orbital edge of jugal (Larsson [2000] (in part adapted from Brochu [1997: character 139])
 - 0 confluent with postorbital bar
 - 1 displaced laterally and ends anterior to postorbital bar (forming posteroventral notch in orbit)
 - 2 displaced laterally and ends at or just behind postorbital bar
 - 3 displaced laterally and ends near posterior corner of infratemporal fenestra
36. Width of anterior process of jugal relative to posterior process (adapted from Clark [1994: character 17])
 - 0 subequal
 - 1 about twice as broad
37. Dorsal surface of jugal beneath infratemporal fenestra (modified from Clark [1994: character 18])
 - 0 ovate cross-section
 - 1 longitudinal crest
38. Anterior process of jugal relative to infratemporal fenestra anteroposterior length (Larsson [2000])
 - 0 subequal
 - 1 much longer
39. Anterior margins of lacrimal and jugal (Larsson [2000])
 - 0 confluent with no notch at anterior contact
 - 1 jugal edge convex producing an anterior notch at contact
40. Jugal participation in margin of antorbital fossa (Wu and Sues [1996: character 14])
 - 0 present
 - 1 absent
41. Lateral surface of anterior process of jugal (modified by Turner and Buckley [2008: character 121] from Pol [1999: character 133] and Ortega et al. [2000: character 145])
 - 0 flat or convex
 - 1 broad shelf below orbit with triangular depression beneath

42. Jugal postorbital process base projection (modified by Turner and Buckley [2008: character 142] from Pol [1999: character 156])
 - 0 posterodorsal
 - 1 dorsal
 - 2 anterodorsal
43. Jugal anterior margin relative to orbit (Pol [1999: character 134])
 - 0 not anterior to
 - 1 anterior to
44. Jugal ventral margin (new combination from Pol et al. [2004: character 179] and Turner and Buckley [2008: character 286])
 - 0 relatively straight
 - 1 gentle concave arch
 - 2 steep concave peak at level of postorbital bar
45. Large foramen on the lateral surface of jugal, near its anterior margin (Zaher et al. [11: character 194])
 - 0 absent
 - 1 present
46. Lateral surface of jugal-ectopterygoid contact (*new character*)
 - 0 inset from lateral jugal margin
 - 1 confluent with lateral jugal margin forming a depression
47. Jugal posterior process exceeds posteriorly the infratemporal fenestra (Pol [1999: character 150])
 - 0 yes
 - 1 no
48. Quadratojugal – postorbital contact (modified by Larsson and Sues [3] from Buscalioni et al. [1992: character 6]; Clark [1994: characters 14 and 19]; Brochu [1997: character 80])
 - 0 absent
 - 1 narrows dorsally and contacts a small region of the postorbital
 - 2 broadens dorsally to contact most of the postorbital bar to diminish the infratemporal fenestra
49. Spina quadratojugal (modified from Norell [1989: character 1]; Brochu [1997: character 69])
 - 0 absent
 - 1 small or low crest
 - 2 prominent
50. Elements at posterior angle of infratemporal fenestra (adapted from Norell [1989: character 10]; Brochu [1997: character 75])
 - 0 quadratojugal
 - 1 quadratojugal and jugal
 - 2 jugal

51. Quadratojugal posteroventral extension (combined from Larsson and Sues [2007: character 30] and Pol [1999: character 155])
 - 0 does not reach quadrate condyles
 - 1 reaches but does not participate in quadrate condyles
 - 2 forms lateral extension to the quadrate condyles and participates in mandibular joint
52. Length of anterior process of quadratojugal (adapted from Brochu [1997: character 83])
 - 0 short or absent
 - 1 long (less than half length of lower temporal bar) -- moderate [1/3 of lower temporal bar]
 - 2 long (greater than half of lower temporal bar)
53. Quadratojugal ornamentation at its base (Pol [1999: character 161])
 - 0 absent
 - 1 present
54. Posterior skull table (modified by Larsson [2000] from Clark [1994: character 24])
 - 0 non-planar (squamosal ventral to horizontal level of postorbital and parietal)
 - 1 planar (postorbital, squamosal, and parietal on same horizontal plane)
55. Cranial table width relative to ventral portion of skull (adapted from Wu et al. [2] character 123)
 - 0 nearly as wide
 - 1 narrower
56. Dorsal and ventral edges of squamosal groove for external ear valve musculature (Larsson [2000])
 - 0 absent
 - 1 ventral edge is lateral to dorsal
 - 2 ventral edge is directly beneath dorsal
57. Posterior region of auditory fossa (Larsson [2000])
 - 0 opens posteriorly
 - 1 bounded posteriorly by a posteroventrolateral extension of the squamosal and exoccipital
58. Squamosal prongs (modified extensively from Clark [1994: characters 35 and 36]; Brochu [1997: character 140])
 - 0 short or absent
 - 1 present, depressed from skull table, unsculpted
 - 2 present, level with skull table, sculpted
 - 3 present, upturned, sculpted
59. Distal squamosal prong (Larsson [2000])
 - 0 tapered
 - 1 broad
60. Posterolateral overhanging rim of supratemporal fossa (modified from Ortega et al. [2000: character 75])
 - 0 absent, anterior opening of temporo-orbital foramen visible in dorsal view
 - 1 present and temporo-orbital foramen partially occluded from dorsal view

61. Squamosal posterolateral region, lateral to paroccipital process (Gasparini et al. [2005: character 249])
 - 0 narrow
 - 1 bearing a subrounded flat surface
62. Posteromedial branch of squamosal orientation (Gasparini et al. [2006: character 250])
 - 0 transverse
 - 1 posterolateral
63. Parietal dorsal surface between supratemporal fenestrae (modified from Clark [1994: character 33])
 - 0 broad sculpted region
 - 1 sagittal crest
64. Postorbital participation in infratemporal fenestra (Wu et al. [1997: character 108])
 - 0 nearly or completely excluded
 - 1 present
65. Postorbital bar sculpturing (if skull sculpted) (modified from Clark [1994: character 25])
 - 0 present
 - 1 absent
66. Postorbital bar (adapted from Norell [1989: character 3]; Clark [1994: 26]; Brochu [1997: character 70])
 - 0 transversely flattened (ectopterygoid does not strongly contact bar)
 - 1 massive (roughly anterolateral elliptical cross-section)
 - 2 slender (cylindrical); roughly anteromedially elliptical
67. Postorbital posteroventral process (modified from Brochu [1997: character 76])
 - 0 absent
 - 1 present as a thin descending process from the postorbital along the quadratojugal
 - 2 present and contacts the quadrate
68. Anterolateral projections on postorbital bar (adapted from Norell [1989: character 2]; Brochu [1997: character 134])
 - 0 absent
 - 1 present
69. Anterior extension of external auditory meatus fossa (Larsson [2000]; modified from Brochu [1997: character 163])
 - 0 squamosal
 - 1 onto posterior margin of postorbital, separated from anterior margin by a vertical ridge (postorbital roof overhangs postorbital-squamosal suture)
 - 2 to anterolateral edge of postorbital
 - 3 along entire length of postorbital and continues into orbit over a thin ramus of the postorbital
70. Vascular opening on lateral edge of dorsal part of postorbital bar (modified from Clark [1994: character 27])
 - 0 absent
 - 1 present

71. Postorbital with prominent anterolateral projection distinct from dorsal corner (adapted from Clark [1994: character 28])
 - 0 absent
 - 1 present
72. Depression on anterodorsal surface of postorbital for a palpebral element (Larsson [2000])
 - 0 absent
 - 1 present
73. Postorbital bar relative to dorsolateral edge of postorbital (adapted from Clark [1994: character 30])
 - 0 continuous
 - 1 inset medially
74. Bar between orbit and supratemporal fossa (adapted from Clark [1994: character 31])
 - 0 broad
 - 1 narrow (fossa nearly covers entire bar)
75. Position of postorbital relative to jugal on ventral end of postorbital bar (modified from Clark [1994: character 16])
 - 0 anterior
 - 1 medial
 - 2 lateral
76. Postorbital-ectopterygoid contact (Pol [1999: character 158])
 - 0 present
 - 1 absent
77. Bones on lateral surface of postorbital bar (Gasparini et al. [2006: character 244])
 - 0 postorbital and jugal
 - 1 only postorbital
78. Premaxillary labial process extending anteriorly beyond tooth row (Larsson [2000])
 - 0 absent
 - 1 present
79. Premaxilla midline extension into anterior margin of external nares (modified from Clark [1994: character 4]; Brochu [1997: character 145]; Wu et al. [1997: character 125])
 - 0 none
 - 1 small projection (less than 10 percent length of nares)
 - 2 present and less than 50 percent
 - 3 present and more than 50 percent but not completely
80. Premaxilla midline extension from posterior margin of external nares (Larsson and Sues [2007: character 50] modified from Pol [1999: character 135]; Larsson [2000])
 - 0 absent
 - 1 present and thin
 - 2 present and thick to form a posterodorsal notch

81. External nares orientation (modified from Clark [1994: character 6])
 - 0 lateral
 - 1 dorsal
 - 2 anterior or anterolateral
82. Circumnarial fossa (Larsson [2000])
 - 0 absent
 - 1 present
83. Single or paired foramina at posterolateral corner of pm above tooth row (*new character*)
 - 0 absent
 - 1 present
84. Foramen on palatal pm-m contact near tooth row (Larsson and Sues [2007: character 60] and Pol [1999: character 149])
 - 0 small or absent
 - 1 large
 - 2 large and connects with an elongate foramen in the external pm-m suture immediately above the tooth line
85. Premaxilla palatal shelves (Larsson [2000])
 - 0 do not meet posteriorly
 - 1 meet posteriorly
86. Incisive foramen (modified from Clark [1994: character 7]; Brochu [1997: character 124])
 - 0 present and large (length equal to or more than half the greatest width of premaxillae)
 - 1 present and small (length less than half the width of the premaxillae)
 - 2 absent (palatal parts of premaxillae in contact along entire length)
87. Premaxilla tooth count (Modified from Norell [1988: character 17]; Brochu [1997: character 97])
 - 0 two
 - 1 three
 - 2 four
 - 3 five
88. Anterior two premaxillary teeth (Larsson [2000])
 - 0 separate
 - 1 nearly confluent
89. Posterodorsal premaxillary process extension (adapted from Brochu [1997: character 145] and Pol [1999: character 138])
 - 0 absent
 - 1 present but not beyond third maxillary alveolus
 - 2 present and beyond third maxillary alveolus

90. Premaxilla-maxilla lateral fossa excavates alveolus of last premaxillary tooth (Larsson and Sues [2007: character 66])
 - 0 no
 - 1 yes
91. Premaxilla-maxilla suture in palatal view, medial to alveolar region (Pol [1999: character 139] and Ortega et al. [2000: character 9])
 - 0 anteromedially directed
 - 1 sinusoidal, posteromedially directed on its lateral half and anteromedially directed along its medial region
 - 2 posteromedially directed
92. Deep fossa between and behind first and second premaxillary teeth to accommodate an enlarged, procumbent first dentary tooth (Larsson and Sues [2007: character 56])
 - 0 absent
 - 1 present
93. Ventral edge of premaxilla location with respect to ventral edge of maxilla (modified from Ortega et al. [2000: character 10])
 - 0 same height
 - 1 ventral
94. Premaxillary palate circular paramedian depressions (Sereno et al. [2001: character 67])
 - 0 absent
 - 1 present located anteriorly on the premaxilla
 - 2 present located at the premaxilla-maxilla suture
95. Procumbent premaxillary alveoli (Zaher et al. [2006: character 195])
 - 0 absent
 - 1 present
96. Premaxillary anterior alveolar margin orientation (Sereno et al. [2001: character 68])
 - 0 vertical
 - 1 inturned
97. Premaxillary tooth row orientation (Sereno et al. [2001: character 69] with new state 2)
 - 0 arched labially from midline
 - 1 angled posterolaterally, at 120° angle
 - 2 set in a relatively straight posterolateral orientation
98. Last premaxillary tooth position to first maxillary tooth (Sereno et al. [2001: character 70])
 - 0 anterior
 - 1 anterolateral
99. Premaxillary and anterior dentary tooth row orientation (Sereno et al. [18])
 - 0 posterolateral
 - 1 nearly transverse

100. Penultimate posterior premaxillary tooth size relative to anterior premaxillary teeth (Clark [1994: character 78])
 - 0 similar
 - 1 much longer
101. Anteromedial extension of incisive foramen (adapted from Brochu [1997: character 153])
 - 0 far from premaxillary tooth row (level of second or third alveolus)
 - 1 abuts premaxillary tooth row
102. Wedge-like anterior process of maxilla on lateral surface of premaxilla-maxilla suture (Gasparini et al. [1993: character 3])
 - 0 absent
 - 1 present
103. Enlarged anterior dentary teeth occlusion at premaxilla – maxilla suture (modified by Larsson and Sues [2007: character 65] from Norell [1988: character 29]; Sereno [1991: character 15]; Clark [1994: chars. 9 and 80]; Brochu [1997: character 77])
 - 0 enlarged teeth absent
 - 1 lingually within an internal fossa (fossa may extend dorsally to form a foramen)
 - 2 labially within a laterally open notch
104. Sculpturing along alveolar margin on lateral surface of maxilla (modified from Wu and Sues [1996: character 29])
 - 0 absent
 - 1 present
105. Maxilla – maxilla contact on palate (adapted from Clark [1994: character 10])
 - 0 only posterior ends not in contact at sutures with palatines
 - 1 complete
106. Ventrolateral edge of maxilla in lateral view (modified from Clark [1994: character 79])
 - 0 straight
 - 1 single convexity
 - 2 double convexity (“festooned”)
107. Posterior extent of maxilla (adapted from Wu and Chatterjee [1993: character 4]; Wu et al. [1997: character 114])
 - 0 posterior to anterior margin of orbit
 - 1 anterior to anterior margin of orbit
108. Maxillary depression (separate from antorbital fenestra) on lateral surface near lacrimal (adapted from Wu et al. [1997: character 127])
 - 0 absent
 - 1 present
109. Sagittal torus on maxillary palatal shelves (Larsson and Sues [2007: character 71])
 - 0 absent
 - 1 present

110. Longitudinal depressions on palatal surface of maxillae and palatines (Gasparini et al. [2006: character 253])
 - 0 absent
 - 1 present
111. Large and aligned neurovascular foramina on lateral maxillary surface (Pol [1999: character 152])
 - 0 absent
 - 1 present
112. Maxillary tooth number (Sereno et al. [2003: character 51])
 - 0,10 or more
 - 1 less than 10
113. Posterior maxillary and dentary teeth implantation (modified from Pol and Apesreguia [2005: character 161] and Ortega et al. [2000: character 19].)
 - 0 thecodont
 - 1 within an incompletely divided alveolar groove
114. Ornamentation on carinae of maxillary and opposing dentary teeth (modified by Larsson and Sues [2007: character 68] from Sereno et al. [2003: character 53]; Ortega et al. [1996: character 11])
 - 0 smooth
 - 1 serrations
 - 2 denticles
115. Compressed crown of maxillary teeth orientation (modified from Pol [1999: character 151])
 - 0 parallel to longitudinal axis of tooth row
 - 1 obliquely disposed
116. Maxillary teeth lateral compression (Pol [1999: character 154]; Ortega et al. [2000: character 104])
 - 0 absent
 - 1 present
117. Position of first enlarged maxillary teeth (modified by Turner and Buckley [2008: character 184] from Ortega et al. [2000: character 156])
 - 0 maxillary teeth relatively homodont
 - 1 second or third alveoli
 - 2 fourth or fifth alveoli
118. Tooth carinae (Ortega et al. [1996: character 11])
 - 0 absent or smooth or crenulated
 - 1 denticulate
119. Cheek teeth crown bases (Ortega et al. [1996: character 13])
 - 0 not constricted
 - 1 constricted
120. Vomer palatal exposure (Buckley et al. [2000: character 115])
 - 0 present
 - 1 absent

121. Palatine secondary palate (modified by Larsson [2000] and Larsson and Sues [2007: character 79] from Clark [1994: character 37])
 - 0 palatines form palatal shelves that do not meet
 - 1 form palatal shelves that meet along anterior 2/3 of secondary palate (posteriorly open V may be filled by pterygoids)
 - 2 palatal shelves of palatines meet along their entire length (linear palatine-pterygoid contact)
122. Palatine – pterygoid suture on secondary palate relative to posterior angle of sub-orbital fenestra (adapted from Brochu [1997: character 85])
 - 0 nearly at
 - 1 far from
123. Posterolateral edges of palatines on secondary palate (adapted from Norell [1988: character 2]; Brochu [1997: character 90])
 - 0 parallel
 - 1 flare laterally to form a shelf
124. Anterior process of palatine on secondary palate (modified by Larsson [2000] and Larsson and Sues [2007: character 78] from Brochu [1997: chars. 108 and 118])
 - 0 pointed
 - 1 rounded
 - 2 wide and squared (flat anteriorly)
125. Palatine-pterygoid contact on palate (Pol and Norell [2004: character 165])
 - 0 palatine overlies pterygoid
 - 1 palatine firmly sutured to pterygoid (Pol and Norell [2004: character 165])
126. Pterygoid secondary palate (modified from Clark [1])
 - 0 absent
 - 1 thin shelf that does not meet
 - 2 secondary palate with anterior margin of choanae located in anterior one-half of pterygoid
 - 3 secondary palate with anterior margin of choanae located in posterior one-half of pterygoid
127. Choanae projection (modified by Larsson and Sues [2007: character 82] from Clark [1994: character 39] and Pol and Norell [2004: character 183])
 - 0 posteroventrally into a midline depression continuous with pterygoid surface
 - 1 posteriorly walled by pterygoids
 - 2 posteriorly walled by pterygoids with a ventrally raised posterior rim
128. Paired anterior palatal fenestra (modified by Pol et al. [15] from Wu et al. [1997: character 128])
 - 0 absent
 - 1 present
129. Palatine orientation (Zaher et al. [11 character 196] modified from Martinelli [2003: character 36])
 - 0 parasagittal along entire length
 - 1 diverge laterally becoming rod-like posteriorly forming palatine bars

130. Posterior pterygoid processes (modified from Larsson [2000])
 - 0 absent or low ridges
 - 1 present and near level of palate
 - 2 present and tall
131. Posteromedial region of pterygoid in occipital aspect (modified from Brochu [1997: character 119])
 - 0 not visible
 - 1 visible but less than basioccipital height
 - 2 visible and subequal in height to basioccipital
132. Combined width of pterygoids in palatal aspect (*new character*)
 - 0 not more than twice wider than long
 - 1 more than twice wider than long
133. Depression on primary pterygoid palate posterior to choana (modified by Ortega et al. [2000: character 149] from Clark [1994: character 42])
 - 0 absent or moderate in size, narrower than palatine bar
 - 1 wider than palatine bar
134. Primary pterygoid palate (Turner and Buckley [2008: character 43] modified from Clark [1994: character 43])
 - 0 forms posterior half of choanal opening
 - 1 forms posterior, lateral, and part of the anterior margin of the choana
 - 2 completely enclose choana
135. Pterygoid – pterygoid contact on primary palatal plane (modified extensively from Clark [1994: character 56]; Brochu [1997: character 113]; Wu et al. [1997: character 56 and 121])
 - 0 completely to basipterygoid processes (but open posteriorly to form a V over basisphenoid)
 - 1 complete with basisphenoid length approximately 1/3 width
 - 2 complete with basisphenoid nearly hidden by a near pterygoid – basioccipital contact
136. Anterior edge of choanae location with respect to posterior margin of suborbital fenestrae (modified from Pol and Norell [2004: character 44] and Clark [1994: character 44])
 - 0 at or anterior to
 - 1 posterior
137. Quadrate process of pterygoid (Pol [1999: character 166])
 - 0 well developed
 - 1 poorly developed
138. Pterygoid flanges (Ortega et al. [2000: character 138])
 - 0 laminar and expanded
 - 1 bar-like
139. Quadrate ramus of pterygoid (modified from Clark [1994: character 38])
 - 0 extends dorsally to laterosphenoid
 - 1 extends dorsally to laterosphenoid and forms ventrolateral edge of trigeminal foramen

- 140. Quadrate ramus of pterygoid in ventral aspect (adapted from Wu et al. [1997: character 119])
 - 0 broad
 - 1 narrow
- 141. Pterygoid flanges (Wu et al. [1997: character 106])
 - 0 thin and laminar
 - 1 dorsoventrally thick, with pneumatic spaces
- 142. Choanal groove (modified by Turner and Buckley [2008: character 69] from Clark [1994: character 69])
 - 0 undivided
 - 1 partially separated
 - 2 completely separated
- 143. Choanal septum shape (Pol and Apesteguia [2005: character 186])
 - 0 narrow vertical bony sheet
 - 1 T-shaped bar expanded ventrally
- 144. Choanal septum, ventral surface (modified by Pol et al. [15] from Turner [2005: character 126])
 - 0 smooth to slightly depressed
 - 1 marked by an acute groove
- 145. Ectopterygoid projection medially on ventral surface of pterygoid flange (Zaher et al. [2006: character 198])
 - 0 minimal
 - 1 broad, extending approximately over the lateral half of the pterygoid flange
- 146. Ectopterygoid medial process (Ortega et al. [2000: character 146])
 - 0 single
 - 1 forked
- 147. Ectopterygoid – maxilla contact (modified by Larsson and Sues [2007: character 91] from Norell [1988: character 19] and Brochu [1997: character 91])
 - 0 absent
 - 1 present but ectopterygoid only abuts maxilla
 - 2 present and ectopterygoid nears maxillary tooth row
 - 3 present and broadly separated from tooth row by maxilla
- 148. Ectopterygoid, relation to postorbital bar (adapted from Clark [1])
 - 0 no support
 - 1 contributes to base of bar
- 149. Ectopterygoid extension along lateral pterygoid flange (modified from Norell [1988: character 32] and Brochu [1997: character 149])
 - 0 not to posterior tip of pterygoid
 - 1 to posterior tip of pterygoid
- 150. Posterior ectopterygoid process along ventral surface of jugal (Larsson [2000])
 - 0 absent
 - 1 very small

151. Quadrate body orientation distal to otoccipital-quadrate contact in posterior view (Pol and Norell [2004: character 181])
 - 0 ventral
 - 1 ventrolateral
152. Cross section of distal end of quadrate (Pol and Norell [2004: character 164])
 - 0 mediolaterally wide and anteroposteriorly thin
 - 1 subquadrangular
153. Quadrate condyles (Ortega et al. [2000: character 53])
 - 0 with poorly developed intercondylar groove
 - 1 medial condyle expands ventrally, separated from the lateral condyle by a deep intercondylar groove
154. Quadrate distal end (Pol [1999: character 167])
 - 0 with only one plane facing posteriorly
 - 1 two distinct faces in posterior view, a posterior one and a medial one bearing the foramen aërum
155. Quadrate major axis orientation (modified by Turner and Buckley [2008: character 149] from Pol [1999: character 166] and Ortega et al. [2000: character 44])
 - 0 posteroventral
 - 1 ventral
 - 2 anteroventral
156. Posterior edge of quadrate body (Clark [1994: character 46])
 - 0 broad medial to tympanum, gently concave
 - 1 posterior edge narrow dorsal to otoccipital contact, strongly concave
157. Squamosal – quadrate contact within the otic aperture to posteriorly bound the external auditory meatus (Larsson [2000], adapted in part from Brochu [1997: char: 102])
 - 0 absent
 - 1 present with a smooth posteroventral margin bordering the otic aperture
 - 2 present with a posteroventral notch in the contact
158. Quadrate – squamosal – otoccipital contact to enclose cranioquadrate space (Clark [1994: character 49])
 - 0 absent
 - 1 present near lateral edge of skull
 - 2 present with quadrate – squamosal contact broad laterally
159. Prominent crest on dorsal surface of distal quadrate that extends proximally to lateral extent of quadrate – exoccipital contact (modified from Brochu [1997: character 112])
 - 0 absent
 - 1 present
160. Preotic siphonal foramina (adapted from Clark [1994: character 45])
 - 0 absent
 - 1 single
 - 2 three or more

- 161. Dorsal primary head of quadrate contact (adapted from Clark [1994: character 47])
 - 0 only squamosal
 - 1 squamosal and (or near) laterosphenoid
- 162. Quadrate – basisphenoid contact (modified from Wu et al. [1997: char: 104])
 - 0 dorsolateral contact
 - 1 dorsolateral and anterolateral contact
- 163. Distal quadrate relative to quadrate body (adapted from Wu et al. [1994: character 22] and Wu et al. [1997: character 105])
 - 0 distinct
 - 1 indistinct ventromedial contact of quadrate body with otoccipital
- 164. Jaw articulation (quadrate condyle), position relative to maxillary tooth row (Wu and Sues [1996: character 24])
 - 0 above or near level
 - 1 below
- 165. Laterosphenoid bridge (modified from Brochu [1997: character 115])
 - 0 absent
 - 1 at least partially complete
- 166. Prominent boss on paroccipital process (Brochu [1997: character 141])
 - 0 absent or reduced, with short process lateral to cranioquadrate opening
 - 1 present, with long process lateral to cranioquadrate opening
- 167. Ventromedial portion of exoccipital adjacent to basioccipital tubera (Larsson [2000])
 - 0 slender
 - 1 hypertrophied
- 168. Large ventrolateral region of paroccipital process (adapted from Clark [1994: character 60])
 - 0 present
 - 1 absent
- 169. Supraoccipital exposure on dorsal skull table (modified from modification by Larsson and Sues [2007: character 107] from Norell [1988: character 11] and Brochu [1997: character 82] and from Turner and Buckley [2008: character 285])
 - 0 absent
 - 1 small, parietal still reaches portion of occipital surface
 - 2 large, parietal excluded from occipital surface
- 170. Mastoid antrum (Clark [1994: character 63])
 - 0 extending into a fossa in supraoccipital
 - 1 extends through a complete transverse canal in supraoccipital
- 171. Otoccipital large ventrolateral part ventral to paroccipital process (Clark [1994: character 60])
 - 0 absent
 - 1 present

172. Basioccipital and ventral part of otoccipital orientation (Gomani [1997: character 32])
 - 0 posteroventrally
 - 1 posteriorly
173. Lateral Eustachian tube openings (Pol [1999: character 146])
 - 0 located posterior to the medial opening
 - 1 aligned anteroposteriorly and dorsoventrally
174. Basisphenoid lateral exposure on braincase (Pol [1999: character 163])
 - 0 absent
 - 1 present
175. Laterosphenoid, capitate process orientation from midline (Brochu [1997: character 130])
 - 0 lateral
 - 1 anteroposterior
176. Posterior surface of supraoccipital (Clark [1994: character 64])
 - 0 nearly flat
 - 1 bilateral posterior prominence
177. Basioccipital tuberosity (Clark [1994: character 57])
 - 0 poorly developed
 - 1 large and pendulous
178. Mandibular symphysis, terminal orientation (*new character*)
 - 0 horizontal, or only slightly anterodorsal
 - 1 anterodorsal at approx. 45 degrees at a distinct angle from jaw line
179. Mandibular symphysis shape in lateral (modified by Turner and Buckley [2008: character 103] from Wu and Sues [1996: character 17])
 - 0 shallow and tapering anteriorly
 - 1 deep and tapering anteriorly
 - 2 deep and anteriorly convex
 - 3 shallow and anteriorly convex
180. Dorsal surface of mandibular symphysis (Pol and Apesteguia [2005: character 184])
 - 0 flat or slightly concave
 - 1 strongly concave and narrow, trough shaped
181. Dentary extension beneath mandibular fenestra (Clark [1994: character 70])
 - 0 present
 - 1 absent
182. Anterior caniniform dentary tooth near third position (*new character*)
 - 0 absent
 - 1 present
183. Dentary teeth height near mid-length of tooth row with respect to remaining teeth in posterior half of mandible (modified from Clark [1994: character 81])
 - 0 equal
 - 1 enlarged

184. Dentary tooth margin curvature between teeth 3 and 10 (adapted from Brochu [1997: character 68])
 - 0 linear
 - 1 gently curved
185. External mandibular fenestra (adapted from Norell [1988: character 14]; Clark [1994: character 75]; Brochu [1997: character 62])
 - 0 absent
 - 1 small and foramen intermandibularis caudalis not visible laterally
 - 2 large and foramen intermandibularis caudalis visible laterally
186. Shape of dentary symphysis in ventral view (modified by Turner and Buckley [2008: character 154] from Pol [1999: character 212])
 - 0 tapering anteriorly forming an angle
 - 1 U-shaped, smoothly curving anteriorly
 - 2 lateral edges longitudinally oriented, convex anterolaterally corner, and extensive transversely oriented anterior edge
187. Lateral surface of posterior region of dentary and anterior region of surangular longitudinal depression (Ortega et al. [1996: character 5])
 - 0 absent
 - 1 present
188. Splenial involvement in mandibular symphysis (adapted from Clark [1994: character 77]; Brochu [1997: character 43] – reduced to 0,1 states to not bias longirostrine taxa)
 - 0 absent
 - 1 present
189. Dentary surface lateral to seventh alveolus (modified by Turner and Buckley [2008: character 158] from Buckley and Brochu [1999: character 105])
 - 0 smooth
 - 1 lateral concavity for the reception of an enlarged maxillary tooth
190. Dorsal edge of dentary orientation to longitudinal axis of skull (modified by Turner and Buckley [2008: character 159] from Ortega et al. [1996: character 1] and Buckley and Brochu [1999: character 107])
 - 0 slightly concave or straight
 - 1 straight with an abrupt dorsal expansion anteriorly
 - 2 single dorsal expansion and concave posterior to this
 - 3 sinusoidal, with two concave waves
191. Posterior peg at symphysis (Pol and Apesteguia [2005: character 180])
 - 0 absent
 - 1 present
192. Dentary compression and ventrolateral surface anterior to mandibular fenestra (modified by Turner and Buckley [2008: character 160] from Ortega et al. [1996: character 2] and Buckley and Brochu [1999: character 108])
 - 0 compressed and vertical
 - 1 not compressed and convex

193. Splenial transverse thickness posterior to symphysis (modified by Turner and Buckley [2008: character 161] from Ortega et al. [1996: character 7] and Buckley and Brochu [1999: character 110])
 - 0 thin
 - 1 robust dorsally
194. Dentary lateral surface below alveolar margin, at mid- to posterior region of tooth row (Pol and Apesteguía [2005: character 188])
 - 0 vertically oriented, continuous with rest of lateral surface of dentary
 - 1 flat surface exposed laterodorsally, divided by a ridge from the rest of the lateral surface of the dentaries
195. Angular-surangular contact relative to medial wall of external mandibular fenestra (adapted by Larsson and Sues [2007: character 115] from Norell [10] character 40; Brochu [6] character 47)
 - 0 continue to posterior angle
 - 1 pass along posteroventral margin
196. Anterior processes of surangular (adapted from Brochu [1997: character 48])
 - 0 single
 - 1 two
197. Coronoid size (modified by Turner and Buckley [2008: character 175] from Ortega et al. [2000: character 98])
 - 0 short and located below dorsal edge of mandible
 - 1 anteriorly extended with posterior region elevated at the dorsal margin of mandible
198. Surangular contribution to glenoid fossa (Buckley and Brochu [1999: character 102])
 - 0 lateral wall only
 - 1 approximately one-third of fossa
199. Surangular extension toward posterior end of retroarticular process (adapted from Norell [1988: character 42]; Brochu [1997: character 51])
 - 0 along entire length
 - 1 pinched off anterior to posterior tip
200. Surangular – articular suture orientation within glenoid fossa (adapted from Brochu [1997: character 162])
 - 0 anteroposteriorly (linear)
 - 1 bowed strongly laterally
201. Insertion area for *M. pterygoideus* posterior on angular (adapted from Clark [1994: character 76])
 - 0 medial
 - 1 medial and lateral
202. Longitudinal ridge along the dorsolateral surface of surangular (Pol and Norell [2004: character 187])
 - 0 absent
 - 1 present

- 203. Sharp ridge on the ventrolateral surface of angular (Pol and Norell [2004: character 186])
 - 0 absent
 - 1 present
- 204. Prearticular (Clark [1994: character 72])
 - 0 present
 - 1 absent (fused to articular)
- 205. Articular cotyle of lower jaw, shape (Wu and Sues [1996: character 23])
 - 0 wider than long
 - 1 longer than wide
- 206. Retroarticular process (modified by Larsson and Sues [2007: character 122] from Benton and Clark [29]; Norell and Clark [1990: character 7]; Clark [1994: character 71]; Brochu [1997: character 50])
 - 0 short, less than twice the length of the articular cotyle
 - 1 elongate, equal to or more than twice the length of the articular cotyle
- 207. Medial edge of retroarticular process (Larsson [2000])
 - 0 concave or linear
 - 1 convex
- 208. Projection of retroarticular process (adapted from Clark [1994: character 71])
 - 0 posteriorly or posteroventrally
 - 1 posterodorsally
- 209. Vertebral centra (Buscalioni and Sanz [1988: character 35])
 - 0 cylindrical
 - 1 spool shaped
- 210. Cervical neural spines (modified by Turner and Buckley [2008: character 90] from Clark [1994: character 90])
 - 0 all anteroposteriorly large
 - 1 only posterior ones rodlike
 - 2 all spines rodlike
- 211. Axial neural spine height (Larsson [2000])
 - 0 high, subequal to centrum height
 - 1 low, less than half centrum height and nearly horizontal
- 212. Axis neural arch lateral process (diapophysis) (adapted from Norell [1989: character 7]; Brochu [1997: char: 4])
 - 0 absent
 - 1 present
- 213. Postzygapophyses of axis (Pol [1999: character 170])
 - 0 well developed, curved laterally
 - 1 poorly developed
- 214. Anteroposterior development of neural spine in axis (Pol [1999: character 168])
 - 0 well developed covering all the neural arch length
 - 1 poorly developed, located over the posterior half of the neural arch

215. Cervical vertebrae (adapted from Clark [1994: character 92])
 - 0 amphicoelous or amphiplatyan
 - 1 procoelous
216. Cervical hypapophyses (modified from Clark [1994: character 91] and Brochu [1997: character 7])
 - 0 absent
 - 1 present only in cervical vertebrae
 - 2 present in cervicals and at least first two dorsal vertebrae
217. Posterior process of cervical rib shaft posterodorsally projecting spine at junction with the tubercular process (Turner [2004: 129])
 - 0 absent
 - 1 present
218. Dorsal vertebrae (adapted from Benton and Clark [29]; Norell and Clark [1990: character 8 and 10]; Clark [1994: character 93]; Brochu [1997: character 18])
 - 0 amphicoelous or amphiplatyan
 - 1 procoelous
219. Number of sacral vertebrae (Buscalioni and Sanz [1988: character 44])
 - 0 two
 - 1 three or more
220. Caudal vertebrae (adapted from Norell and Clark [1990: character 9])
 - 0 all amphicoelous or amphiplatyan
 - 1 all procoelous
 - 2 first caudal vertebra gently biconvex and rest procoelous
221. Transverse process of sacral vertebrae orientation (Gasparini et al. [2006: character 255])
 - 0 lateral
 - 1 markedly deflected ventrally
222. Scapular blade width relative to length of scapulocoracoid articulation (Buckley and Brochu [1999: character 106])
 - 0 no more than twice
 - 1 broad, greater than twice
223. Anterior and posterior margins of scapula in lateral aspect (Clark [1994: character 82]; Brochu [1997: character 22]; Turner and Buckley [2008: character 82])
 - 0 symmetrically concave in lateral view
 - 1 anterior edge more strongly concave than posterior edge
 - 2 dorsally narrow with straight edges
224. Deltoid crest of scapula (adapted from Brochu [1997: character 23])
 - 0 present
 - 1 absent
225. Coracoid length relative to scapula (adapted from Clark [1994: character 83])
 - 0, 1/2
 - 1 subequal

- 226. Proximomedial articular surface on humerus (modified from Sereno [1991: character 4])
 - 0 present (strongly arched edge)
 - 1 absent (weakly arched edge)
- 227. Longitudinal axis of humeral shaft in lateral aspect (Larsson [2000])
 - 0 straight
 - 1 sigmoid (distal end curves anteriorly)
- 228. M. teres major and M. dorsalis scapulae insertion on humerus (Brochu [1997: character 29])
 - 0 separate, scars distinguished dorsal to deltopectoral crest
 - 1 insert with common tendon, single insertion scar
- 229. Olecranon process of ulna (Brochu [1997: character 27])
 - 0 narrow and subangular
 - 1 wide and rounded
- 230. Radiale and ulnare length (modified from Benton and Clark [1988: character Crocodylomorpha E]; Wu and Sues [1996: character 40])
 - 0 short (endochondral)
 - 1 long (perichondral)
 - 2 long with a distinct proximomedial process on the radiale
- 231. Anterior process of ilium length relative to length of posterior process (Clark [1994: character 84])
 - 0 similar
 - 1 one-quarter or less
- 232. Dorsal margin of iliac blade (modified from Brochu [1997: char: 28])
 - 0 rounded with a smooth border
 - 1 flat
- 233. Posterior iliac process (Larsson [2000])
 - 0 dorsoventrally expanded with a blunt end
 - 1 nearly absent
- 234. Supra-acetabular crest (Buscalioni and Sanz [1988: character 49])
 - 0 present
 - 1 absent
- 235. Contribution of pubis to acetabulum (Clark [1994: character 86])
 - 0 partially excluded by anterior process of ischium
 - 1 completely excluded from acetabulum
- 236. Anterior margin of femur (Buckley and Brochu [1999: character 102])
 - 0 linear
 - 1 bears flange for coccygeofemoralis musculature
- 237. Proximal-most portion of fibular head (modified by Pol and Gasparini [2009: character 272] from Turner [2004: character 128])
 - 0 straight-sided to weakly developed posteriorly
 - 1 sharply projecting posteriorly, forming distinct extension

238. Fibular articular facet of femur (adapted from Clark [1994: character 87])
0 large
1 very small
239. Lateral edge of proximal articular surface of femur (lesser trochanter) (Larsson [2000])
0 rounded
1 squared with an enlarged ischiotrochantericus muscle scar
240. Fourth trochanter on femur (modified from Sereno [1994: character 35])
0 absent
1 present but low
241. Tibia length relative to femur length (adapted from Sereno [1991: character 27])
0 subequal or longer
1 shorter
242. Calcaneal facet for fibula and distal tarsal 4 (Sereno [1991: character 3])
0 separate
1 contiguous
243. Calcaneal tuber (adapted from Sereno [1991: character 2 and 29]; Parrish [1993: character 1 and 9])
0 absent or rudimentary
1,45 degrees posterolaterally
2 posteriorly
244. Fore and hind limb lengths (Larsson [2000])
0 hind limb much longer than forelimb
1 subequal
245. Gap in cervico-thoracic dorsal armor (Ortega et al. [2000: character 109])
0 absent
1 present
246. Number of dorsal osteoderms per transverse row (adapted from Norell and Clark [1990: character 12]; Sereno [1994: character 22]; Clark [1994: character 97]; Brochu [2000: character 37])
0 none (dorsal osteoderms absent)
1 two
2 four or more
247. Dorsal osteoderm shape (modified from Norell and Clark [1990: character 16]; Clark [1994: character 95]; Brochu [1997: character 36])
0 square
1 wider than long but less than three times wider than long
2 more than three times wider than long
248. Anterior edge of dorsal parasagittal osteoderms (Turner and Buckley [2008: character 96] modified from Norell and Clark [1990: character 13]; Clark [1994: character 96]; Brochu [1997: character 40])
0 straight
1 discrete convexity on anterior margin
2 with anterolateral process on anterior edge

- 249. Keel on dorsal osteoderms (adapted from Buscalioni et al. [1992: character 22]; Clark [1994: character 101]; Brochu [1997: character 35])
 - 0 absent
 - 1 present
- 250. Dorsal trunk osteoderm, anteroposterior keel position (Sereno et al. [2003: character 65])
 - 0 medial or paramedian
 - 1 lateral margin
- 251. Ventral trunk osteoderms (adapted from Buscalioni et al. [1992: character 21]; Clark [1994: character 100]; Brochu [1997: character 39])
 - 0 absent
 - 1 present and osteoderms are single
 - 2 present and osteoderms are paired ossifications sutured together
- 252. Tail osteoderms (adapted from Clark [1994: character 99])
 - 0 absent
 - 1 dorsal only
 - 2 completely surrounded

References

- Benton MJ, Clark JM (1988) Archosaur phylogeny and the relationships of the Crocodylia. In: Benton MJ (Ed.) *The Phylogeny and Classification of the Tetrapods, Vol 1: Amphibians, Reptiles, Birds*. Clarendon Press, Oxford: 295–338.
- Brochu CA (1997) Phylogenetics, taxonomy, and historical biogeography of Alligatoroidea. *Journal of Vertebrate Paleontology* 6: 9–100.
- Buckley GA, Brochu CA (1999) An enigmatic new crocodile from the Upper Cretaceous of Madagascar. *Special Papers in Palaeontology* 60: 149–175.
- Buckley GA, Brochu CA, Krause DW, Pol D (2000) A pub-nosed crocodyliform from the Late Cretaceous of Madagascar. *Nature* 405: 941–944.
- Buscalioni AD, Sanz JL (1988) Phylogenetic relationships of the Atoposauridae (Archosauria, Crocodylomorpha). *Historical Biology* 1: 233–250
- Buscalioni AD, Sanz JL, Casanovas ML (1992) A new species of the eusuchian crocodile *Diplocynodon* from the Eocene of Spain. *Neues Jahrbuch für Geologie und Paläontologie, Abhandlungen* 187: 1–29.
- Clark JM (1994) Patterns of evolution in Mesozoic Crocodyliiformes. In: Fraser NC, Sues H-D, eds. *In the Shadow of the Dinosaurs: Early Mesozoic Tetrapods*. Cambridge: Cambridge University Press. pp. 84–97.
- Gasparini Z, Fernandez M, Powell J (1993) New Tertiary sebecosuchians (Crocodylomorpha) from South America: phylogenetic implications. *Historical Biology* 7: 1–19.
- Gasparini Z, Pol D, Spalletti LA (2006) An unusual marine crocodyliform from the Jurassic-Cretaceous boundary of Patagonia. *Science* 311: 70–73.

- Gomani EM (1997) A crocodyliform from the Early Cretaceous dinosaur beds, northern Malawi. *Journal of Vertebrate Paleontology* 17: 280–294
- Larsson HCE (2000) Ontogeny and phylogeny of the archosauriform skeleton [Ph.D. thesis]. Chicago: University of Chicago. 500 p.
- Larsson HCE, Sues HD (2007) Cranial osteology and phylogenetic relationships of *Hamadasuchus rebouli* (Crocodyliformes: Mesoeucrocodylia) from the Cretaceous of Morocco. *Zoological Journal of the Linnean Society* 149: 533–567.
- Martinelli AG (2003) New cranial remains of the bizarre notosuchid *Comahuesuchus brachybuccalis* (Archosauria, Crocodyliformes) from the Late Cretaceous of Río Negro Province (Argentina). *Ameghiniana* 40: 559–572.
- Norell MA (1988) Cladistic approaches to paleobiology as applied to the phylogeny of alligatorids [Ph.D. thesis]. New Haven: Yale University.
- Norell MA (1989) The higher level relationships of the extant Crocodylia. *Journal of Herpetology* 23: 325–335.
- Norell MA, Clark JM (1990) A reanalysis of *Bernissartia fagesii*, with comments on its phylogenetic position and its bearing on the origin and diagnosis of the Eusuchia. *Bulletin de l'Institut Royal des Sciences Naturelles de Belgique* 60: 115–128.
- Ortega F, Buscalioni AD, Gasparini Z (1996) Reinterpretation and new denomination of *Atacisaurus crassiproratus* (Middle Eocene; Issel, France) as cf. *Iberosuchus* (Crocodylomorpha: Metasuchia). *Geobios* 29: 353–364.
- Ortega F, Gasparini Z, Buscalioni AD, Calvo JO (2000) A new species of *Araripesuchus* (Crocodylomorpha, Mesoeucrocodylia) from the Lower Cretaceous of Patagonia (Argentina). *Journal of Vertebrate Paleontology* 20: 57–76.
- Parrish JM (1993) Phylogeny of the Crocodylotarsi, with reference to archosaurian and crurotarsan monophyly. *Journal of Vertebrate Paleontology* 13: 287–308.
- Pol D (1999) El esqueleto postcraneano de *Notosuchus terrestris* (Archosauria: Crocodyliformes) del Cretácico Superior de la Cuenca Neuquina y su información filogenética [M.Sc. thesis]. Buenos Aires: Universidad de Buenos Aires. 158 p.
- Pol D, Apesteguía S (2005) New *Araripesuchus* remains from the early Late Cretaceous (Cenomanian-Turonian) of Patagonia. *American Museum Novitates* 3490: 1–38.
- Pol D, Gasparini Z (2009) Skull anatomy of *Dakosaurus andiniensis* (Thalattosuchia: Crocodylomorpha) and the phylogenetic position of Thalattosuchia. *Journal of Systematic Palaeontology* 7: 163–197.
- Pol D, Ji S-H, Clark JM, Chiappe LM (2004) Basal crocodyliforms from the Early Cretaceous Tugulu Group (Xinjiang, China), and the phylogenetic position of *Edentosuchus*. *Cretaceous Research* 25: 603–622.
- Pol D, Norell MA (2004) A new crocodyliform from Zos Canyon Mongolia. *American Museum Novitates* 3445: 1–36.
- Turner AH, Buckley GA (2008) *Mahajangasuchus insignis* (Crocodyliformes: Mesoeucrocodylia) cranial anatomy and new data on the origin of the eusuchian-style palate. *Journal of Vertebrate Paleontology* 28: 382–408.
- Sereno PC (1991) Basal archosaurs: phylogenetic relationships and functional implications. *Journal of Vertebrate Paleontology*, Memoir 2 11(4, Supplement): 1–53.

20011?0{3,4}?0{0,1}0???00???{1,2}??0?1000?2???001??1010000?2???0?{0,1}11??21100
0?10???{1,2,3}?0?11??0???{0,1}???0??1?1?0?00000??1?02?01?0?0011000000?0???0?10??
?00010??011?00?????01{0,1}10????21?10???2?0000?000000?1??00000?100???0???00?0
??

Hsisosuchus chungkingensis

21011004000000?002000000000000201000101001100002011?11120200000010
 001000100?0111000012301?00?0?01-?00111-?00?10121??0---00110000000000
 0001000?001?{0,1}??10?1101100000-001000?000??1?01?01?00?1?0?00?001?0010
 ?????00?0?0?0100?1??2??????1????101101012

Pelagosaurus typus

2001201000111000000000000110000010000001001000010011000000-0100100
 0000000021100010001?2?1?0000000000?0011-0001000000-0011101101000000
 000{0,1}101010?00000110000011000110000000110??01000?--21110-0??01??0??0
 0000101?001?00?0?0?01?1???1010100?1?011{1,2}001120-11

Steneosaurus bollensis

100120100011100000000000011000002-0000010110?0?00011000000-01011100
 00000002?1000200011211-0000000000000?1-000{0,1}000000-00?100010100100
 000001?1010?001000100000110?0110?1000?110??110?000--21010-0100?0100100
 00010100101000?0001?11100??1010100?100111001121011

Metriorhynchus superciliosus

00012110001110110001001001100000100000000?1000?00011000000-01111100
 00000002?0001100001101-00000000000000-1-0001000000-00?210110100000000
 0?101010?0000-01000001100011001000?110??110?0-0--0?110-0?00-0100?000000
 010011?000?0001?01110?0001100?0001010-0---00

Geosaurus suevicus

0001311000111011000?0020011000002-00010?0010?0??0011000000-?111?10000
 000002??00010?0??101-?00?000000?00?1-000?000000-0?0????????????????????
 ???0??10?0??0??00?????010?0?0--00110-???0-0???000?00?1??11100??0?0??01110?0?0
 1?00?0001000?0---00

Uruguaysuchus aznarezi

20011?0{3,4}?0{0,1}???0?0??????1??0?2??011??1?1?0?0??0???11??{0,1}?0??0????????
 ?????2??21?2?1???0??{0,2}??0??011100??10?2010{0,1}1?1?????????0?0???{1,2}?0?0?
 ?????111{1,2}??1???1?????0???00001?001{1,2}?01001????????1??1???0??????0?0????
 ??21??0111????????001???

Notosuchus terrestris

1011100200100010000111200101012011011001011000110000?1110100000112
 ?01001101101202002123?1-0000000001-0001010?01112110001110{0,1}1011100
 0100000?1110011110101111112121101?101210000100010100020{0,1}1001001
 0??01?100?100002??0100?010011?10????1??0110????????1101???

Malawisuchus mwakasyngutiensis

1011100{3,4}000000000{1,2}010?10?10{0,1}0120010110-10000??11000?011?0100
 ?00112??100?10{0,1}??1{1,2}220?2??2010?00?00{0,2}001?0101000??111200101111
 0{0,1}10100?00000000?1?1000?110?011101?2111101?1012?00?0?0001?1?0020010
 000?100?01?100?1010?2???01?0?0?01??00???????1?1??0?11?20010??

Mariliasuchus amarali

10113-0{3,4}?0????100??10??0110{0,1}??2???1101-00101001??0?0111?1100001120
 0300111110??220?01?2?1-0000100001?000101000111001111?1-12101111010010
 00?1010011200000011112?21101??0???0010?00??0100020010010?1?1?010100110
 10??

Comahuesuchus brachybuccalis

10123-0{3,4}?0{0,1}0??100?????011010?????????-00??1???0????1???0?00??????????10
 ??22????{2,3}?1?2?0?100000??0011?0?0110?0?10?11??1??01???1??????????101?0?0?11
 11???1??0?1?2????1??00?0???1010210?1??????0????????????????????????????????
 ???????

Sphagesaurus huenei

10113-?{3,4}?0?0????0?????0??????01101-101000110?0?1????????11200?0????101
 ?22002000?1?0?000000010000101000110011-0111??11?10????00010?1?200?????0
 1?11?????0??????110?0010??0????0???1??0????????????01????????????????????
 ???????

Baurusuchus pachecoi

1000{1,3}?0310??00?00?0?0110011?01?01001111?10110?11010{0,1}010110-000?1
 1210100110110020200{0,1}1?20100000000001?02111100011010111112102101
 00{0,1}{0,1}010{1,2}010?1110?1111??01111112?11101??01210000?0012011012{0,
 1}110200100?001?110100000??????0100??101???000?1???0?{1,2}1??0????

Baurusuchus salgadoensis

10001003100000100{1,2}0?01000110012010011111111100?1010{0,1}010110-00
 0011210100110???022200{0,1}1?2010??0?000001?02111100011?00011??21021010
 0{0,1}?0?0{1,2}1?0?10??1?1?0?01??1{1,2}2??1101???2?00???00120110121110200?
 00???1?110?0010????????????????????????????????

Anatosuchus minor

200210040000000002020?10010100?10021110100110001001211120110000112
 103001101?0122210?1{1,2}3010?000001010?00011000010?00?001?1???1?1000{0,1
 }0002??0?0?1000????01?12122?11101?1?11?0?0??00020?00122010000000???0?1011
 ?100????????0?0110100??2????????????011011??

20121004000000000{1,2}0{1,2}0?10010100221020110000110001011211120110
000112203001100?003221021130102000001010000011100010120100100-?210
100000002010?{0,1}1210001?0?01102112011100?1011?0000?0002010012201001
00001?00010111010?2????01?0???????????????????????????2001?1?

200210030000000002010010010001200021101100100?01011101110??00001120
0310110110120211212201-000?002000-00111100010110011111102101001?000
1000?1021100110101010112?11?11?1?111000010000110?12{0,1}010100?00??11?
10010110????00021010011????021??01111?????01101102

```
{1,2}002??0??010??0????????10?0?2???11???010??10????11??????01122??0?10?????
??????1?0?0?0??????01110??1?100010?11??11?1002??0020?0?1121100{1,2,3}????????
???1?????1??????1??0{0,1}??1?1?0111?{0,1}100001????????????1????????????????????
?????????????
```

2002100{3,4}000000000?0{1,2}2??001000?2001?11??100100?110?0?011?0??000011
2{1,2}??10?10100??02?121?3?1???0?{0,1}020?1?0011110?010100110111???1?100??0?
?100011120000{1,2,3}???01{0,1}111?2?11?10?10??100?010000110112001?110000?
??1?101111101????0021000?1101000?21??001111???????10????

2002100{3,4}000000000?0?0??0?1000??0002{0,1}1??100100?01000?011?01100001
121?3?01101?0?2?2??{1,2}??2?1???0?0??0?1?0011100?01010001???1???1?1?0???00100
0?1021100{1,2,3}?0?010?11?2?1??01?10?1?000??0000?1???20010?1?0?0???1?100?111
0?1?????1???011???0???1??0??1???????011011??

2002100{3,4}0000000002010?00101010?001211111001000010012111202100001
121?31011011012221120?3?1?0?000020?100011100?010120111111??11?1002200
02000110211003?0?01111122111?01?11?010000100001?111?0???0?0?0?????????????
????????????????010????????????????1????1??2

[illegible]

Sebecus icaeorhinus

10002?0{3,4}10?000?0?20{0,1}0010?10101?{1,2}1101101101110001?0201112021?
 ??0112???????1?0?{1,2}?21?1002011010000000110211200?0100101111?11001010
 0{0,1}{1,2}000{1,2}0???1?????111010010122111100?11101010???001??111?{0,1}00
 02???0?1?0?0?010?11?????0?0?0????????????????11???????????

Hamadasuchus rebouli

2002200400100000020{1,2}0010010101?20001101100110001102111120200000
 11220310111100122210101201101000000010021120010101101111020021010
 022000200011020?002110100001220111001111010100110010?111?0?10200????
 ???

Stolokrosuchus lapparenti

200110040001100002010000010011?11121001100110001102211120210000112
 103101101101212101003121010000000111211210101011012011{1,2}??01?1002
 2?0{0,1}200011?{1,2}???11?11001012210110011111?0101100010010020010-011
 00?0?100101?1??

Uberabasuchus terrificus

20020003000?00000{1,2}0?201001000121000110110{0,1}11000{0,1}0021111202
 10000112?01?01101?0121210???3111?0?00001?1211200??10?1011011{1,2}?????0
 ?????????????????????01{1,2}2?11100???0??????0{1,2}011?1100112001??1??1?0001
 0001?????0??0?0????????????????????1?????

Peirosaurus tormini

20022?0?0?0?0?0?2?{1,2}0?100?1??0????????????????11???0?00????????????12?210
 ?00311?0?0?000001112112????10?0?10?1{1,2}????????????????????????????0??
 1????????0???1?1{1,2}??1?????????1?????0????????????????????????????0?10??

Lomasuchus palebrosus

20022?0?00001000020{1,2}2010?1000122012100?100110?01?0211112?200?00112
 {1,2}0??0110110????100??1?{0,1}?0??0?000?1211200101011011011{1,2}??21?1002
 2?0020001102000?1????????2?111?0?1110?01001000?0?11?{1,2}?0???0?0?????0???
 ?????????????????????????????????????

Mahajangasuchus insignis

2002100{2,3,4}01000?0002?1201001001??111210??100120101011{0,1}11121310
 000112203100102100?110011{1,2}{2,3}?1?2?000000?00021121000100001100?21
 0211100011012000?1021000211?100001{1,2}2001101?10?210100?00120111111
 001200101??1?11101010011???0210?0?110?01??210001101111121?10110??

Kaprosuchus saharicus

20021004010000000201201001001??111210??10012010{0,1}01111112?31000011
 2??310010{1,2}10011100{0,1}1{1,2}101??1000110?1002112100010?001100?2--21
 1100011012000?1021000{2,3}110100001?20?1?01???010?0???01200?1?110002001
 001?1??11110100?0????????????????1????????????????

Goniopholis simus

20023-0100101000011{1,2}00110100-022013110?-00110001201?1112121100011
 2?02110101?0001100{0,1}113010?000000000002112010010?0002001110210100
 11?0020?0?1020?0021??10000122101100???10?010??00030?111?1?{1,2}03?110???0?
 ?000100?01???100?0?0?01????{1,2}???1?0?1????011201{1,2}?

Pholidosaurus purbeckensis

21013-0000101100000?0001?110?0?20121000-0?1??0012011?1121111000111??{1,
 2}110101???????1???2???0?????0{0,1}?1-000?10?000?00?1?0?111001010120?0?1?{1,
 ,2}0?00110?100001{1,2}2001100?1?1000???0?????-??10-??0????????0???0?????0?
 ???1????1???10???????122111?

Dyrosaurus phosphaticus

10013-1101101000?0010001?10010122-11100-0210??01-02?01121211001?112?21
 10101?00111000112020?00?000000??201-000?100000?00?2110111001010120???1
 ?20010211?100?012200110001110001??1110??1?--??10-??00???1???00?01?0??11??0?
 ?0?0???10????00?10??11????12?0-??

Terminonaris robusta

20013-1100101?00000?00010110-0?21?{2,3}1000-0?1??001201?1112?201000??1??{
 1,2}110101??0001000013020?01101111000201-000010?000?0?111001{0,1}1000?1
 0{0,1}20?0?10{1,2}0000?10?0000??20???00?1?10?0?0?1100??1?--1101?-0??1???00?1??
 1010?101?10000000?010100??211011001111111?122112?

Sarcosuchus imperator

20023-0100{0,1}0110010010001011010?20011000-011100011011111211110001
 11012110101?0000100011302-2011011111001{0,1}1-0000101000200110011110
 01110120001102?000110?1000012200110001?10?01???100?010--11010-0110110
 011000101101????0000000?10?????11011????????122111{1,2}

Laganosuchus thaumastos

20??
 ?????????00??00??030110011100001
 00?-001011010110??

Bernissartia fagesii

20023-0{2,3}00101000000{1,2}1111?10010?{1,2}003110?-0{0,1}11?00121?11112??
 ?10?011{1,2}1??100101??0{0,1}{0,1}200???301???0?000000?01112?0?010100120??20
 0{0,1}11100{1,2}?101{1,2}1?0??0????211?10?0122??1100???1?1????000-11101000
 301?0-??01?001100011?1??011?000????0????????????12{0,1}0101?

Isisfordia duncani

20023-0300?01000000?0000010010?20131111-0011000{0,1}211?1112111100011
 2??{1,2}?0010???01010001130101000000000010110000010100100112111121001
 01022000?10200002?0?100001{1,2}20?1100?1011?0100?00???000?{1,2}?0????0?1?
 ?????????1{0,1}1?101{1,2}?101?01??01??2100??0?1?1?{1,2}11200101{1,2}

Gavialis gangeticus

21013-000010110010010001011011100011001-00100001200111121101000112?
 1110010100000100011301020000000000011-0000100000-0012100131001110
 221001100--00211110000122001?0?0?11010101103001--11010-010011001010
 010101111?101201020010101012100110011111??02011002

Leidyosuchus canadensis

20023-030010100001020010010001120021100-00110001100111121201000112
 01210010100011100110301010000000000211200001010012011200113200111
 0221101100--00310?10000122011100?0010101011100300111110103?1?0010?10
 10010101????1?1?2????1?1?2?0?1?1?1??0?200101?

Crocodylus niloticus

20023-030010100001020000010011121031100-01110001220011121101000112
 012100101000101000113010200000000000211200001000002011110113100111
 0221001100--002100100001220111001001010101110030011111000301001100
 011001010111001012010200201011121001100111112012001002

Alligator mississippiensis

20023-040010100002122120010011120121001-01110001100111121101000112
 11210010100010100111301010000000001011120000101001201120121320022
 102210011020000310010000122011100100101010111003001112100030100110
 0101001011111001012010200201011121001100111112012001001

Apomorphy list

List of apomorphic states by node for one of the four minimum-length trees in the maximum-parsimony analysis (Fig. 43A). Ambiguous transformations (using delayed character-state transformation) are indicated with an asterisk.

Hsisosuchus + *Mesoeucrocodylia*

21(0), 43(1), 85(1)*, 112(0), 127(1), 157(1)*, 158(1)*, 160(1), 188(1), 251(1)*

Mesoeucrocodylia

8(3), 26(1)*, 48(1), 52(1)*, 64(1), 104(1), 105(1), 120(1)*, 121(1), 125(1), 128(0), 140(1), 162(1), 166(1), 211(1)*, 225(1)

Thalattosuchia

5(2), 7(1), 8(0), 11(1)*, 12(1), 13(1), 18(0), 27(1), 31(0), 33(1)*, 37(0), 39(0), 54(0), 55(0), 56(0), 58(0), 61(1), 69(0), 73(0), 75(2), 78(0), 79(0), 81(1)*, 100(0), 103(0)*, 110(1), 138(1), 160(0), 161(0), 171(1), 172(1)*, 177(1), 182(0), 197(1)*, 208(1), 221(1)*, 224(1), 230(1), 234(1), 240(0), 241(1)*, 244(0), 252(1)

Pelagosaurus and *Steneosaurus*

23(0), 77(1), 149(0)*, 185(2)*, 186(1), 206(1)*, 232(1), 248(2)*

Metriorhynchus and *Geosaurus*

1(0), 6(1), 15(1), 16(1), 62(1), 63(1)*, 87(1), 185(0), 187(1)*, 212(1)*, 223(0), 226(1), 230(0), 233(1), 238(0), 242(0), 246(0), 251(0), 252(0)

Metasuchia

20(1)*, 36(1), 59(1)*, 66(2), 67(1), 80(1)*, 81(2)*, 111(1), 116(1)*, 117(1)*, 124(2)*, 135(1), 139(1), 147(1), 148(1), 156(1), 158(2), 163(0)*, 168(1), 181(1)*, 196(1), 199(1)*, 201(1), 204(1), 216(1), 231(1), 235(1), 247(0)

Notosuchia

58(1), 72(1)*, 79(2)*, 119(1)*, 149(0)*, 151(0), 152(1), 154(1)*, 155(1), 164(1), 169(1), 185(2)*, 200(0), 207(1)*, 210(1)*, 213(0), 236(1)*, 248(0)

Uruguaysuchidae

4(2)*, 35(2), 69(3), 82(1), 84(2), 97(2), 103(0)*, 113(1), 142(2)*, 180(1), 191(1)*, 205(1)*, 222(1)*, 237(1), 250(1)

Araripesuchus wegeneri, *Araripesuchus buiterraensis*, *Uruguaysuchus*, *Anatosuchus*, and *Simosuchus*

28(1), 38(1), 52(2), 53(1), 56(2)*, 80(2)*, 135(2), 143(1)*, 153(1)*

Uruguaysuchus, Anatosuchus, and Simosuchus

100(0), 117(0), 182(0), 183(0)

Anatosuchus and Simosuchus

8(4)*, 32(1)*, 39(0)*, 44(1), 87(3)*, 97(1), 99(1)*, 104(0), 155(2), 179(2), 180(0), 186(2)*, 199(0)*, 203(1)*

Araripesuchus wegneri and Araripesuchus buiterraensis

124(1), 130(2), 144(1), 167(1)

Araripesuchus rattoides, Araripesuchus tsangatsangana, Araripesuchus patagonicus, and Araripesuchus gomesii

190(1)

Araripesuchus tsangatsangana, Araripesuchus patagonicus, and Araripesuchus gomesii

70(1)*, 80(0)*, 83(1)*, 182(0), 206(1)*, 216(2)*, 247(1)*

Araripesuchus patagonicus and Araripesuchus gomesii

116(0), 143(1)*, 144(1)

Baurusuchus, Mariliassuchus, Comahuesuchus, Sphagesaurus, Malawisuchus, and Notosuchus

1(1), 15(1), 22(1), 30(1)*, 51(0)*, 107(1)*, 112(1), 145(1), 146(1), 153(1)*, 169(2), 183(0), 219(1)

Mariliassuchus, Comahuesuchus, Sphagesaurus, Malawisuchus, and Notosuchus

3(1), 28(1), 67(0), 80(2)*, 103(0)*, 104(0), 182(0), 184(0), 194(1), 205(1)*

Sphagesaurus, Malawisuchus, and Notosuchus

47(1)*, 84(2), 106(0)*, 124(1), 135(0), 179(1), 214(1)*

Malawisuchus and Notosuchus

34(1)*, 59(0)*, 113(1), 114(2), 159(1)*, 210(2)*

Mariliassuchus and Comahuesuchus

5(3)*, 25(1), 45(1), 95(1), 129(1)*, 191(1)*

Baurusuchus

4(0)*, 9(1), 27(1), 33(1)*, 38(1), 41(1), 44(1), 50(1), 55(0), 57(1), 58(0), 78(0), 118(1), 121(2), 178(1), 179(2), 187(1), 190(2), 202(1)

Neosuchia

4(2)*, 32(1), 44(1), 53(1), 56(2)*, 70(1)*, 106(2), 131(1), 135(2), 142(2)*, 157(2), 172(1)*, 190(2), 239(1)*

Sebecia

30(1)*, 51(2), 72(1)*, 79(2)*, 82(1), 90(1), 114(1), 119(1)*, 179(1)*, 193(1)*, 208(1)

Hamadasuchus, Sebecus, Stelokrosuchus, Peirosaurus, and Lomasuchus

5(2), 8(4), 49(1), 69(3), 84(1)*, 85(0)*, 92(1)*, 109(1)*, 131(2)*, 165(1)*, 167(1)*

Sebecus, Stelokrosuchus, Peirosaurus, and Lomasuchus

34(1), 86(0), 101(1), 154(1)*, 159(1)

Stelokrosuchus, Peirosaurus, and Lomasuchus

13(1), 35(2), 37(0), 87(3), 88(1), 102(1), 113(1)*, 130(2)*

Peirosaurus and Lomasuchus

21(2)

Mahajangasuchidae, Pholidosauridae, and Crocodylia

29(1), 57(1), 69(2)*, 78(0), 81(1)*, 91(2), 126(1), 132(1), 134(1), 147(2)*, 160(0), 186(1), 206(1)*, 209(1)*, 241(1)*

Mahajangasuchidae

10(1), 21(2), 33(1)*, 34(1)*, 35(2)*, 37(0), 44(2), 46(1), 50(1)*, 58(3), 69(3), 107(1), 121(2)*, 143(1), 164(1), 178(1), 179(2)*, 188(0)*, 193(1)*, 198(1), 202(1)

Pholidosauridae, Bernissartia, Isisfordia, and Crocodylia

5(3), 11(1), 13(1), 18(1), 32(2), 35(3)*, 49(2), 60(1), 87(3), 100(0)*, 117(2), 130(1), 179(3)*, 190(3), 192(1), 195(1)*, 217(0), 234(1)

Pholidosauridae

8(1), 24(1)*, 71(1), 116(0), 247(1), 248(2), 250(1)

Dyrosaurus, Terminonaris, Pholidosaurus, and Sarcosuchus

4(1), 18(0)*, 23(0), 39(0)*, 66(1), 89(2), 104(0), 124(0), 170(0)*, 176(1), 247(2)

Terminonaris, Pholidosaurus, and Sarcosuchus

27(1), 37(0), 79(0)*, 80(0), 94(1)*, 96(1), 97(1), 98(1), 99(1), 149(0), 216(0)*, 232(1)

Pholidosaurus and Sarcosuchus

14(1)*, 58(1), 103(1), 147(1)*

Laganosuchus, *Bernissartia*, *Isisfordia*, and Crocodylia

188(0)*, 200(0)

Bernissartia, *Isisfordia*, and Crocodylia

18(0)*, 121(2)*, 124(1)*, 169(1)*, 208(1), 215(1)*, 245(1)*, 246(2)*, 248(0)*

Isisfordia and Crocodylia

23(0), 58(1)*, 80(0)*, 126(2), 134(2), 181(0)*, 218(1), 220(1), 227(1)*

Crocodylia

30(1), 31(1)*, 51(0), 59(0), 68(1)*, 76(0)*, 126(3), 136(1)*, 142(0), 166(0), 174(1), 176(1), 210(1)*, 216(2)*, 220(2), 229(1)*, 251(0)

Brevirostres

18(1), 20(2), 119(1)*, 149(0)*, 160(1), 165(1)*, 169(0), 211(0), 223(2), 228(1), 243(2)*, 244(0)*

Alligatoroidea

35(2), 49(1), 84(1), 91(1), 113(1)*, 122(0), 127(2), 147(3)